BERICHTE
aus dem Fachbereich Geowissenschaften
der Universität Bremen

No. 242

Riedinger, N.

PRESERVATION AND DIAGENETIC OVERPRINT OF GEOCHEMICAL AND GEOPHYSICAL SIGNALS IN OCEAN MARGIN SEDIMENTS RELATED TO DEPOSITIONAL DYNAMICS

Berichte, Fachbereich Geowissenschaften, Universität Bremen, No. 242, 91 pages, Bremen 2005

ISSN 0931-0800

The "Berichte aus dem Fachbereich Geowissenschaften" are produced at irregular intervals by the Department of Geosciences, Bremen University.

They serve for the publication of experimental works, Ph.D.-theses and scientific contributions made by members of the department.

Reports can be ordered from:

Monika Bachur

Forschungszentrum Ozeanränder, RCOM

Universität Bremen

Postfach 330 440

D 28334 BREMEN

Phone: (49) 421 218-65516

Fax: (49) 421 218-65515

e-mail: MBachur@uni-bremen.de

Online available titles: http://elib3.suub.uni-bremen.de/publications/diss/html

Citation:
Riedinger, N.
Preservation and diagenetic overprint of geochemical and geophysical signals in ocean margin sediments related to depositional dynamics.
Berichte, Fachbereich Geowissenschaften, Universität Bremen, No. 242, 91 pages, Bremen, 2005.

ISSN 0931-0800

Preservation and diagenetic overprint of geochemical and geophysical signals in ocean margin sediments related to depositional dynamics

Dissertation
zur Erlangung des
Doktorgrades in den Naturwissenschaften
am Fachbereich Geowissenschaften
der Universität Bremen

vorgelegt von
Dipl. Geol. Natascha Riedinger
Bremen, April 2005

Tag des Kolloquiums:

22. Juni 2005

Gutachter:

Prof. Dr. H.D. Schulz
Prof. Dr. U. Bleil

Prüfer:

Prof. Dr. K.-U. Hinrichs
PD Dr. S. Kasten

Preface

This study was conducted as part of the Research Center Ocean Margins (RCOM) at the University of Bremen funded by the Deutsche Forschungsgemeinschaft (DFG). This work is submitted as a dissertation and has been supervised by Prof. Dr. Horst D. Schulz, under the guidance of PD Dr. Sabine Kasten, within the scope of subproject C1 "*Gauging diagenetic processes versus terrigenous and biogenic influx from physical, chemical and mineralogical attributes of sedimentary deposits in high productivity systems* ".

The present work is a supplement of four separate manuscripts based primarily on my own investigations, analytical work, data processing, and numerical modeling. Additionally, the abstracts of two further manuscripts, to which I contributed analytical work and co-authorship, are integrated into this thesis. The manuscripts have either been published or submitted for publication in international journals. In the introductory chapter a general introduction is outlined and a conclusion at the end of this thesis presents the main results, followed by an acknowledgement written in German. All data sets generated in the frame of this study are available via the geological data network Pangaea.

The aim of this thesis was the investigation of non-steady state diagenetic processes in deeper subsurface marine sediments of different depositional environments. The first study area, the western Argentine Basin, was selected based on prior work by Dr. Christian Hensen and co-workers. They pointed out the strong influence of the high dynamic depositional conditions in this area and its imprint on the geochemical record *(C. Hensen, M. Zabel, K. Pfeifer, T. Schwenk, S. Kasten, N. Riedinger, H.D. Schulz, and A. Boetius: Control of sulfate pore-water profiles by sedimentary events and the significance of anaerobic oxidation of methane for the burial of sulfur in marine sediments*). This paper deals with the reconstruction of sedimentary events, reflected in sulfate pore water profiles, by applying numerical modeling on geochemical and physical properties. Furthermore, the influence of anaerobic oxidation of methane on sulfur burial was examined. The investigations in this area were continued to study the diagenetic impact under such highly variable depositional settings on the geochemical as well as the magnetic record. Distinct minima in the magnetic susceptibility at the current sulfate/methane transition at three sites were reconstructed, applying numerical modeling on geochemical records (*N. Riedinger, K. Pfeifer, S. Kasten, J.F.L. Garming, C. Vogt, and C. Hensen: Diagenetic alteration of magnetic signals by anaerobic oxidation of methane related to a change in sedimentation rate*). One of these study sites was then chosen for detailed investigations of its rock-magnetic properties, with a comprehensive characterization of diagenetic alteration affecting magnetic mineral assemblages (*J.F.L. Garming, U. Bleil, and N. Riedinger: Alteration of magnetic mineralogy at the sulfate methane transition: Analysis of sediments from the Argentine continental slope*). Furthermore, studies on sediments from the western Argentine Basin were carried out, to investigate the effect of deeper buried reactive minerals on geochemical and microbiological systems (*N. Riedinger and S. Kasten: Alteration of manganese minerals and release of ferrous iron in deeper subsurface marine sediments from the western Argentine Basin*). The second study

area, the northern Cape Basin, was selected due to its contrasting depositional environment compared to the Argentine Basin. The diagenetic impact on the geochemical record in a rather static depositional system was studied and the preservation of reactive minerals, such as barite, in deeper subsurface sediments was discussed *(N. Riedinger, S. Kasten, J. Gröger, C. Franke, and K. Pfeifer: Active and buried authigenic barite fronts in sediments from the eastern Cape Basin*). In contrast to the prior manuscripts, the last paper presents results of laboratory experiments, which aimed at demonstrating that pyrite, although being assumed stable under anoxic conditions, can undergo biomediated alteration in anoxic marine environments (*N. Riedinger, S. Kasten, and M. Krüger: Microbial alteration of pyrite under anoxic conditions*).

Content

Abstract

In marine sediments, early diagenetic processes have a strong impact on the primary signals of the sedimentary records. This limits the application of such signals as paleoenvironmental proxies or stratigraphic tools.

The focus of this work is to study the impact of non-steady state diagenesis on primary geochemical and geophysical properties. We investigated the influence of depositional dynamics on diagenetic processes, by studying sediments recovered in the western Argentine Basin as well as in the northern Cape Basin. These two areas are characterized by contrasting depositional conditions as well as different input of organic matter.

The western Argentine Basin is characterized by highly dynamic depositional conditions, and thus represents a suitable sedimentary environment to study non-steady state processes. Geochemical and geophysical investigations were carried out on sediments from selected sites. The main process which drives diagenetic alteration in these sediments is the anaerobic oxidation of methane (AOM). This biogeochemical process leads to a depletion of sulfate at the sulfate/methane transition (SMT), a few meters below the sediment surface. The shape of the pore water sulfate profiles is influenced by sedimentary events. Such events can be reconstructed and a timing can be estimated by numerical modeling based on geochemical and physical properties. Linear profiles of sulfate pore water concentrations at some of the investigated sites indicate constant low sedimentation rates for a period of time. These sites are characterized by distinct gaps in magnetic susceptibility within the sulfidic zone. The nearly complete loss of magnetic susceptibility is shown to result from the reduction of sulfate by the process of AOM. This process releases H_2S into the pore water, which leads to the alteration of iron (oxyhydr)oxides to iron sulfides. Results of numerical modeling of geochemical data suggest that during the Pleistocene/Holocene transition a drastic decrease in sedimentation rate occurred, which caused a stagnation of the SMT. This fixation caused an enhanced diagenetic dissolution of ferrimagnetic iron minerals within the sulfidic zone. In this sediment interval a distinct overall fining of the grain-size of magnetic particles was found, which can be attributed to intense diagenetic alteration of the magnetic minerals. Further analyses of the rock magnetic properties revealed that the depletion in the magnetic signal results from complete pyritization.

Furthermore, in the sediments of the western Argentine Basin pore water concentration profiles of H_2S and manganese suggest that manganese is precipitated in the sulfidic zone. Above and below the sulfidic zone dissolved manganous ions occur. In addition, ferrous iron is released into the pore water in the methanic zone. We assume that the reduction of reactive manganese and iron minerals in the methanic zone could be related to biomediated processes. Identifying the exact reaction pathways as well as the microorganisms involved in these processes will advance the understanding of processes in the deep biosphere, especially concerning the availability of terminal electron acceptors.

In contrast to the western Argentine Basin, the eastern Cape Basin is characterized by relatively constant depositional conditions. Investigations of sediments from this area reveal the occurrence of distinct barium enrichments at the SMT. These authigenic barite fronts are formed by the reaction of upward diffusing barium with interstitial sulfate. At one study site, barite enrichments in sulfate-depleted sediments buried a few meters below the SMT were observed. The occurrence/preservation of these barite enrichments is presumably associated with a decelerated dissolution of barite, which could be explained by high concentrations of dissolved barium in the pore water. Furthermore, the alteration of barite into witherite via the transient phase barium sulfide could be another mechanism leading to the preservation of a former barite peak. Calculation of the enrichment time and the results of numerical modeling imply that a rapid relocation of the barite front to a shallower depth occurred between the last glacial maximum (LGM) and the Pleistocene/Holocene transition. We suggest that the upward shift of the SMT, which leads to the establishment of a new barite front, can be explained by an increase in the upward flux of methane. The most likely mechanism which has caused the rapid upward migration of the SMT is the burial of high amounts of organic matter below the SMT, followed by an increase in the rate of methanogenesis and upward flux of methane.

In addition to the investigations of sediments from natural environments, laboratory experiments were carried out. We studied the possible diagenetic alteration of pyrite under anoxic conditions which in general is assumed to be stable in this redox environment. To reveal the capability of bacteria to perform the process of pyrite reduction to iron monosulfide (FeS) with H_2 as the required electron donor, different experimental setups were continuously sampled over a time period of about one year. The results of microbiological and geochemical investigations imply, that the reduction of pyrite to FeS does indeed occur and is mediated by bacteria, although the postulated reaction could not be satisfactorily verified by our experiment. However, we assume that the microbial reduction of pyrite is a likely mechanism to explain alteration of supposedly stable minerals in anoxic marine environments.

The results of this thesis show that the sediments in the two contrasting depositional environments are both affected by diagenetic processes under non-steady state conditions. While in the Argentine Basin the strong changes in sedimentation rates are the main mechanisms leading to non-steady state conditions, the dominant process in the Cape Basin is a change in the upward flux of methane. The burial of reactive phases in deeper marine sediments can fuel biogeochemical processes. Thus, even in deeper sediments non-steady state diagenesis strongly influences geophysical and geochemical properties, which are used for the interpretation of the sedimentary record.

Zusammenfassung

In marinen Sedimenten haben frühdiagenetische Prozesse einen großen Einfluss auf die Erhaltung primärer Signale und limitieren daher die Anwendbarkeit eines breiten Spektrums von sedimentären Proxy-Parametern.

Im Mittelpunkt dieser Arbeit steht die Untersuchung der Auswirkung von instationären Prozessen auf primäre geochemische und geophysikalische Eigenschaften. Der Einfluss der Ablagerungsdynamik auf diagenetische Prozesse wurde untersucht. Zu diesem Zweck wurden Sedimente untersucht, die im westlichen Argentinienbecken sowie im östlichen Kapbecken genommen wurden. Diese beiden Gebiete sind durch gegensätzliche Ablagerungssysteme sowie den unterschiedlichen Eintrag von organischem Material charakterisiert.

Das westliche Argentinienbecken ist durch hochdynamische Ablagerungsbedingungen geprägt und eignet sich damit sehr gut für Studien instationärer Prozesse. An Sedimenten von ausgewählten Standorten wurden geochemische und geophysikalische Untersuchungen durchgeführt. Der Hauptprozess, der für die diagenetische Überprägung dieser Sedimente verantwortlich ist, ist die anaerobe Oxidation von Methan (AOM). Dieser biogeochemische Prozess führt zum Verbrauch von Sulfat an der Sulfat/Methan-Übergangszone (SMT), wenige Meter unterhalb der Sedimentoberfläche. Die Form der Sulfat-Porenwasserprofile wird durch sedimentäre Ereignisse beeinflusst. Durch Anwendung von numerischen Modellen auf geochemische und physikalische Eigenschaften können solche Ereignisse rekonstruiert und datiert werden. Lineare Sulfat-Porenwasser Profile an einigen der untersuchten Standorte deuten auf eine zeitweilig konstante Sedimentation hin. Diese Gebiete sind durch eine deutliche Abnahme der magnetischen Suszeptibilität im Bereich der sulfidischen Zone gekennzeichnet. Der nahezu vollständige Verlust der magnetischen Suszeptibilität in diskreten Horizonten ist auf die Reduktion von Sulfat durch den Prozess der AOM zurückzuführen. Dieser Prozess setzt Schwefelwasserstoff (H_2S) in das Porenwasser frei, was zu einer Umwandlung der Eisen(hydr)oxide in Eisensulfide führt. Ergebnisse der numerischen Modellierung von geochemischen Daten deuten auf einen drastischen Rückgang der Sedimentationsrate am Pleistozän/Holozän-Übergang hin, der zu einer Fixierung der SMT führte. Die Fixierung dieser geochemischen Grenze verursachte eine erhöhte diagenetische Lösung ferrimagnetischer Minerale in der sulfidischen Zone. In diesem Sedimentintervall wurde eine deutliche Verfeinerung der Korngröße magnetischer Partikel beobachtet, die sich aus der intensiven diagenetischen Umwandlung der magnetischen Minerale ergibt. Weitere Analysen der gesteinsmagnetischen Eigenschaften ließen erkennen, dass der Einbruch im magnetischen Signal aus dem Prozess der vollständigen Pyritisierung resultiert.

In den Sedimenten des Argentinienbeckens deuten des weiteren Porenwasser-Konzentrationsprofile von Mangan und H_2S auf eine Fällung von Mangan in der sulfidischen Zone hin. Ober- und unterhalb dieser Zone tritt dagegen gelöstes Mangan auf. Zusätzlich wird in der methanhaltigen Zone Eisen in das Porenwasser freigesetzt. Unsere Ergebnisse legen nahe, dass die Reduktion von reaktiven Eisen- und Manganmineralen in der methanhaltigen

Zone unter der Beteiligung von Mikroorganismen abläuft. Die Identifizierung dieser Prozesse könnte helfen die Prozesse in der tiefen Biosphäre, besonders im Bezug auf die Verfügbarkeit terminaler Elektronenakzeptoren, zu erklären bzw. das Verständnis zu vertiefen.

Im Gegensatz zum westlichen Argentinienbecken ist das Kapbecken durch über die Zeit relativ konstante Ablagerungsbedingungen charakterisiert. Untersuchungen an Sedimenten aus diesem Gebiet zeigen das Vorkommen deutlicher Barium-Anreicherungen an der SMT. Diese authigenen Baryt-Fronten entstehen durch die Reaktion von nach oben diffundierendem Barium mit dem im Porenwasser gelösten Sulfat. An einem der untersuchten Standorte wurden in den sulfatfreien Sedimenten, einige Meter unterhalb der SMT, Baryt-Anreicherungen gefunden. Das Vorkommen bzw. die Erhaltung dieser Baryt-Anreicherungen ist vermutlich mit einer verlangsamten Lösung der Baryt-Kristalle verbunden, die durch die hohe Konzentration von Barium im Porenwasser erklärt werden könnte. Des weiteren könnte die Umwandlung von Baryt in Whiterit, mit Bariumsulfid als Übergangsphase, zu einer Erhaltung der ehemaligen Baryt-Anreicherung führen. Berechnungen der Zeit, die zur Bildung dieser Anreicherungen erforderlich war, und Resultate von numerischen Modellierungen deuten auf eine Verlagerung der Baryt-Front in geringere Tiefen zwischen dem Letzten Glazialen Maximum und dem Pleistozän/Holozän-Übergang hin. Die Aufwärtsbewegung der SMT, die zu der Bildung einer neuen Baryt-Front führte, kann durch eine Zunahme des Methanflusses erklärt werden. Diese Zunahme ist vermutlich auf hohe Gehalte organischen Materials unterhalb der SMT und eine daraus resultierende erhöhte Methanbildungsrate zurückzuführen.

Zusätzlich zu den Untersuchungen an natürlichen Sedimenten wurden Laborexperimente zur möglichen Umwandlung von Pyrit durchgeführt, der unter anoxischen marinen Bedingungen als stabil angenommen wird. Um zu zeigen, dass Bakterien den Prozess der Reduktion von Pyrit zu Eisenmonosulfid (FeS) mit H_2 als Elektronendonor vermitteln können, wurden unterschiedlich angesetzte Versuche über den Zeitraum von einem Jahr beprobt. Die Resultate der mikrobiologischen und geochemischen Untersuchungen weisen auf eine durch Bakterien vermittelte Reduktion von Pyrit zu FeS hin, auch wenn diese postulierte Reaktion in unseren Experimenten nicht zufriedenstellend bestätigt werden konnte.

Die Ergebnisse dieser Arbeit zeigen, dass die beiden untersuchten und durch unterschiedlich sedimentäre Bedingungen geprägten Ablagerungssysteme durch diagenetische Prozesse unter instationären Bedingungen beeinflusst werden. Während im Argentinienbecken maßgeblich die vorherrschenden Ablagerungsprozesse zu den instationären Bedingungen führen, ist im Kapbecken hauptsächlich die Veränderung des aufwärts gerichteten Methanflusses hierfür verantwortlich. Die Einbettung reaktiver Minerale in tieferen marinen Sedimenten kann die dortigen biogeochemischen Prozessen antreiben bzw. verstärken. Somit werden geophysikalische und geochemische Sedimenteigenschaften, die zur Interpretation von Sedimentabfolgen herangezogen werden, auch in tieferen Sedimenten durch instationäre diagenetische Prozesse stark beeinflusst.

Introduction

Marine sediments provide unique archives to study changes in paleoclimatic conditions and their impact on continental and marine environments. The reconstruction of these environments requires the development of specific proxies. However, the sedimentary record is often influenced by early diagenetic processes which have a strong impact on the reliability of paleoceanographic proxy records. Diagenetic overprint does not only occur directly after deposition but can also cause alteration of sediment composition long after initial deposition. This substantially influences geochemical, mineralogical, and geophysical signals and further complicates the interpretation of the sedimentary record.

Early diagenesis and redox zonation

The degradation of organic matter starts in the water column during sinking of particles and aggregates, and continues in the sediment using oxygen as the preferred electron acceptor. When oxygen is exhausted microorganisms switch to alternative terminal electron acceptors. The general sequence of electron acceptors used is oxygen, nitrate, manganese oxides, iron oxides, and sulfate. This succession corresponds to a decreasing energy yield of oxidized organic carbon (e.g. Froelich et al., 1979). These oxidation processes often lead to the establishment of typical domains in marine sediments, which are described as redox zonations (Fig. 1). In the oxic zone oxygen in interstitial waters is still available, while in anoxic environments the pore waters contain no measurable amounts of dissolved oxygen. The anoxic environment can be further subdivided into post-oxic, sulfidic, and methanic environments as described by Berner (1981). In post-oxic environments diagenesis has proceeded beyond the oxic stage and nitrate, manganese oxides and iron oxides are used as oxidants. Sulfidic environments are characterized by the formation of hydrogen sulfide due to bacterial reduction of dissolved sulfate, and a continued decomposition of organic matter by fermentation results in the formation of methane, in the methanic zone.

The mineralization of organic matter proceeds via biologically mediated redox reactions, which drive most of the early diagenetic processes (Froelich et al., 1979). The products of this mineralization are afterwards involved in secondary reactions including redox reactions, sorption, dissolution and precipitation processes. Thus, the stability of reactive minerals is successively reduced and numerous biotic and abiotic processes are activated causing alteration and remineralization of sediment components. These processes can lead to an overprint of constituents for example used as proxies in paleoceanography or stratigraphy. Thus, there is a need to understand and quantify the processes that occur in these systems.

Iron oxide minerals, which are a common component of marine sediments (e.g. Haese et al., 2000), have a proxy potential for selective environmental reconstructions. They are important carriers of magnetostratigraphic and paleomagnetic information (Frederichs et al., 1999; Bleil, 2000).

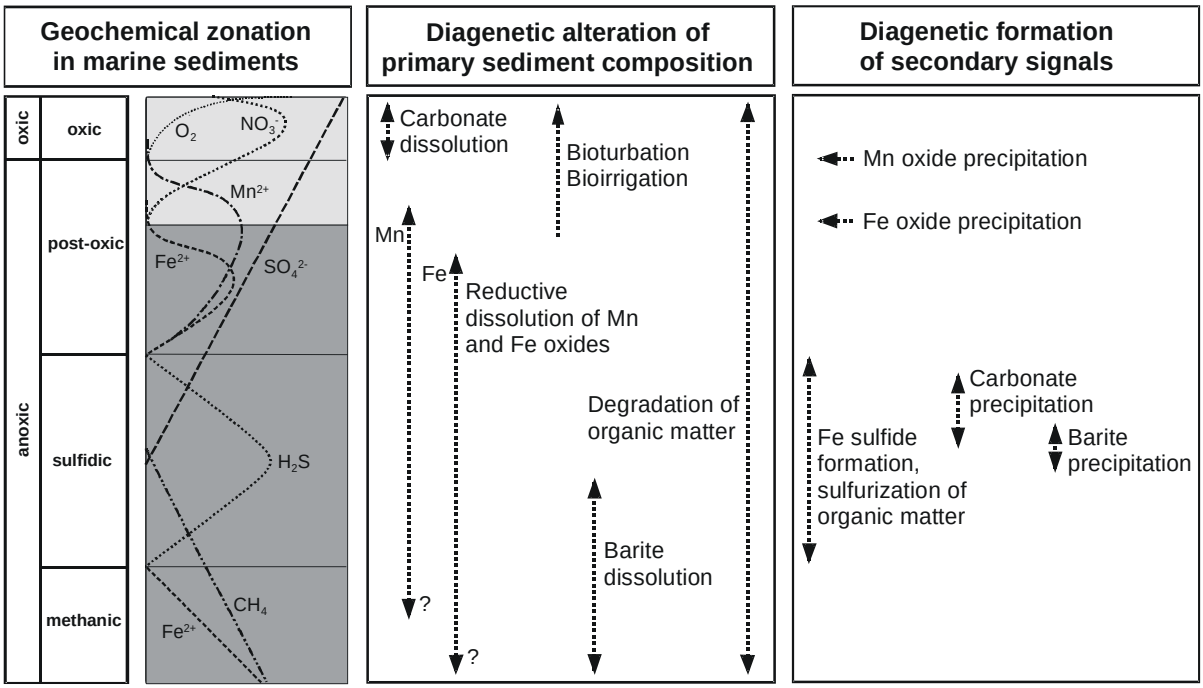

Fig. 1. Schematic representation of redox zonation in marine sediments as well as the most important early diagenetic processes for the alteration of the primary sediment composition and for the formation of secondary signals in the sedimentary record, modified after Kasten et al. (2003). The classification of the different early diagenetic environments according to Berner (1981) is shown on the left side. Pore water profiles of the dissolved terminal electron acceptors (TEA) and the products of the different TEA processes are depicted here as well. This illustration represents a particular situation in which the sulfate pore water profile is primarily shaped by the reaction with upward diffusing methane, i.e. by anaerobic oxidation of methane.

The alteration of these primary signals limits the application of iron oxides as a proxy. After deposition primary iron mineral inventories pass through a sequence of early diagenetic alteration. This can lead to strong modification of primary iron oxide/hydroxides and rock magnetic properties and precipitation of secondary minerals, particularly across the FeII/FeIII redox boundary (e.g. Wilson et al., 1986; Tarduno and Wilkison, 1996; Kasten et al., 1998; Funk et al., 2003) and in the post-oxic zone where sulfate is reduced (e.g. Passier et al., 1998).

A further good example for the impact of diagenetic processes on paleoceanographic proxies, is barium or barite in deep-sea sediments. The accumulation of barium in the solid phase has been discussed as a proxy for productivity (e.g. Bishop, 1988; Dymond et al., 1992; Gingele and Dahmke, 1994; Paytan et al., 1996). The link between productivity and the amount of barium in the sediment is thought to be established by the formation of distinct barite ($BaSO_4$) particles associated with the decay of organic matter in the water column (Goldberg and Arrhenius, 1958; Church, 1979; Chow & Goldberg, 1960; Dehairs et al., 1980; Bishop, 1988; Dehairs, 1991; Ganeshram et al., 2002). When barite is buried in the zone where sulfate is depleted, it will be dissolved and barium will be released into the pore water. Thus, diagenetic processes such as the anaerobic oxidation of methane (AOM), which lead to the alteration of primary Ba-signals, are one of the most important limitations for application of barium as a proxy for paleoproductivity (e.g. von Breymann et al., 1992).

Non-steady state processes and mechanisms

Early diagenetic processes are often assumed to proceed under steady state conditions, where inputs of reactive minerals and overlying water properties remain constant (Kasten et al., 2003). However, the balance between fluxes and sedimentation rate is very delicate, as pointed out by Pruysers et al. (1993). Thus, steady state conditions persisting over a long period of time are unlikely in most sedimentary environments and non-steady state conditions can be considered to be the more common situation (Kasten et al., 2003). The main mechanisms and processes which lead to non-steady state conditions can be summarized under: 1) oceanographic conditions, 2) depositional dynamics, 3) sedimentary input, and 4) methane flux.

Changes in oceanographic conditions comprise oxygen and/or nutrient supply and temperature changes. These factors primarily affect the benthic boundary layer. Processes within deeper subsurface sediments are more influenced by depositional dynamics such as gravity mass flows, slumps, slides, turbidites, or sudden changes in sedimentation rate. High sedimentation rates can lead to a preservation/shielding of reactive mineral phases e.g. iron (oxyhydr)oxides (Roberts and Turner, 1993). These reactive phases then influence early diagenetic processes in the deeper sediments. Deeper sediments are furthermore affected by both qualitative and quantitative changes of particle input. Distinct modification of mineral assemblages mostly occurs in and around organic matter rich layers (e.g., sapropels), marking episodic productivity extremes or enhanced preservation of organic matter (Passier et al., 1996). The last discussed mechanism leading to non-steady state conditions, is a change in the upward flux of methane. Gas hydrate disintegration, increase in the formation of thermogenic methane, or methane formation within TOC rich layers can increase the methane flux and thus lead to an upward shift of the sulfate/methane transition (SMT). Although sediment sequences may have deposited under constant conditions over time, they can be subject to different degrees of diagenetic overprint driven by influences from below e.g. burial of organic matter rich layers or gas hydrate disintegration.

The schematic representation in Fig. 2 points out the broad spectrum of mechanisms and processes which can lead to non-steady state conditions. This emphasizes the wide occurence of non-steady state conditions compared to steady state situations. Suitable indices of non-steady-state diagenetic environments are elements and minerals precipitated and immobilized under suboxic to anoxic conditions. In this regard, authigenic barite precipitation is greatly influenced by non-steady state diagenesis. A drastic decrease in sedimentation rates can fix such a barite front at a discrete interval, which leads to the formation of a large barite deposit (Torres et al., 1996). Furthermore, the formation of a new barite enrichment can be triggered by a decrease in the methane flux, which shifts the position of the SMT downward (Dickens, 2001). Therefore, decreases in the upward methane flux, and thus, former positions of the SMT, can be reconstructed by barite fronts preserved above the SMT. Thus, under the premise that the SMT moves down, authigenic barite enrichments provide a good indicator

for non-steady state conditions. If the SMT moves up, former barite fronts are generally assumed to be destroyed by dissolution (Dickens, 2001).

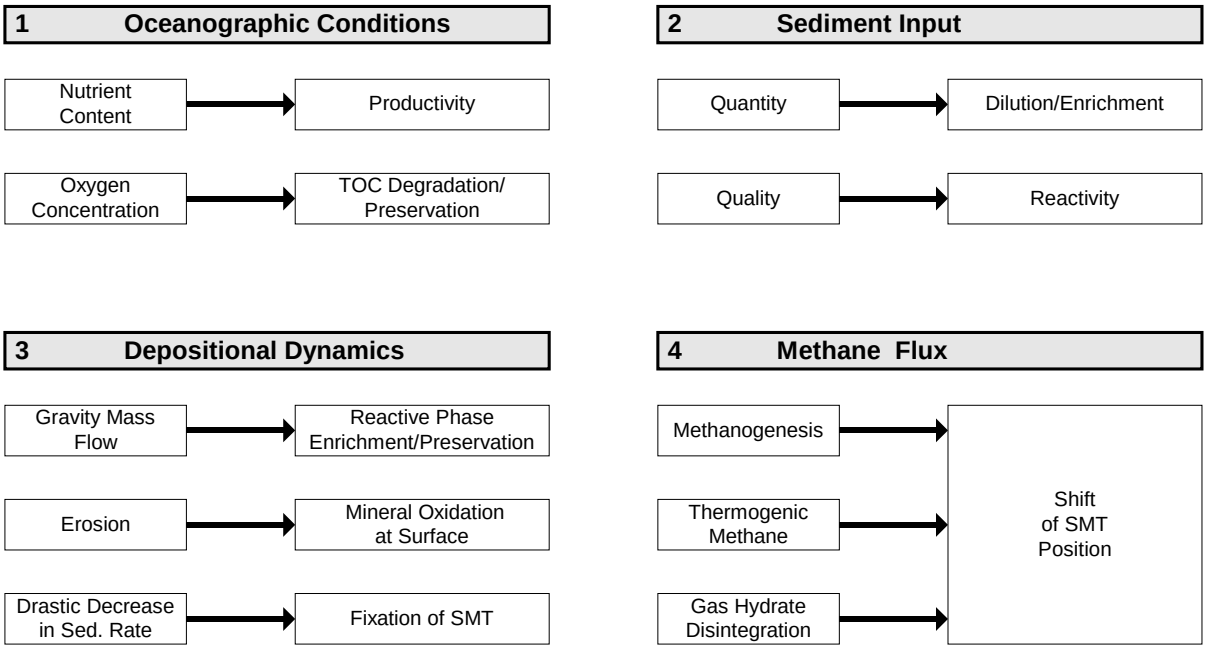

Fig. 2. Examples of processes and mechanisms which can lead to non-steady state conditions.

Overall, depositional dynamics, qualitative and/or quantitative changes in sediment input, and changes in the upward flux of methane can have a strong influence on the diagenetic processes in deeper buried marine sediments. The alteration of minerals, which can lead to a loss of the primary signal, can proceed long time after initial deposition of the sediments. This non-steady state diagenetic impact on minerals in deeper buried sediments, is the focus of this work.

Microbial processes in deeper subsurface sediments

Prokaryotes of subseafloor sediments have been estimated to constitute as much as one-third of the Earth's total living biomass (Whitman et al., 1998) and biogeochemical reactions with high turnover rates take place. In the last decades it could be shown that processes, which were assumed to be chemically driven are often microbially mediated. These biomediated processes can lead to the alteration of reactive minerals. In sediments throughout the world ocean prokaryotic activity occurs among others in the form of sulfate reduction and/or methanogenesis (D'Hondt et al., 2002). Boetius et al. (2000) could demonstrate that the anaerobic oxidation of methane (AOM) by sulfate is mediated by a consortium of methane-consuming archaea and sulfate-reducing bacteria. Sulfate reduction driven by AOM releases hydrogen sulfide (H_2S) and bicarbonate into the pore water according to the following net equation (Barnes and Goldberg, 1976; Bernard, 1979; Blair and Aller, 1995; Borowski et al., 1996; Niewöhner et al., 1998):

$$CH_4 + SO_4^{2-} \rightarrow HCO_3^- + HS^- + H_20 \qquad (1)$$

The process of AOM strongly affects the sedimentary solid phase. The released HCO_3^- ions can potentially lead to the precipitation of Mn and Ca carbonate phases (e.g. Kasten et al., 2003). Hydrogen sulfide liberated by AOM is responsible for the alteration of Mn-oxides and iron (oxyhydr)oxides into sulfides (Fig. 1), which is a very important geochemical process leading to the loss and new formation of magnetic signals (Kasten et al., 1998; Passier et al., 1998).

The overprint of magnetic attributes is a major cause for the loss of paleomagnetic and magnetostratigraphic records in marine sediments (Canfield and Berner, 1987; Channell and Hawthorne, 1990; Karlin, 1990; Roberts and Turner, 1993; Furukawa and Barnes, 1995; Passier et al., 1998; Channell and Stoner, 2002). The strong influence on the magnetic signal is caused by the conversion of ferrimagnetic iron oxides, which carry remanent magnetism, to paramagnetic iron sulfides (Berner, 1970; Canfield et al., 1992). Pyrite is the thermodynamically stable endmember of the transformation of iron oxide/hydroxides to iron sulfides via intermediate minerals (Berner, 1970; Roberts and Turner, 1993; Coleman and Raiswell, 1995). At excess H_2S in pore water, pyrite is formed by the oxidation of FeS by H_2S (Morse and Cornwell, 1987; Butler and Rickard, 2000), which causes a drop in the magnetic signal. If free H_2S is not available, metastable iron sulfides like pyrrhotite (Fe_7S_8) or greigite (Fe_3S_4) can persist for a considerable period of time (Berner, 1967, 1982). These intermediate minerals are ferrimagnetic and can lead to the formation of a strong secondary magnetic signal (Fig. 3). This emphasizes, that the formation of authigenic iron sulfides is critical to sedimentary paleomagnetic studies, because of the alteration of magnetic signals.

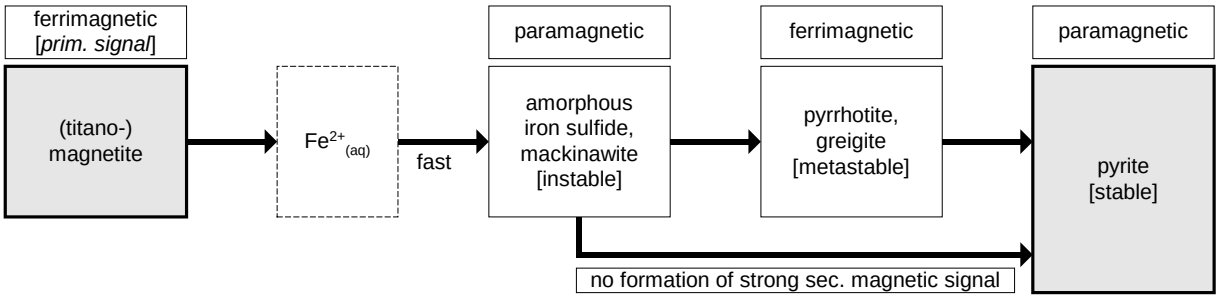

Fig. 3. Simplified major pathways of the transformation of iron oxides to iron sulfides in anoxic marine environments, in relation to the alteration of the magnetic record. If pyrite is precipitated directly from amorphous iron sulfide or mackinawite there is no formation of a secondary strong magnetic signal. Pyrrhotite and greigite are instable in the presence of hydrogen sulfide, where pyrite is the stable endmember. For more details and references see text.

In addition to AOM, there are further biotic processes in deeper subsurface sediments which affect reactive minerals, such as iron and manganese reduction (D'Hondt et al., 2004). In areas with high accumulation rates reactive minerals are buried rapidly and considerable amounts can be shielded from reduction (Damuth, 1977; Canfield and Berner, 1987; Finney et

al., 1988; Roberts and Turner, 1993). The availability of these minerals can even activate some of the microbial processes in the deeper sediments. Preserved minerals in these depths, such as reactive iron phases, can be reduced by microorganisms coupled to the oxidation of H_2 in anoxic marine sediments (Lovley et al., 1989; Lovley, 1993). Thus, by providing terminal electron acceptors reactive minerals buried in deeper sediments can have great influence on biogeochemical processes in the deeper biosphere.

To explore life in deeply buried marine sediments expeditions of the Ocean Drilling Program (ODP) were undertaken. The occurrence of microbial activity and abundant cells in these deep sediments could be documented (e.g. D'Hondt et al., 2002; Schippers et al., 2005). The availability of substrates for microbial activity in the deeply buried sediments is rather low. Because of the high amounts of prokaryotes in the deep biosphere the calculated metabolic activities relating to the single cell is quite low. However, due to the possible existence of dormant cells, specific rates of active cells might be much higher. Despite the ubiquity of life in deeper marine sediments, little is known about which organisms are responsible for which metabolic activities in these sediments. Their effects on global biogeochemical cycles as well as on geochemical and biological resources are poorly understood (D'Hondt et al., 2002, 2004).

REFERENCES

Barnes, R.O. and Goldberg, E.D. (1976) Methane production and consumption in anoxic marine sediments. *Geology* **4**, 297-300.

Bernard, B.B. (1979) Methane in marine sediments. *Deep-Sea Res.* **26** 429-443.

Berner, R.A. (1967) Thermodynamic stability of sedimentary iron sulfides. *Am. J. Sci.* **265**, 773-785.

Berner, R.A. (1970) Sedimentary pyrite formation. *Am. J. Sci*. **268**, 1-23.

Berner, R.A. (1981) A new geochemical classification of sedimentary environments. *J. Sed. Petrol*. **51**, 359-365.

Berner, R.A. (1982) Burial of organic carbon and pyrite sulfur in the modern ocean: Its geochemical and environmental significance. *Am. J. Sci*. **282**, 451-473.

Bishop, J.K. (1988) The barite-opal-organic carbon association in oceanic particular matter. *Nature* **24**, 341-343.

Blair, N.E. and Aller, R.C. (1995) Anaerobic methane oxidation on the Amazon shelf. *Geochim. Cosmochim. Acta* **59**, 3707-3715.

Bleil, U. (2000) Sedimentary Magnetism. In *Marine Geochemistry* (eds. H.D. Schulz and M. Zabel). Springer, pp. 73-84.

Boetius, A., Ravenschlag, K., Schubert, C.J., Rickert, D., Widdel, F., Gieseke, A., Amann, R., Jørgensen, B.B., Witte, U., and Pfannkuche, O. (2000) A marine microbial consortium apparently mediating anaerobic oxidation of methane. *Nature* **407**, 623-626.

Borowski, W.S., Paull, C.K., and Ussler, W. (1996) Marine porewater sulfate profiles indicate in situ methane flux from underlying gas hydrate. *Geology* **24**, 655-658.

Butler, I.B. and Rickard, D. (2000) Framboidal pyrite formation via the oxidation of iron (II) monosulfides by hydrogen sulfide. *Geochim. Cosmochim. Acta* **64**, 2665-2672.

Canfield, D.E. and Berner, R.A. (1987) Dissolution and pyritization of magnetite in anoxic marine sediments. *Geochim. Cosmochim. Acta* **51**, 645-659.

Canfield, D.E., Raiswell, R., and Bottrell, S. (1992) The reactivity of sedimentary iron minerals toward sulfide. *Am. J. Sci*. **292**, 659-683.

Channell, J.E.T. and Hawthorne, T. (1990) Progressive dissolution of titanomagnetites at ODP Site 653 (Tyrrhenian Sea). *Earth Planet. Sci. Lett.* **96**, 469-480.

Channell, J.E.T. and Stoner, J.S. (2002) Plio-Pleistocene magnetic polarity stratigraphies and diagenetic magnetite dissolution at ODP Leg 177 Sites (1089, 1091, 1093 and 1094). *Mar. Micropal*. **45**, 269-290.

Chow, T.J. and Goldberg, E.D. (1960) On the marine geochemistry of barium. *Geochim. Cosmochim. Acta* **20**, 192-198.

Church, T.M. (1979) Marine Barite. In *Marine Minerals* (ed. R.G. Burns). Rev. Mineral., Miner. Soc. Am. **6**, pp. 175-209.

Coleman, M.L. and Raiswell, R. (1995) Source of carbonate and origin of zonation in pyritiferous carbonate concretions: Evaluation of a dynamic model. *Am. J. Sci*. **295**, 282-308.

Dehairs, F., Chesselet, R., and Jedwab, J. (1980) Discrete suspended particles of barite and the barium cycle in the open ocean. *Earth Planet. Sci. Lett.* **49**, 915-931.

Dehairs, F., Stroobants, N., and Goeyens, L. (1991) Suspended barite as a tracer of biological activity in the Southern Ocean. *Mar. Chem.* **35**, 399-410.

D'Hondt, S., Rutherford, S., and Spivack, A.J. (2002) Metabolic activity of subsurface life in deep-sea sediments. *Science* **295**, 2067-2070.

D'Hondt, S., Jørgensen, B.B., Miller, D.J., et al. (2004) Distributions of microbial activities in deep subseafloor sediments. *Science* **306**, 2216-2221.

Dickens, G.R. (2001) Sulfate profiles and barium fronts in sediment on the Blake Ridge: Present and past methane fluxes through a large gas hydrate reservoir. *Geochim. Cosmochim. Acta* **65**, 529-543.

Dymond, J., Suess, E., and Lyle, M. (1992) Barium in deep-sea sediment: A geochemical proxy for paleoproductivity. *Paleoceanography* **7**, 163-181.

Finney, B.P., Lyle, M.W., and Heath, G.R. (1988) Sedimentation at MANOP site H (eastern equatorial Pacific) over the past 400 000 years: Climatecally induced redox variations and their effects on transition metal cycling. *Paleoceanography* **3**, 169-189.

Frederichs, T., Bleil, U., Däumler, K., von Dobeneck, T., and Schmidt, A.M. (1999) The magnetic view on the marine paleoenvironment: parameters, techniques and potentials of rock magnetic studies as a key to paleoclimatic and paleoceanographic changes. In *Use of proxies in paleoceanography: examples from the South Atlantic* (eds. G. Fischer and G. Wefer). Springer, pp. 575-599.

Froelich, P.N., Klinkhammer, G.P., Bender, M.L., Luedtke, N.A., Heath, G.R., Cullen, D., Dauphin, P., Hammond, D., Hartman, B., and Maynard, V. (1979) Early oxidation of organic matter in pelagic sediments of the eastern equatorial Atlantic: suboxic diagenesis. *Geochim. Cosmochim. Acta* **43**, 1075-1090.

Funk, J.A., von Dobeneck, T., and Reitz, A. (2003) Integrated rock magnetic and geochemical quantification of redoxomorphic iron mineral diagenesis in Late Quaternary sediments from the Equatorial Atlantic. In *The South Atlantic in the Late Quaternary: Reconstruction of material budget and current systems* (eds. G. Wefer, S. Mulitza, and V. Ratmeyer). Springer, pp. 237-260.

Furukawa, Y. and Barnes, H.L. (1995) Reactions forming pyrite from precipitated amorphous ferrous sulfide. In *Geochemical transformation of sedimentary sulfur* (eds. M.A. Vairavamurthy and M.A.A. Schoonen). ACS Symposium Series **612**, 194-205.

Ganeshram, R.S., Franc, R., Commeau, J., and Brown-Leger, S. L. (2003) An Experimental Investigation of Barite Formation in Seawater. *Geochim. Cosmochim. Acta* **67**, 2599-2605.

Gingele, F. and Dahmke, A. (1994) Discrete barite particles and barium as tracers of paleoproductivity in South Atlantic sediments. *Paleoceanography* **9**, 151-168.

Goldberg, E.D. and Arrhenius, G.O.S. (1958) Chemistry of Pacific pelagic sediments. *Geochim. Cosmochim. Acta* **13**, 153-212.

Haese, R.R., Schramm, J., Rutgers van der Loeff, M.M., and Schulz, H.D. (2000) A comparative study of iron and manganese diagenesis in continental slope and deep sea basin sediments off Uruguay (SW Atlantic). *Int. J. Earth Sci.* **88**, 619-629.

Karlin, R. (1990) Magnetite diagenesis in marine sediments from the Oregon Continental Margin. *J. Geophys. Res*. **95**, 4405-4419.

Kasten, S., Freudenthal, T., Gingele, F.X., and Schulz, H.D. (1998) Simultaneous formation of iron-rich layers at different redox boundaries in sediments of the Amazon deep-sea fan. *Geochim. Cosmochim. Acta* **62**, 2253–2264.

Kasten, S., Zabel, M., Heuer, V., and Hensen, C. (2003) Processes and signals of nonsteady-state diagenesis in deep-sea sediments and their pore waters. In *The South Atlantic in the Late Quaternary: Reconstruction of material budget and current systems* (eds. G. Wefer, S. Mulitza, and V. Ratmeyer). Springer, pp. 431-459.

Lovley, D.R., Phillips, E.J.P., and Lonergan, D.J. (1989) Hydrogen and formate oxidation coupled to dissimilatory reduction of iron or manganese by Alteromonas putrefaciens. *Appl. Environ. Microbiol*. **55,** 700-706.

Lovley, D.R. (1993) Dissimilatory metal reduction. *Annu. Rev. Microbiol*. **47** 263-290.

Morse, J.W. and Cornwell (1987) Analysis and distribution of iron sulfide minerals in recent anoxic marine sediments. *Mar. Chem*. **22**, 55-69.

Niewöhner, C., Hensen, C., Kasten, S., Zabel, M., and Schulz, H.D. (1998) Deep sulfate reduction completely mediated by anaerobic methane oxidation in sediments of the upwelling area off Namibia. *Geochim. Cosmochim. Acta* **62**, 455-464.

Paytan, A., Kastner, M., and Chavez, F.P. (1996) Glacial to interglacial fluctuations in productivity in the Equatorial Pacific as indicated by marine barite. *Science* **274**, 1355-1357.

Passier, H.F., Middelburg, J.J., van Os, B.J.H., and de Lange, G.J. (1996) Diagenetic pyritisation under eastern Mediterranean sapropels caused by downward sulphide diffusion. *Geochim. Cosmochim. Acta* **60**, 751–763.

Passier, H.F., Dekkers, M.J., and de Lange, G.J. (1998) Sediment chemistry and magnetic properties in an anomalously reducing core from the eastern Mediterranean Sea. *Chem. Geol*. **152**, 287–306.

Pruysers, P.A., de Lange, G.J., Middelburg, J.J., and Hydes, D.J. (1993) The diagenetic formation of metal-rich layersin sapropel-containing sediments in the rastern Mediterranean. *Geochim. Cosmochim. Acta* **57**, 579-595.

Roberts, A.P. and Turner, G.M. (1993) Diagenetic formation of ferrimagnetic iron sulphide minerals in rapidly deposited marine sediments, South Island, New Zealand. *Earth Planet. Sci. Lett*. **115**, 257-273.

Schippers, A., Neretin, L.N., Kallmeyer, J., Ferdelman, T.G., Cragg, B.A., Parkes, R.J., and Jørgensen, B.B. (2005) Prokaryotic cells of the deep sub-seafloor biosphere identified as living bacteria. *Nature* **433**, 861-864.

Tarduno, J.A. and Wilkison, S.L. (1996) Non-steady state magnetic mineral reduction, chemical lock-in, and delayed remanence acquisition in pelagic sediments. *Earth Planet. Sci. Lett*. **144**, 315–326.

Torres, M.E., Brumsack, H.J., Bohrmann, G., and Emeis, K.C. (1996) Barite fronts in continental margin sediments: A new look at barium remobilization in the zone of sulfate reduction and formation of heavy barites in diagenetic fronts. *Chem. Geol.* **127**, 125-139.

von Breymann, M.T., Brumsack, H., and Emeis, K.-C. (1992) Depositional and diagenetic behavior of barium in the Japan Sea. In *Proc. ODP, Sci. Resul.* **127/128** (eds. K.A. Pisciotto, J.C. Ingle, M.T. von Breymann, J. Barron, et al.). College Station, Texas, pp. 651-663.

Whitman, W.B., Coleman, D.C., and Wiebe, W.J. (1998) Prokaryotes: the unseen majority. *Proc. Nat. Sci. U.S.A.* **95**, 6578-6583.

Wilson, T.R.S., Thomson, J., Hydes, D.J., Colley, S., Culkin, F., and Sørensen, J. (1986) Oxidation fronts in pelagic sediments: Diagenetic formation of metal-rich layers. *Science* **232**, 972-975.

Control of sulfate pore-water profiles by sedimentary events and the significance of anaerobic oxidation of methane for the burial of sulfur in marine sediments

C. Hensen[1], M. Zabel[1], K. Pfeifer[1], T. Schwenk[1], S. Kasten[1], N. Riedinger[1], H.D. Schulz[1], and A. Boetius[2]

[1] *Fachbereich Geowissenschaften, Universität Bremen, Klagenfurter Str., 28359 Bremen, Germany*

[2] *Max-Planck Institute for Marine Microbiology, Celsiusstrasse 1, 28359 Bremen, Germany*

Abstract

Gravity driven mass-flow deposits proven by sedimentary and digital echosounder data are indicative for prevailing dynamic sedimentary conditions along the continental margin of the western Argentine Basin. In this study we present geochemical data from a total of 23 gravity cores. Pore-water SO_4 is generally depleted within a few meters below the sediment surface by anaerobic oxidation of methane (AOM). The different shapes of SO_4 profiles (concave, kink- and s-type) can be consistently explained by sedimentary slides possibly in combination with changes in the CH_4 flux from below, thus, mostly representing transient pore-water conditions. Since slides may keep their original sedimentary signature, a combined analysis and numerical modeling of geochemical, physical properties, and hydro acoustic data could be applied in order to reconstruct the sedimentary history. We present first order estimates of the dating of sedimentary events for an area where conventional stratigraphic methods failed to this day. The results of the investigated sites suggest that present day conditions are the result of events that occurred decades to thousands of years ago and promote a persisting mass transport from the shelf into the deep-sea, depositing high amounts of reactive compounds. The high abundance of reactive iron phases in this region maintains low hydrogen sulfide levels in the sediments by a nearly quantitative precipitation of all reduced sulfate by AOM. For the total region we estimate a SO_4 (or CH_4) flux of 6.6×10^{10} moles per year into the zone of AOM. Projected to the global continental slope and rise area, this may sum up to about 2.6×10^{12} moles per year. Provided that the sulfur is completely fixed in the sediments it is about twice the global value of the recent global sulfur burial in marine sediments of 1.2×10^{12} moles per year as previously estimated. Thus, AOM obviously contributes very significantly to the regulation of global sulfur reservoirs, which is hitherto not sufficiently recognized. This finding may have implications for global geochemical models, as sulfur burial is an important control factor in the development of atmospheric oxygen levels over time.

Diagenetic alteration of magnetic signals by anaerobic oxidation of methane related to a change in sedimentation rate

N. Riedinger[*1], K. Pfeifer[1], S. Kasten[1], J.F.L. Garming[1], C. Vogt[1], and C. Hensen[2]

[1] *Fachbereich Geowissenschaften, Universität Bremen, Klagenfurter Straße, 28359 Bremen, Germany*

[2] *GEOMAR – Forschungszentrum für Marine Geowissenschaften, Wischhofstr. 1-3, 24148 Kiel, Germany*

Abstract

Geochemical and rock magnetic investigations of sediments from three sites on the continental margin off Argentina and Uruguay were carried out to study diagenetic alteration of iron minerals driven by anaerobic oxidation of methane (AOM). The western Argentine Basin represents a suitable sedimentary environment to study non-steady state processes because it is characterized by highly dynamic depositional conditions. Mineralogical and bulk solid phase data document that the sediment mainly consists of terrigenous material with high contents of iron minerals. As a typical feature of these deposits, distinct minima in magnetic susceptibility (κ) are observed. Pore water data reveal that these minima in susceptibility coincide with the current depth of the sulfate/methane transition (SMT) where HS^- is generated by the process of AOM. The released HS^- reacts with the abundant iron (oxyhydr)oxides resulting in the precipitation of iron sulfides accompanied by a nearly complete loss of magnetic susceptibility. Modeling of geochemical data suggest that the magnetic record in this area is highly influenced by a drastic change in mean sedimentation rate (SR) which occurred during the Pleistocene/Holocene transition. We assume that the strong decrease in mean SR encountered during this glacial/interglacial transition induced a fixation of the SMT at a specific depth. The stagnation has obviously enhanced diagenetic dissolution of iron (oxyhydr)oxides within a distinct sediment interval. This assumption was further substantiated by numerical modeling in which the mean SR was decreased from 100 cm kyr^{-1} during glacial times to 5 cm kyr^{-1} in the Holocene and the methane flux from below was fixed to a constant value. To obtain the observed geochemical and magnetic patterns, the SMT must remain at a fixed position for approximately 9000 years. This calculated value closely correlates to the timing of the Pleistocene/Holocene transition. The results of the model show additionally that a constant high mean SR would cause a concave-up profile of pore water sulfate under steady state conditions.

1. INTRODUCTION

Iron (oxyhydr)oxides are a common component of marine sediments (e.g. Canfield, 1989; Haese et al., 2000), and are important carriers of magnetostratigraphic and paleomagnetic information (Frederichs et al., 1999; Bleil, 2000). After deposition primary iron mineral assemblages pass through a sequence of early diagenetic zones in which the minerals undergo alterations. Strong modifications of iron (oxyhydr)oxides and rock magnetic properties during the early stages of diagenesis across the Fe redox boundary have been documented by numerous studies (Wilson, 1986; Tarduno and Wilkison, 1996; Funk et al., 2003a and b; Reitz et al., 2004). The early diagenetic transformation of iron (oxyhydr)oxides in marine sediments is linked to different pathways. One important process is the reaction with hydrogen sulfide via sulfate reduction (Berner, 1970; Froelich et al., 1979; Canfield, 1989; Lovley, 1991; Haese et al., 1998). Besides sulfate reduction driven by the bacterial degradation of organic matter, which typically occurs at high rates in the upper layers of the sediment (Jørgensen, 1982; Ferdelman et al., 1999), the process which ultimately leads to the complete consumption of interstitial sulfate in marine sediments is the anaerobic oxidation of methane (AOM). This important biogeochemical process finds its geochemical expression in a characteristic sulfate/methane transition (SMT) typically located one to a few meters below the sediment surface. Sulfate reduction driven by AOM releases adequate amounts of hydrogen sulfide into the pore water (Barnes and Goldberg, 1976; Bernard, 1979; Blair and Aller, 1995; Borowski et al., 1996; Niewöhner et al., 1998; Jørgensen et al., 2004). The liberated hydrogen sulfide leads to diagenetic alteration of primary geochemical and geophysical properties and the formation of distinct secondary signals in the zone of AOM (Passier et al., 1998; Kasten et al., 2003; Neretin et al., 2004).

The extent of geochemical and magnetic overprint occurring at geochemical boundaries and reaction fronts, particularly in deeper sediments is poorly understood. An important geochemical process in the zone of AOM is the transformation of magnetic iron minerals (Kasten et al., 1998; Passier et al., 1998). One of the major minerals to carry remanent magnetism in sediments is the ferrimagnetic mineral (titano-)magnetite. The conversion of magnetite to iron sulfides during sediment diagenesis is a major cause of the loss of the magnetostratigraphic record in marine sediments (Karlin and Levi, 1983, 1985; Channell and Hawthorne, 1990; Karlin, 1990; Passier et al., 1998; Channell and Stoner, 2002). Ferrimagnetic iron oxides can be altered to paramagnetic iron sulfides (Berner, 1970; Canfield et al., 1992) and the magnetic signal can change dramatically (Canfield and Berner, 1987; Channell and Hawthorne, 1990; Channell and Stoner, 2002). An often cited mechanism is the formation of the iron sulfide pyrite via an intermediate sulfide mineral like greigite (Berner, 1967; Roberts and Turner, 1993). These latter minerals are ferrimagnetic and their preservation would lead to the formation of a strong secondary magnetic signal (Roberts and Turner, 1993; Kasten et al., 1998; Jiang et al., 2001; Neretin et al., 2004). Intermediate iron sulfides are metastable, but they can persist for a considerable period of time if hydrogen sulfide is entirely consumed (Berner, 1982; Kao et al., 2004). Pyrite is thermodynamically

more stable and thus will be the end-member of the transformation from iron (oxyhydr)oxides to iron sulfides (Berner, 1970; Coleman and Raiswell, 1995). However, if hydrogen sulfide is present in pore water, the oxidation of iron monosulfides by hydrogen sulfide can form pyrite directly without a greigite intermediate (Morse and Cornwell, 1987; Rickard et al., 1995; Butler and Rickard, 2000). Therefore, the diagenetic formation of iron sulfides in aquatic sediments has a strong effect on the interpretation of paleomagnetic data (Roberts and Turner, 1993; Furukawa and Barnes, 1995; Neretin et al., 2004).

The continental margin off Argentina and Uruguay represents a suitable sedimentary environment to study non-steady state processes because it is characterized by highly dynamic depositional conditions (Ewing et al., 1971; Biscaye and Dasch, 1971; Ledbetter and Klaus, 1987; Hensen et al., 2000, 2003). The sediment has a high content of ferric iron minerals and specific variations in magnetic signals (Sachs and Ellwood, 1988). Extensive geochemical and geophysical studies were carried out by Hensen et al. (2003) on sediments from the western Argentine Basin. Focusing on the reconstruction of mainly modern sedimentary history, especially gravity-driven mass flows, gravity cores with non-steady state sulfate pore water profiles (concave, kink-, and s-type) were investigated. In this study, we present geochemical, magnetic and mineralogical data for three sediment cores from the continental margin off Argentina and Uruguay. These coring sites are characterized by a rather homogenous recent sedimentation and linear sulfate pore water profiles. We investigate the influence of depositional settings and AOM on the diagenetic overprint of iron (oxyhydr)oxides and the resulting change in the magnetic record and we present results of numerical modeling of the processes involved.

2. MATERIALS AND METHODS

2.1. Location and Geological Settings

The study area is located in the western South Atlantic on the continental margin off Argentina and Uruguay (Fig. 1). The investigated gravity cores (Table 1) were taken during expeditions M46/2 and M46/3 of the RV *Meteor* (Bleil et al., 2001; Schulz et al., 2001). The gravity cores were retrieved east of the Rio de la Plata at the western boundary of the Argentine Basin. Sedimentation in this area is controlled by two main processes: gravity-controlled sediment transport and strong current circulation (Ewing and Leonardi, 1971; Klaus and Ledbetter, 1988). Terrigenous input originates from the numerous fluvial tributaries along the coast of Argentina and Uruguay (Iriondo, 1984; Piccolo and Perillo, 1999). The sediments are transported directly down-slope along the western margin of the Argentine Basin by gravity-controlled processes (Ewing et al., 1971; Biscay and Dasch, 1971; Klaus and Ledbetter, 1988; Sachs and Ellwood, 1988; Romero and Hensen, 2002; Hensen et al., 2003). These gravity-driven mass transports, such as debris flows and turbidity currents, are the main pathways of sediment supply into the deeper basin.

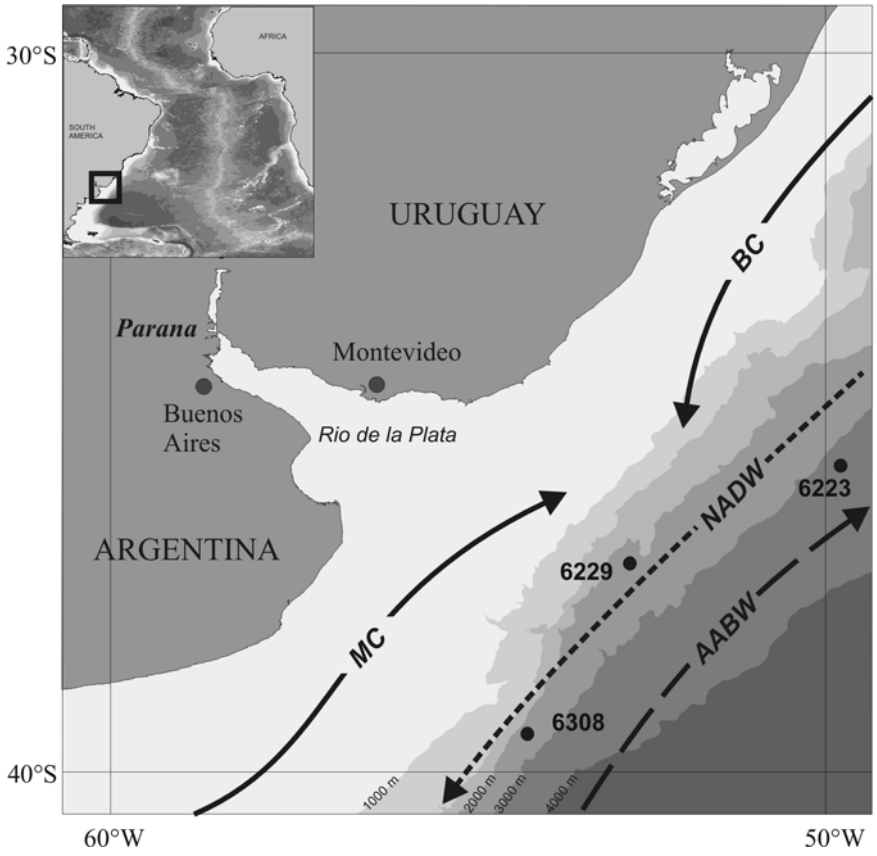

Fig. 1. Location map of the study area offshore of the Rio de la Plata. Arrows indicate simplified pathways of the main currents (solid line presents the surface water currents MC (Malvinas Current) and BC (Brazil Current), while the lower level and bottom water currents are marked by dashed lines with NADW=North Atlantic Depth Water and AABW=Antarctic Bottom Water).

The second important process controlling sedimentation in this area is the strong currents along the continental margin. The currents in the upper water column are the southward flowing Brazil Current and the northward flowing Malvinas (Falkland) Current (Peterson and Stramma, 1991). These two currents meet in the Brazil Malvinas Confluence (BMC), located in front of the Rio de la Plata. The confluence of the two different water masses leads to an increase in primary production over a large area (Antoine et al., 1996; Behrenfeld and Falkowski, 1997), which results in relatively high inputs of organic carbon into the sediment.

Table 1. Studied gravity cores with the location and water depth.

Station	Longitude [W]	Latitude [S]	Water Depth [m]	Core Length [m]
GeoB 6223-6	49°40.86’	35°44.42’	4280	8.67
GeoB 6223-5[a]	49°40.86’	35°44.43’	4280	8.15
GeoB 6229-6	52°39.00’	37°12.41’	3446	9.50
GeoB 6308-4	53°08.70’	39°10.00’	3620	11.66

[a] Core GeoB 6223-5 is the parallel core at site GeoB 6223 subjected to magnetic analysis.

The suspended load of the Rio de la Plata is carried by northerly currents and thus forms a tongue of fine-grained sediment which is deposited parallel to the shore line off the coast of Uruguay (Ewing and Lonardo, 1971; Ledbetter and Klaus, 1987; Frenz et al., 2003). Between depths of 2000 and 4000 m, the water column is governed by the southward-flowing North Atlantic Deep Water (NADW). Below 4000 m, the strong currents carry Antarctic Bottom Water (AABW) to the north. These currents flow parallel to the continental margin supplying benthic diatoms from higher latitudes (Romero and Hensen, 2002). The AABW dominates the transport of predominantly fine-grained sediment below 4000 m water depth. The currents winnow and entrain sediments deposited by gravity-controlled mass flows, and the fine material is transported into the deep basin (Groot et al., 1967; Ewing et al., 1971; Ledbetter and Klaus, 1987; Sachs and Ellwood, 1988).

The composition of the sediments in the study area is characterized by low calcium carbonate concentrations, but with relatively high amounts of organic carbon, biogenic opal and iron (oxyhydr)oxides. Due to the sediment composition and the highly dynamic sedimentary conditions, few to no reliable stratigraphic information for this region exists (Romero and Hensen, 2002; Hensen et al., 2003).

2.2. Sampling

To prevent warming of the sediments after retrieval on board, all core segments were immediately placed in a cooling laboratory and were maintained at a temperature of about 4°C. Gravity cores were cut into 1-m segments on deck, and syringe samples were taken from the bottom of every segment for methane analysis. Higher resolution sampling for methane was carried out in the cooling room by sawing 4x4 cm rectangles into the PVC liner. Syringe samples of 5 ml of sediment were taken every 20 to 25 cm. For hydrogen sulfide analyses at higher concentrations, 1 mL sub-samples of the pore water were added to a ZnAc-solution in order to fix all hydrogen sulfide present as ZnS (see also Hensen et al., 2003).

Within the first two days after recovery, gravity cores were cut lengthwise into two halves and processed within a glove box under argon atmosphere. Conductivity and temperature were measured on the archive halves. On the working halves, pH and Eh were determined by punch-in electrodes and sediment samples were taken every 25 cm for pressure filtration. Solid phase samples for total digestions, sequential extractions and mineralogical analyses were taken at 10-cm intervals and kept in gas-tight glass bottles under argon atmosphere. The storage temperature for all sediments was -20°C to avoid dissimilatory oxidation of reduced species. Teflon squeezers were used for pressure filtration. The squeezers were operated with argon at a pressure that was gradually increased up to 5 bar. The pore water was retrieved through 0.2 µm cellulose acetate membrane filters.

2.3. Pore Water Analysis

The parameters hydrogen sulfide, sulfate, alkalinity, phosphate, and iron (Fe^{2+}) were determined by standard methods, as described in detail by Schulz (2000), within a few hours after retrieval of the pore water. All further analyses were carried out at the University of Bremen. Methane was measured with a gas chromatograph (Varian 3400) equipped with a splitless injector, by injecting 20 µL of the headspace gas. The concentrations were subsequently corrected for sediment porosity. Aliquots of the remaining pore water were diluted and acidified with HNO_3 for determination of cations using atomic absorption spectrometry (AAS, Unicam Solaar 989 QZ) and inductively coupled plasma atomic emission spectrometry (ICP-AES) techniques (Perkin Elmer Optima 3000 RL). For further information regarding analytical methods and devices, we refer to the homepage of the geochemistry group under http://www.geochemie.uni-bremen.de at the University of Bremen.

2.4. Solid Phase Analysis

All solid phase analyses were performed on anoxic subsamples. For total digestion, the samples were freeze-dried and homogenized in an agate mortar. About 50 mg of the sediment was digested in a microwave system (MLS – MEGA II and MLS – ETHOS 1600) and was treated with a mixture of 3 mL HNO_3, 2 mL HF, and 2 mL HCl. Dissolution of the sediments was performed at 200°C at a pressure of 30 bar. The solution was fully evaporated, redissolved with 0.5 mL HNO_3 and 4.5 mL deionized water (MilliQ) and homogenized. Finally, the solution was filled up to 50 mL with MilliQ. Major and minor elements were measured by ICP-AES. The accuracy of the measurements was verified using standard reference material USGS-MAG-1. The reference material element concentrations were within certified ranges. The precision of ICP-AES analyses was better than 3%.

The concentrations of reactive Fe phases were determined following the method described by Haese et al. (2000). In the first step, 150-250 mg of the wet sample was treated with 20 mL of an ascorbate solution (a weak reducing agent) containing sodium citrate, sodium carbonate, and ascorbate acid and extracted over 24 hours. In the second step, the ascorbate residuum was treated with 20 mL of a dithionite solution consisting of acetic acid, sodium citrate, and sodium dithionite and kept in suspension for one hour. The extractions of ascorbate and dithionite were diluted 1:10 and measured by ICP-AES. Standards were prepared using the corresponding matrix.

For the determination of inorganic carbon (IC) and total organic carbon (TOC) contents, freeze-dried and homogenized samples of cores GeoB 6229-6 and GeoB 6308-4 were measured using a LECO CS-300 carbon sulfur analyzer. For organic carbon, the samples were treated with 12.5% HCl, washed two times with MilliQ and dried at 60°C. The accuracy, checked by marble standards, was ± 3%. The samples of core GeoB 6223-6 were measured using a Shimadzu TOC with SSM 5000A carbon analyzer. Inorganic carbon was measured by

adding 35% phosphoric acid to the sample and heating up to 250°C. The accuracy is ± 3%, and the limit of detection is below 0.05% for a 100 mg sample.

The data set of pore water and solid phase measurements is available via the geological data network Pangaea (http://www.pangaea.de/PangaVista?query=@Ref26445).

2.5. Mineral Analysis

Mineral identification was carried out by X-ray diffraction (XRD), which was performed at a few selected depths of core GeoB 6229-6 (75, 375, 545, 675, and 725 cm) using Philips X´Change (Cu-tube) with fixed divergence slit. The measurement was carried out with a first angle of 3° 2Θ and a last angle of 100° 2Θ. The step size was 0.02° 2Θ, with measurement time of 12 s/step. Samples from core GeoB 6223-6 (255, 525, 655 cm) and core GeoB 6308-4 (555 and 655 cm) were measured using an X'Pert Pro MD, X'Celerator detector system, with a step size of 0.033° 2Θ, and the calculated time per step was 219.7 seconds. Quantification of the mineral content was carried out with QUAX (for further information see Vogt et al., 2002). Scanning electron microscope (SEM) analysis was performed on selected samples.

2.6. Magnetic Susceptibility Measurement

The magnetic susceptibility data for site GeoB 6223 were obtained on the parallel core GeoB 6223-5 on board the RV *Meteor*. Determination of susceptibility on the archive halves of the gravity cores GeoB 6229-6 and GeoB 6308-4 took place at the University of Bremen. The susceptibility measurements were performed using a non-magnetic automated core conveyor system equipped with a commercial Bartington Instruments MS2 susceptibility meter with an F- type spot sensor. The measurement interval was 2 cm and 1 cm, respectively.

2.7. Geochemical Modeling

AOM and the associated diagenetic processes were simulated with the non-steady state transport and reaction model CoTReM. A detailed description of this computer software is given in the CoTReM User's Guide (Adler et al., 2000; http://www.geochemie.uni-bremen.de/downloads/cotrem/index.htm) and by Adler et al. (2001). The upper 20 m of the sediment (model area) was subdivided into cells of 5 cm thickness. The time-step to fulfill numerical stability was set to 10^{-1} yr, and the porosity of the sediment was set to 75%. Transport mechanisms were molecular diffusion (D_s) for all solutes in the pore water and the sedimentation rate (SR) for the solid phase and pore water. Diffusion coefficients were corrected for tortuosity (Boudreau, 1997) using a temperature of 2°C. The bottom water concentration of species defines the upper boundary condition. The lower boundary is defined as an open/transmissive boundary which means that the gradient of the last two cells is extrapolated to allow diffusion across the boundary. For methane, a fixed concentration was defined at the lower boundary which creates the gradient necessary to simulate the measured influx of methane into the model area from below. For geochemical reactions, 0^{th} order

kinetics were used by defining maximum reaction rates. These rates are used as long as the educt species are available in sufficient amounts. If the amount decreases, the rates were automatically reduced to the available amount of reactants in each cell to avoid negative concentrations (for further details see Hensen et al., 2003). All input parameters are given in the respective section below.

3. RESULTS AND DISCUSSION

3.1. Sediment Composition

Sediment composition and grain size are two important parameters that affect diagenetic processes (Roberts and Turner, 1993). These attributes vary in all three cores. While the sediment of cores GeoB 6229 and GeoB 6308 is quite variable in grain size, the sediment in core GeoB 6223-6 is rather fine-grained, as identified macroscopically and by SEM. At all sites, the composition of the sediment is dominated by lithogenic components, as indicated by the major mineral assemblages of selected samples from all three cores (20-28 wt% quartz, 18-35 wt% feldspar and 23-44 wt% phyllosilicates). The lowest amounts of phyllosilicates were found at site GeoB 6308. Additionally, solid phase concentrations of Al and Ti indicate a high terrigenous input (Fig. 2).

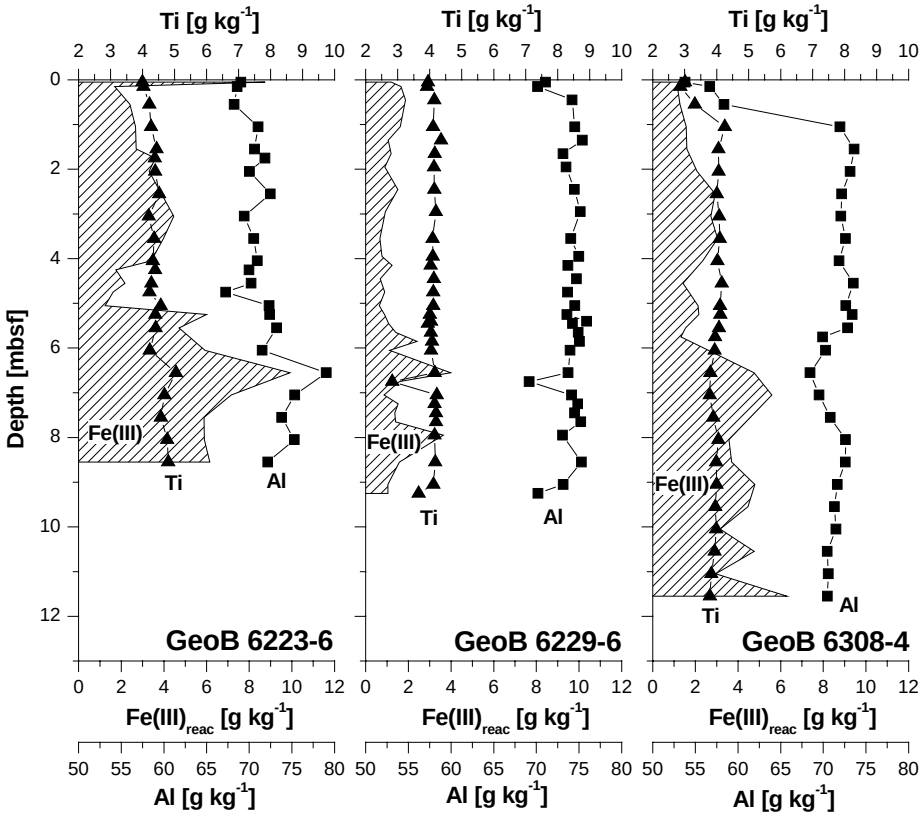

Fig. 2. Solid phase data for Al (solid squares) and Ti (solid triangles) indicating the dominance of terrigenous input. The cross-hatched area indicates the amount of reactive Fe(III) phases.

Total concentrations of Al and Ti positively correlate in sediments of the southernmost site GeoB 6308-4 (R^2=0.93), which is not the case for the other two sites (GeoB 6229-6: R^2=0.60 and GeoB 6223-6: R^2=0.75). We attribute this finding to variable depositional processes. The comparatively high content of glauconite (3-17 wt%) detected by XRD in the sediment from all three cores gives evidence for mass flow deposition events. In general, glauconite in recent sediment is an indicator of slow rates of clastic deposition in shallow marine environments (Odin and Matter, 1981; Harris and Whiting, 2000). The presence of this mineral at all three sites suggests erosion of near shore/shelf sediments and redeposition at greater water depths on the continental slope. A further characteristic component of the sediments of this area is the relatively high amount (up to 1 wt%) of reactive iron (oxyhydr)oxides (Fig. 2).

All three cores display a distinct change in sediment composition in the uppermost section. Total organic carbon (TOC) reaches values of up to 1.1 wt% close to the sediment surface, while the mean content for the deeper sediment is about 0.7 wt% (Fig. 3). Correspondingly, calcium carbonate also has the highest overall concentrations in the uppermost sediments.

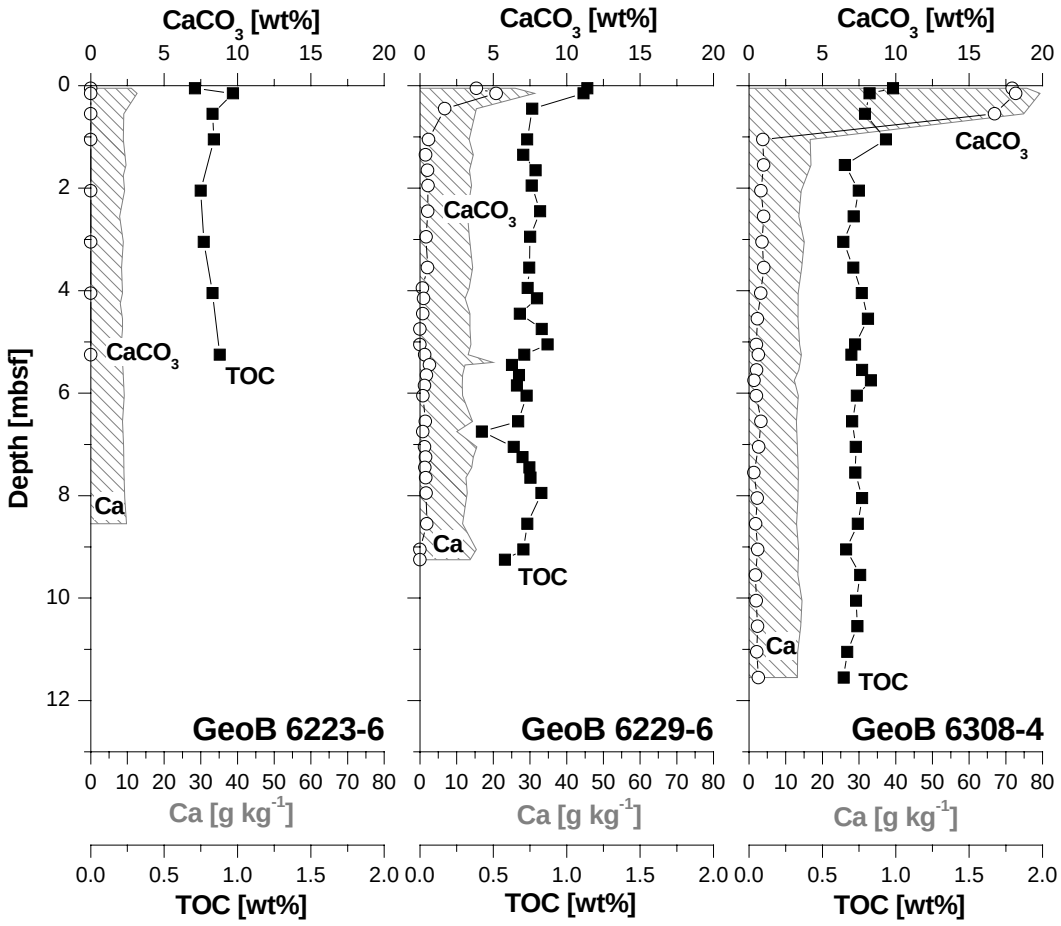

Fig. 3. Solid phase concentrations of total Ca (cross-hatched area), calcium carbonate (open circles), and total organic carbon (TOC, solid squares). The TOC in the upper layer of core GeoB 6308-4 is diluted by the higher amount of $CaCO_3$. There is no measurable carbonate in the sediment of core GeoB 6223-6, but there is a higher organic carbon content in the uppermost centimeters before it decreases toward the sediment surface.

The calcium carbonate contents are generally low and are well correlated with the total concentration of calcium obtained from acid digestion. The lack of carbonate in the deepest core GeoB 6223-6 can be due to the depositional system, e.g., dilution by terrigenous input, or because of its depth lying below the lysocline resulting in dissolution of carbonate (Archer, 1996; Frenz et al., 2003). At site GeoB 6229, $CaCO_3$ concentrations of up to 5 wt% were determined, and, at the southernmost site GeoB 6308, high $CaCO_3$ contents of up to 18 wt% are found in the uppermost layer (Fig. 3). A similar transition from terrigenous dominated to carbonate enriched sediments in the upper sediment layers is also found in sediments of the Amazon Fan (e.g. core GeoB 1514-6 of Kasten et al., 1998). In these sediments, a sedimentation change is found at about 60 cm, with $CaCO_3$ gradually increasing upward. While the glacial sedimentation rate (SR) for the Amazon Fan area amounts to a few meters per kyr (Flood et al., 1995), stratigraphic data for the upper 35 cm at site GeoB 1514 indicate a Holocene age with a SR of 3.5 cm kyr^{-1} (Schneider et al., 1991). A similar transition from terrigenous dominated to more calcareous sediments in the upper sediment layers for the investigated sites would suggest a Holocene SR of about 3 to 7 cm kyr^{-1}. This is in good agreement with unpublished stratigraphic data by O. Romero (pers. comm.) from Argentine Basin sites (e.g. GeoB 6340 at 44°54,95'S, 58°05,78'W, water depth 2785 m), which reveal a SR of a few cm per kyr in the Holocene. Although the mean SR in the investigated area is not the same as for the Amazon Fan, similar patterns in sediment composition are consistent with a comparable decrease in mean SR during the glacial/interglacial transition.

3.2. Diagenetic Alteration

The sulfate pore water profiles for all three studied cores show a linear decrease with depth, which indicates a currently steady state situation (Fig. 4). The SMT is located between 5 and 5.5 mbsf (meters below seafloor) in each case. In cores GeoB 6229-6 and GeoB 6308-4, excess hydrogen sulfide could be detected at depths of 4-7 and 4-6 mbsf, respectively. The sulfidic sediment intervals are characterized by distinct minima in magnetic susceptibility (Fig. 4). Based on the pore water data, we suggest that the characteristic decrease in magnetic susceptibility (κ), which is a widespread phenomenon in sediments of the continental margin off Argentina and Uruguay, is caused by diagenetic processes within the zone of AOM. Except for the decrease in magnetic susceptibility in the uppermost centimeters of core GeoB 6308-4, which is due to dilution by $CaCO_3$, we attribute the decrease in magnetic susceptibility to the reduction of iron (oxyhydr)oxides by hydrogen sulfide and subsequent formation of iron sulfides as described by Karlin and Levi (1983) and Channell and Hawthorne (1990).

Because of the current relatively high fluxes of methane and sulfate into the SMT at all three sites (Fig. 4), we suggest that deep sulfate reduction is primarily driven by AOM (Niewöhner et al., 1998). Thus, hydrogen sulfide is produced by a reaction of sulfate and methane (e.g. Barnes and Goldberg, 1976):

$$CH_4 + SO_4^{2-} \rightarrow HCO_3^- + H_2O + HS^-. \qquad (1)$$

The species distribution of hydrogen sulfide is pH dependent (Pyzik and Sommer, 1981). Based on the measured pH values (7.2 to 8.0), we conclude that HS^- is the predominant hydrogen sulfide species in the sediment of the studied cores.

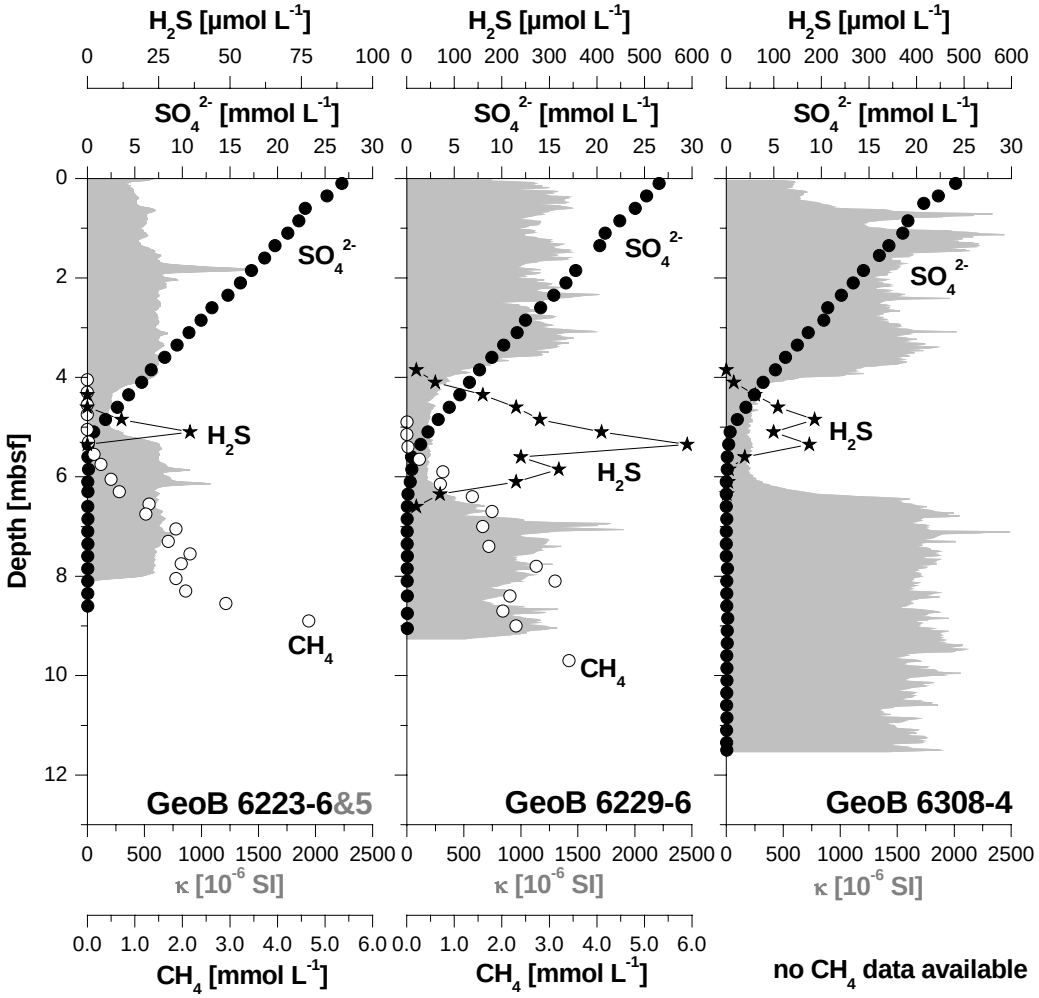

Fig. 4. Sulfate (solid circles), methane (open circles) and sulfide (solid stars) pore water profiles (pore water data for methane, sulfate and sulfide for core GeoB 6223-6 and sulfate for core GeoB 6229-6 are taken from Hensen et al., 2003) and the magnetic susceptibility (gray area) (note that the offset for data from core GeoB 6223-5 is probably due to the measurements coming from a parallel core). Except for the decrease in magnetic susceptibility at the top of the core GeoB 6308-4, due to the dilution by higher carbonate concentrations, the decrease in susceptibility is restricted to the sulfidic zone.

The concentration of measured reactive iron (oxyhydr)oxides for cores GeoB 6223-6 and GeoB 6308-4 is low (Fig. 2) in the interval where magnetic susceptibility data show a minimum (Fig. 4). In this zone, the iron (oxyhydr)oxides are almost completely reduced and only relict concentrations are left. For the process of iron (oxyhydr)oxide reduction, the assumed reactions for lepidocrocite (Eq. 2) (as an example for iron (oxyhydr)oxides) and for magnetite (Eq. 3) are:

$$2FeOOH + HS^- + 5H^+ \rightarrow 2Fe^{2+} + S^0 + 4H_2O \quad (2)$$

$$Fe_3O_4 + HS^- + 7H^+ \rightarrow 3Fe^{2+} + S^0 + 4H_2O. \quad (3)$$

The available dissolved ferrous iron reacts directly with HS^- (Berner, 1970; Pyzik and Sommer, 1981) according to the following equation:

$$Fe^{2+} + HS^- \rightarrow FeS_{(s)} + H^+. \quad (4)$$

The precipitated amorphous iron sulfide is highly unstable and transforms rapidly to other iron sulfide phases (Schoonen and Barnes, 1991). Morse (2002) discussed that the oxidation of FeS by hydrogen sulfide (Eq. 5) is the faster process compared to the oxidation by elemental sulfur as discussed by Berner (1970). In addition, Rickard (1997) pointed out that pyrite formation through oxidation by HS^- is thermodynamically favored:

$$FeS_{(s)} + HS^-_{(aq)} + H^+_{(aq)} \rightarrow FeS_{2(s)} + H_{2(g)} \quad (5)$$

In contrast to the intermediate iron sulfides, pyrrhotite ($Fe_{x-1}S$) and greigite (Fe_3S_4), the iron disulfide pyrite is paramagnetic and therefore has a low magnetic susceptibility and does not contribute to the remanent magnetization of a sediment. As both pyrite and marcasite are paramagnetic, we term all iron disulfides as pyrite for simplicity. Thus, the dissolution of magnetite and the precipitation of pyrite would cause a strong decrease in magnetic susceptibility. Such a decrease of the magnetic signal can be observed in the susceptibility (κ) at all three sites (Fig. 4).

3.3. Magnetic Susceptibility Profiles

We have explained the mechanisms of alteration of iron (oxyhydr)oxides to iron sulfides within the zone of AOM, but we still have to explain the occurrence of iron (oxyhydr)oxides below the SMT. We assume that there are only a few possible processes that can cause a decrease of iron (oxyhydr)oxides that is limited to the zone of AOM and that leads to a localized minimum in magnetic susceptibility.

One process would be the reoxidation of ferrous iron below the sulfidic zone. The oxidation could be driven by Mn(II) released during reduction of Mn-oxides (Aller and Rude, 1988; Postma and Appelo, 2000; Schippers and Jørgensen, 2002). This process could explain the existence of iron (oxyhydr)oxides below the SMT where no hydrogen sulfide is present. Detailed rock magnetic and scanning electron microscope (SEM) analyses performed on magnetic minerals of samples from core GeoB 6229-6 by Garming et al. (in press) reveal that the magnetic mineral assemblages above and below the zone of AOM are similar and that the authigenic formation of iron oxides can therefore be excluded.

Another process that could potentially cause a distinct loss in magnetic susceptibility in the zone of AOM is a variation in the parameters controlling the position of the SMT. The depth at which the SMT is established is driven mainly by the upward flux of methane and the downward diffusion of sulfate, which is directly influenced by the SR. We simulated different scenarios with the numerical model CoTReM, to investigate whether a constant mean SR alone can lead to the observed profiles of magnetic susceptibility. Under steady state conditions prevailing over a long period of time, with continuous sedimentation and no change in the upward flux of methane, the zone of AOM would keep a fixed offset with respect to the sediment surface (Borowski et al., 1996; Kasten et al., 2003). This process would lead to a continuous reduction of iron (oxyhydr)oxides within the SMT and below. The degree of reduction to which every sediment layer is subject would thereby be coupled to the rate at which the zone of AOM moves upward as a function of SR. The dissolution rate is dependent on the reactivity of the iron (oxyhydr)oxides and their grain size, and the time period over which they are in contact with hydrogen sulfide (Pyzik and Sommer, 1981; Karlin and Levi, 1983, 1985; Canfield and Berner, 1987; Canfield, 1992; Roberts and Turner, 1993).

Hensen et al. (2003) give a detailed description for reaction kinetics of hydrogen sulfide with a continuum of different Fe(III)-phases. The reaction rates are sensitive to dissolved Fe and HS^- in the model approach because HS^- is involved in two reactions (Eq. 3 and 4). For simplicity, we consider only magnetite (Fe_3O_4) and adapt a maximum reaction rate of 3×10^{-5} mol L^{-1} yr^{-1} to account for the measured hydrogen sulfide concentration compared to rates of between 5.5×10^{-6} mol L^{-1} yr^{-1} and 1.2×10^{-4} mol L^{-1} yr^{-1} in Hensen et al. (2003). The initial concentration of Fe_3O_4 is set to 1 wt%, which is reduced to iron monosulfide (FeS) in the sulfidic zone. A compilation of input parameters for all simulation runs is given in Table 2, where the lower boundary is defined at a model depth of 20 m (while the figures are only displayed to a depth of 13 m).

Table 2. Parameters used in modeling of magnetic susceptibility profiles for different sedimentation rates.

Parameters		
Model area[a]:	20 m	
Cell discretization:	5 cm	
Time step:	1×10^{-1} yr	
Sediment porosity:	75%	
Temperature:	2°C	
Input concentration		
Magnetite (Fe_3O_4):	1 wt%	
	Upper boundary	Lower boundary
Sulfate (SO_4^{2-}):	26 mmol L^{-1}	0 mmol L^{-1}
Methane (CH_4):	0 mmol L^{-1}	45 mmol L^{-1}

[a] **The model area is the sediment column incorporated in the approach.**

During simulation of a relatively low mean SR of 5 cm kyr^{-1} (Fig. 5a), the SMT moves slowly upward resulting in the complete transformation of the initially present magnetite into iron sulfides (Fig. 5b).

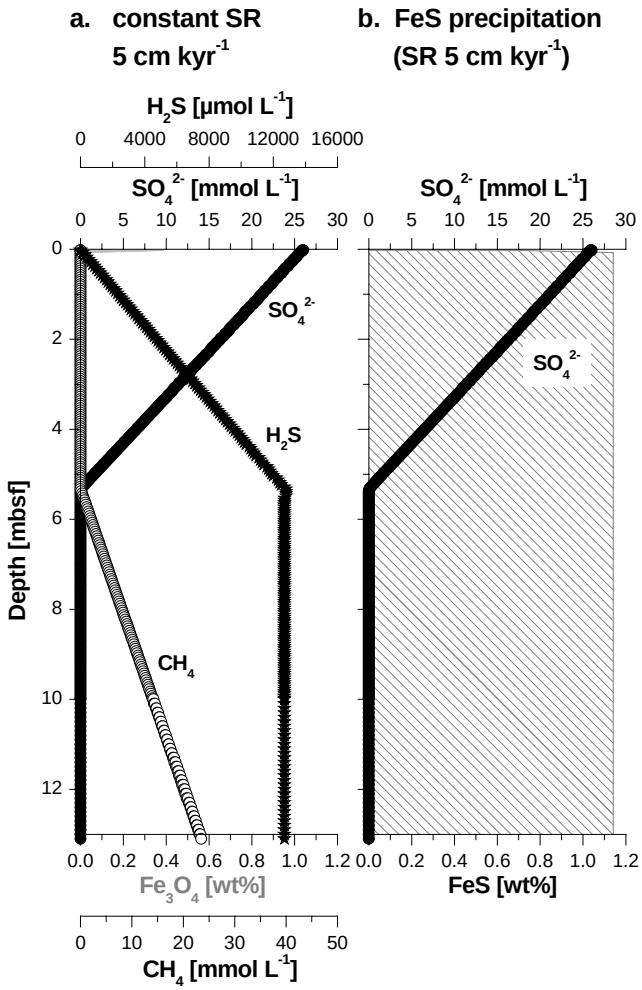

Fig. 5. Modeling results for diagenetic alteration of magnetite to iron monosulfide. a. Sulfate, methane and sulfide profiles at a constant mean SR of 5 cm kyr^{-1}. b. All iron (oxyhydr)oxides are altered into iron monosulfides.

In contrast, more rapid sedimentation can lead to the preservation of a considerable amount of magnetic iron oxides and therefore to a preservation of the magnetic record, as also discussed by Canfield and Berner (1987). Model runs with a high mean SR of 200 cm kyr^{-1} result in fast burial of magnetite (Fig. 6a), with reduction of only a small amount (about 1/5) of Fe_3O_4 (Fig. 6b). These model runs demonstrate that the observed patterns cannot be formed under conditions of constant mean SR.

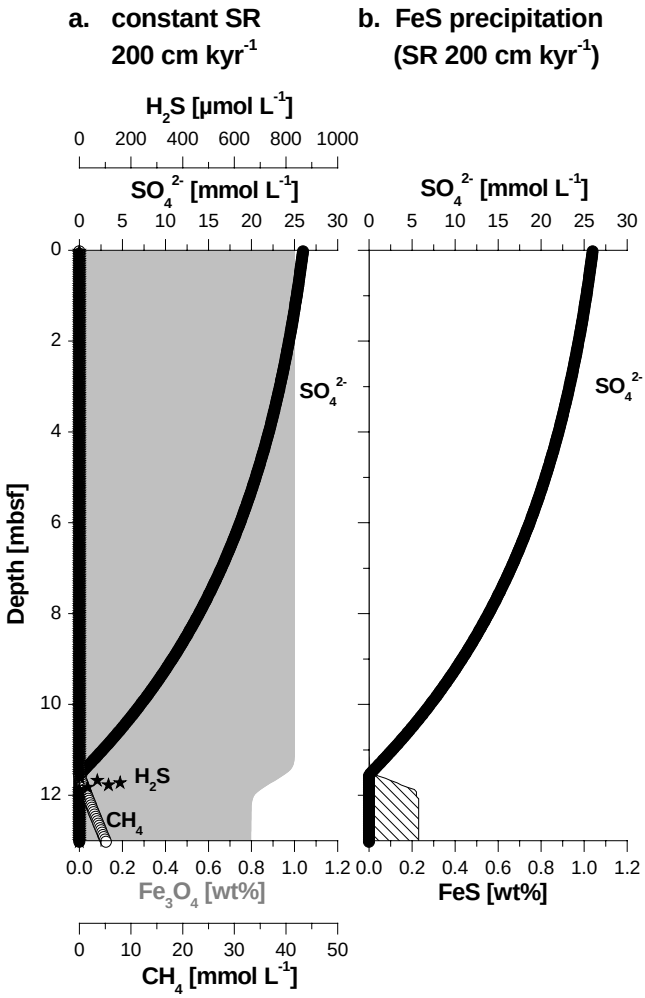

Fig. 6. Model results for a constant mean SR of 200 cm kyr^{-1}. a. The high mean SR leads to good preservation of magnetite below the SMT. The pore water profile for sulfate shows a concave-up shape. b. Only a small amount of iron sulfide is precipitated in this scenario.

Different scenarios were modeled to assess the influence of variations in depositional and/or geochemical conditions on the position of the SMT. A sudden increase in the upward methane flux would push up the SMT and result in a concave-up sulfate pore water profile (Hensen et al., 2003; Kasten et al., 2003). At a constant high mean SR, this concave-up profile would remain and the observed linear sulfate profile would not be seen. At low mean SR, the SMT would move rapidly upward due to the increased methane flux until a new steady state with a linear sulfate pore water profile is regained. But, as shown in the simulation of constant mean SR (Fig. 5a), at a low mean SR all available reactive iron (oxyhydr)oxide would be altered and thus the increased methane flux would not produce the observed localized magnetic susceptibility minimum.

After demonstrating that variations in the upward methane flux alone cannot produce the observed patterns, we simulated the effect of changing mean SR. Kasten et al. (1998) demonstrated that the strong decrease in SR for Amazon Fan sediments as a consequence of

the glacial/interglacial transition was responsible for the fixation of the SMT for a prolonged period of time. To test whether the observed profiles of magnetic susceptibility could be explained by a drastic decrease in mean SR, we modeled scenarios of different mean SR with a constant methane flux over time. The history of sedimentary events for the three studied sites are not known in detail. We therefore assume, as the starting condition for the model, a high mean SR of 100 cm kyr^{-1} (Fig. 7a). This mean SR includes all possible mechanisms of sediment deposition. This mean SR is sufficiently high to limit the contact time between the iron oxides and the sulfidic pore water, and thus to alter only one third of the initially present iron into iron sulfides. With a subsequent decrease in the rate of sedimentation to about 5 cm kyr^{-1}, estimated from $CaCO_3$ concentrations in the solid phase (see section 3.1), the SMT moves upward until a steady state is regained (Fig. 7b). In this scenario, there is a complete transformation of all available iron oxides to iron monosulfides in the SMT and subsequently in the expending zone of excess hydrogen sulfide (Fig. 7c).

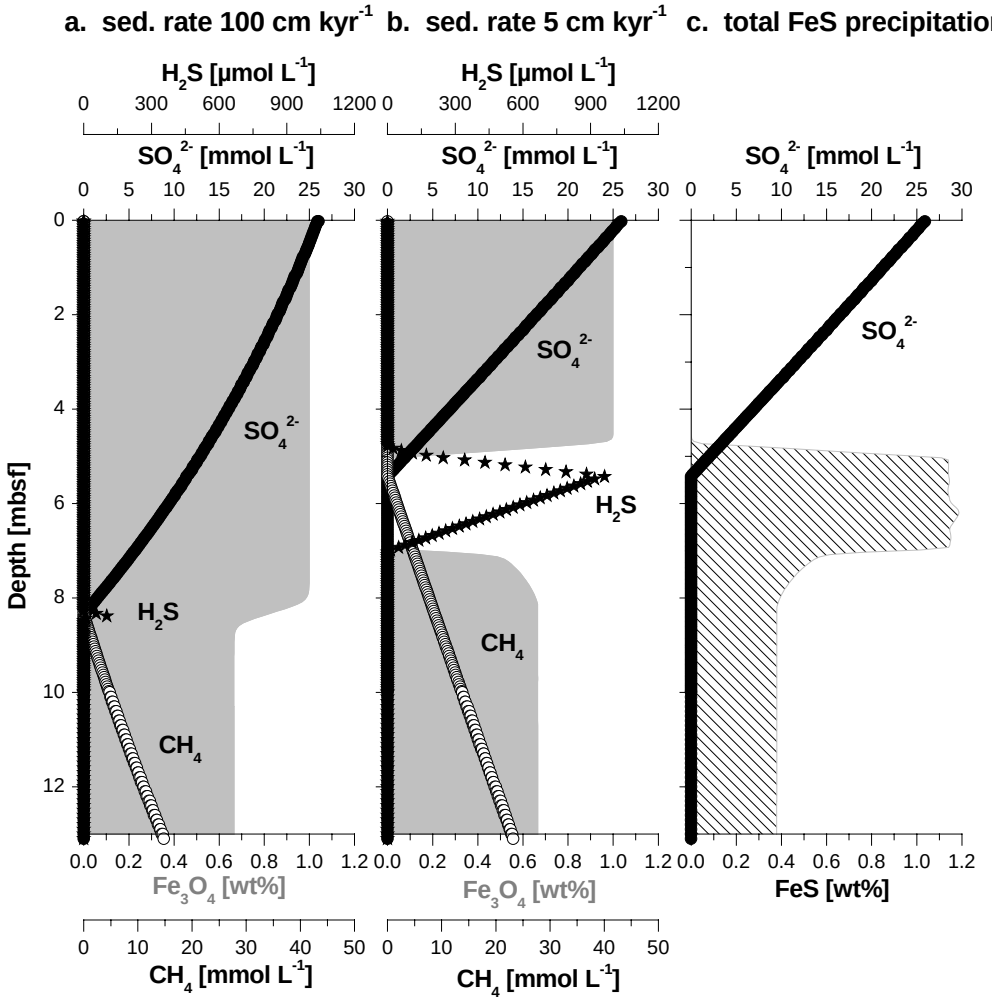

Fig. 7. Modeling results for diagenetic alteration of magnetite to iron monosulfide with a major change of mean SR (for sediment porosity of 75%). a. A mean SR of 100 cm kyr^{-1} leads to reduction of only about one third of the Fe_3O_4. b. If the mean SR is decreased to 5 cm kyr^{-1}, a time interval of approximately 8000 years is needed to reduce the total amount of magnetite for an interval of 2 m thickness. c. The cross-hatched area indicates the total amount of precipitated monosulfides for the modeled scenario with change in mean SR.

Although the results of our approach are strongly dependent on the boundary parameters, the estimation correlates well with a change in mean SR at the glacial/interglacial transition. This process causes a pronounced loss in magnetic susceptibility in a particular sediment interval. The time needed for the complete conversion of magnetite into iron sulfides in an interval of 2 m (e.g. GeoB 6308-4) is about 8000 years.

A further interesting finding of the simulation is the concave-up sulfate profile at high constant mean SR. This shape of the sulfate profile has previously been described for non-steady state conditions such as an increased methane flux (Kasten et al., 2003), upward-directed advective flow (e.g. Aloisi et al., 2004) or by transient diagenesis after a sedimentary event has occurred (Hensen et al., 2003). An example of a transient event is a single submarine slide event, which results in a kink-type profile (de Lange, 1983; Zabel and Schulz, 2001) that is smoothed to a concave-up and finally a linear profile by diffusion. As shown by our model outcome, the concave-up sulfate profile can also result from high mean SR under steady state conditions. This could be explained by the high sulfate accumulation compared to the diffusion flux of sulfate.

3.4. Solid Phase Enrichment of Iron and Sulfur

For core GeoB 6308-4, the solid phase profiles of total iron and sulfur (Fig. 8) indicate an enrichment of iron sulfides between 6 and 7 mbsf. Similar solid phase peaks of total iron and sulfur are found at site GeoB 6223, where XRD analyses of the sample taken at 525 cm prove the presence of pyrite (2.5 wt%). The accumulation of authigenic iron sulfides within this distinct interval could be explained by diffusion of ferrous iron from below reacting with hydrogen sulfide (e.g. Kasten et al., 1998). At site GeoB 6223, ferrous iron is detected in pore water directly below the solid phase iron enrichment (Fig. 8). Another explanation for the enrichment of iron in the solid phase could be in consequence of an initial enrichment of iron (oxyhydr)oxides at this particular layer due to a sedimentary event. The iron (oxyhydr)oxides will be reduced and the ferrous iron can be transformed directly into iron sulfide. As the enrichment of total iron and sulfur in core GeoB 6308-4 is located below the distinct susceptibility minimum, we suggest that the reduction of the magnetic minerals ((titano-)magnetite) has not yet taken place and that only the more reactive iron phases have been reduced.

Under the premise of a decrease in mean SR, and hence a fixation of the zone of AOM for a specific length of time, we calculated the time needed to produce the total amount of solid phase sulfur in the sediments of site GeoB 6223 at 525 cm and at site GeoB 6308 at 625 cm. The calculation is described in detail by Kasten et al. (1998). We simulated the enrichment of solid phase sulfur by downward diffusion of sulfate, assuming that the sulfur contained in the solid phase was fixed due to the precipitation of iron sulfide as a result of hydrogen sulfide liberated by AOM.

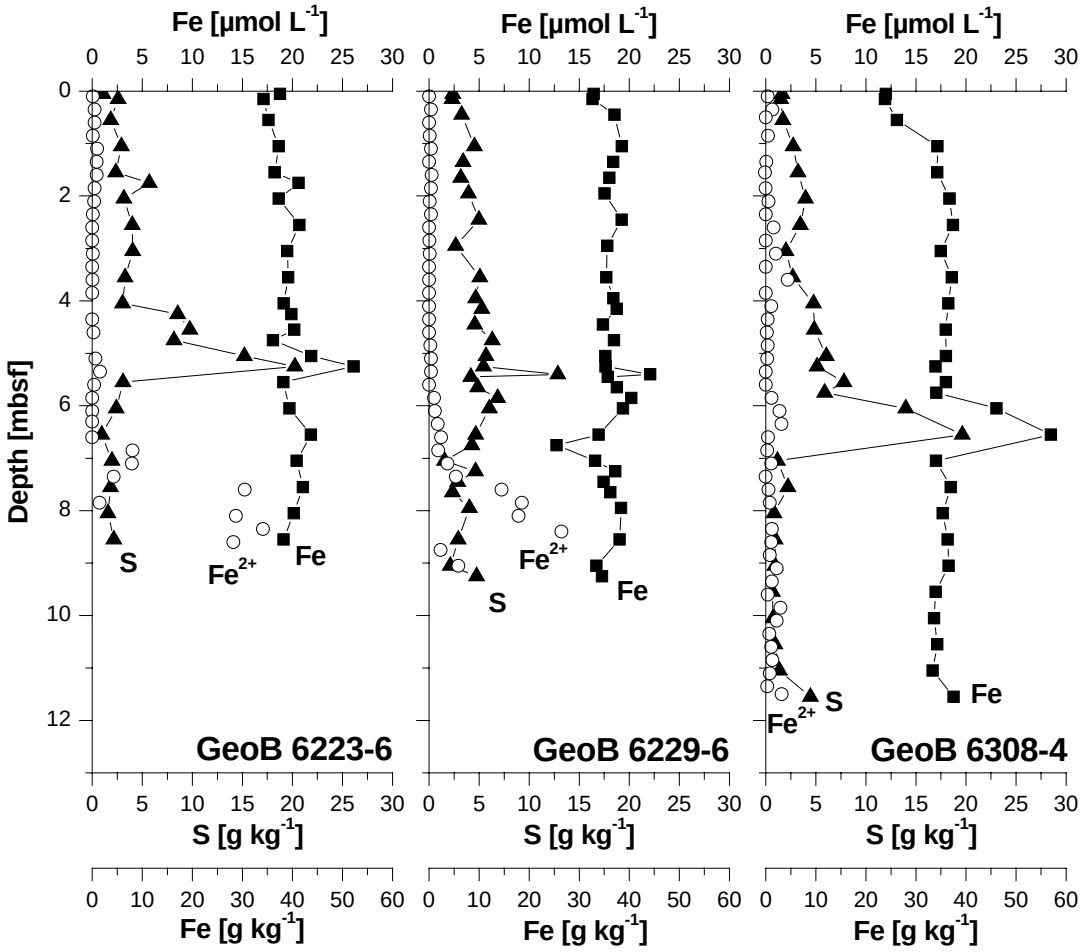

Fig. 8. Total sulfur (solid triangles) and total iron (solid squares) concentrations of the solid phase. Correlation of the iron and sulfur peak at sites GeoB 6223 and GeoB 6308 indicates an iron sulfide enrichment. The iron minimum in the sediment of core GeoB 6229-6 correlates with a turbidite sequence. Open circles indicate ferrous iron pore water concentrations.

Assuming a linear sulfate pore water profile over the whole time of iron sulfide formation, the flux of pore water sulfate is calculated using Fick's first law, with a diffusion coefficient in free solution (D_0) for sulfate of 165 cm^2 yr^{-1} (after Iversen and Jørgensen, 1993). The sediment dry density averages 2.2 g cm^{-3}, and the temperature is 2°C. The presumed mean Holocene SR amounts to 5.0 cm kyr^{-1}. If we assume a porosity of 70% for the sediment of core GeoB 6223-6 and 75% for core GeoB 6308-4, the time needed to produce the measured sulfur peak would be about 9000 years. This calculated result is in good agreement with the outcome of the model above. Based on the model results, we suggest that the only scenario that produces the observed localized loss in magnetic susceptibility is a non-steady state diagenetic scenario involving a drastic decrease in mean SR, from a few hundred cm to about 5 cm per 1000 years, during the Pleistocene/Holocene transition leading to a fixation of the SMT for a period of 8000 to 9000 years.

4. CONCLUSIONS

A marked localized minimum in magnetic susceptibility in distinct sediment intervals of Argentine Basin deposits is observed, which correlates with the current position of the SMT. To explain the diagenetic impact of AOM on magnetic susceptibility, we modeled different geochemical and depositional scenarios. The model results indicate that the depletion of iron (oxyhydr)oxides and the resulting strong decrease in magnetic susceptibility within the sulfidic zone around the current depth of the SMT is an effect of the rather low and constant mean SR since the beginning of the Holocene, compared to the high mean SR of one to several meters per kyr during the last Glacial. The drastic change in mean SR results in a fixed or slow moving SMT, which increases the time of contact between iron (oxyhydr)oxides and the liberated hydrogen sulfide, leading to enhanced dissolution of iron (oxyhydr)oxides and formation of the paramagnetic iron sulfide pyrite in this particular sediment layer. Furthermore, the results of the model indicate that a constant high mean SR is able to cause a concave-up pore water sulfate profile. Such concave-up sulfate profiles have been previously interpreted to result from either non-steady state depositional conditions or from upward-directed advective flow. In the scenarios that we have modeled, the concave-up sulfate profile would be a steady state case. A low mean SR with a fixation of the SMT is necessary to produce an enrichment of iron and sulfur in the solid phase, as can be found in the sediment at sites GeoB 6223 and GeoB 6308. We calculated the time needed to produce the total amount of sulfur in the solid phase to be about 9000 years, which corresponds well with the estimation of the model and the Pleistocene/Holocene transition.

However, the stagnation of the SMT caused a loss of magnetic signal by diagenetic destruction of magnetite due to AOM. Another influence of AOM on sediment magnetism can be e.g. a magnetic enhancement via growth of greigite. This important but different magnetic effect was described by Neretin et al. (2004). The two effects are both results of similar processes, except that pyritization seems to have been arrested in the study by Neretin et al. (2004), which has led to preservation of greigite nodules with magnetizations 10-100 times greater than surrounding sediments. The net result is that non-steady state diagenesis can have varying effects on the magnetic record. Thus, diagenetic transformation of iron oxides to iron sulfides in the zone of AOM that corresponds to a loss and new formation of magnetic signals, should be considered in the interpretation of magnetic records.

Acknowledgements. We thank the captains and crews of the RV *Meteor* for their strong support during the two cruises M46/2 and M46/3. For technical assistance on board and in the home laboratory, we are indebted to S. Hinrichs, S. Siemer, K. Enneking and S. Hessler. We highly appreciate magnetic data provided by and discussions with T. Frederichs and SEM analyses carried out by H. Mai. Furthermore, we thank V. Heuer, K. Plewa and M. Schweizer for laboratory support. F. Aspetsberger, K. Seiter, O. Romero and M. Zabel are thanked for detailed comments on an earlier version of the manuscript. Two reviewers, R.R. Haese and A.P. Roberts, are greatly acknowledged for constructive and detailed comments, which improved the quality of the manuscript. Our special appreciation goes to U. Bleil and H.D. Schulz for helpful discussions. This research was funded by the Deutsche Forschungsgemeinschaft as part of the DFG-Research Center 'Ocean Margins' of the University of Bremen No. RCOM0289. *Associate editor:* D. E. Canfield

REFERENCES

Adler, M., Hensen, C., and Schulz, H.D. (2000) CoTReM – Column Transport and Reaction Model. http://www.geochemie.uni-bremen.de/downloads/cotrem/index.htm, User Guide, Version 2.3.

Adler, M., Hensen, C., Wenzhöfer, F., Pfeifer, K., and Schulz, H.D. (2001) Modeling of subsurface calcite dissolution by oxic respiration in supralysoclinal deep-sea sediments. *Mar. Geol.* **177**, 167-189.

Aller, R.C. and Rude, P.D. (1988) Complete oxidation of solid phase sulfides by manganese and bacteria in anoxic marine sediments. *Geochim. Cosmochim. Acta* **52**, 751-765.

Aloisi, G., Wallmann, K., Drews, M., and Bohrmann, G. (2004) Evidence for the submarine weathering of silicate minerals in Black Sea sediments: Possible implications for the marine Li and B cycles. *Geochem. Geophys. Geosyst.* **5**, 1-22.

Antoine, D., Andre, J.-M., and Morel, A. (1996) Oceanic primary production: 2. Estimation at global scale from satellite (coastal zone color scanner) chlorophyll. *Glob. Biogeochem. Cycles* **10**, 57-69.

Archer, D. (1996) A data-driven model of the global calcite lysocline. *Glob. Biogeochem. Cycles* **10**, 511-526.

Barnes, R.O. and Goldberg, E.D. (1976) Methane production and consumption in anoxic marine sediments. *Geology* **4**, 297-300.

Behrenfeld, M.J. and Falkowski, P.G. (1997) Photosynthetic rates derived from satellite-based chlorophyll concentration. *Limnol. Oceanogr*. **42**, 1-20.

Bernard, B.B. (1979) Methane in marine sediments. *Deep-Sea Res*. **26A**, 429-443.

Berner, R.A. (1967) Thermodynamic stability of sedimentary iron sulfides. *Am. J. Sci.* **265**, 773-785.

Berner, R.A. (1970) Sedimentary pyrite formation. *Am. J. Sci*. **268**, 1-23.

Berner, R.A. (1982) Burial of organic carbon and pyrite sulfur in the modern ocean: Its geochemical and environmental significance. *Am. J. Sci*. **282**, 451-473.

Biscaye, P.E. and Dasch, E.J. (1971) The rubidium, strontium, strontium-isotope system in deep-sea sediments: Argentine Basin. *J. Geophys. Res.* **76**, 5087-5096.

Blair, N.E. and Aller, R.C. (1995) Anaerobic methane oxidation on the Amazon shelf. *Geochim. Cosmochim. Acta* **59**, 3707-3715.

Bleil, U. (2000) Sedimentary Magnetism. In *Marine Geochemistry* (eds. H.D. Schulz and M. Zabel). Springer, pp. 73-84.

Bleil, U. and cruise participants (2001) Report and preliminary results of *Meteor* cruise M 46/3 Montevideo – Mar del Plata, 04.01. - 07.02.2000, *Ber. Fachb. Geowiss. Univ. Bremen* **172**.

Borowski, W.S., Paull, C.K., and Ussler, W. (1996) Marine porewater sulfate profiles indicate in situ methane flux from underlying gas hydrate. *Geology* **24**, 655-658.

Boudreau, B.P (1997) *Diagenetic models and their implementation: modelling transport and reactions in aquatic sediments*. Springer.

Butler, I.B. and Rickard, D. (2000) Framboidal pyrite formation via the oxidation of iron (II) monosulfides by hydrogen sulfide. *Geochim. Cosmochim. Acta* **64**, 2665-2672.

Canfield, D.E. and Berner, R.A. (1987) Dissolution and pyritization of magnetite in anoxic marine sediments. *Geochim. Cosmochim. Acta* **51**, 645-659.

Canfield, D.E. (1989) Reactive iron in marine sediments. *Geochim. Cosmochim. Acta* **53**, 619-632.

Canfield, D.E., Raiswell, R., and Bottrell, S. (1992) The reactivity of sedimentary iron minerals toward sulfide. *Am. J. Sci*. **292**, 659-683.

Channell, J.E.T. and Hawthorne, T. (1990) Progressive dissolution of titanomagnetites at ODP Site 653 (Tyrrhenian Sea). *Earth Planet. Sci. Lett.* **96**, 469-480.

Channell, J.E.T. and Stoner, J.S. (2002) Plio-Pleistocene magnetic polarity stratigraphies and diagenetic magnetite dissolution at ODP Leg 177 Sites (1089, 1091, 1093 and 1094). *Mar. Micropal*. **45**, 269-290.

Coleman, M.L. and Raiswell, R. (1995) Source of carbonate and origin of zonation in pyritiferous carbonate concretions: Evaluation of a dynamic model. *Am. J. Sci*. **295**, 282-308.

de Lange, G.J. (1983) Geochemical evidence of a massive slide in the southern Norwegian Sea. *Nature* **305**, 420-422.

Ewing, M. and Leonardi, A.G. (1971) Sediment transport and distribution in the Argentine Basin. 5. Sedimentary structure of the Argentine margin, basin, and related provinces. *Phys. Chem. Earth* **8**, 125-251.

Ewing, M., Eittreim, S.L., Ewing, J.I., and Le Pichon, X. (1971) Sediment transport and distribution in the Argentine Basin. 3. Nepheloid layer and processes of sedimentation. *Phys. Chem. Earth* **8**, 51-77.

Ferdelman, T.G., Fossing, H., Neumann, K., and Schulz, H.D. (1999) Sulfate reduction in surface sediments of the southeast Atlantic continental margin between 15°38'S and 27°57'S (Angola and Namibia). *Limnol. Oceanogr*. **44**, 650-661.

Flood, R.D., and cruise participants (1995) *Proc. ODP, Init. Repts.* **155**, Ocean Drilling Program.

Frederichs, T., Bleil, U., Däumler, K., von Dobeneck, T., and Schmidt, A.M. (1999) The magnetic view on the marine paleoenvironment: parameters, techniques and potentials of rock magnetic studies as a key to paleoclimatic and paleoceanographic changes. In *Use of proxies in paleoceanography: examples from the South Atlantic* (eds. G. Fischer and G. Wefer). Springer, pp. 575-599.

Frenz, M., Höppner, R., Stuut, J.-B.W., Wagner, T., and Henrich, R. (2003) Surface sediment bulk geochemistry and grain-size composition related to the oceanic circulation along the South American margin in the Southwest Atlantic. In *The South Atlantic in the Late Quaternary: Reconstruction of material budget and current systems* (eds. G. Wefer, S. Mulitza, and V. Ratmeyer). Springer, pp. 347-373.

Froelich, P.N., Klinkhammer, G.P., Bender, M.L., Luedtke, N.A., Heath, G.R., Cullen, D., Dauphin, P., Hammond, D., Hartman, B., and Maynard, V. (1979) Early oxidation of organic matter in pelagic sediments of the eastern equatorial Atlantic: suboxic diagenesis. *Geochim. Cosmochim. Acta* **43**, 1075-1090.

Funk, J.A., von Dobeneck, T., and Reitz, A. (2003a) Integrated rock magnetic and geochemical quantification of redoxomorphic iron mineral diagenesis in Late Quaternary sediments from the

Equatorial Atlantic. In *The South Atlantic in the Late Quaternary: Reconstruction of material budget and current systems* (eds. G. Wefer, S. Mulitza, and V. Ratmeyer). Springer, pp. 237-260.

Funk, J.A., von Dobeneck, T., Wagner, T., and Kasten, S. (2003b) Late Quaternary sedimentation and early diagenesis in the equatorial Atlantic ocean: Patterns, trends and processes deduced from rock magnetic and geochemical records. In *The South Atlantic in the Late Quaternary: Reconstruction of material budget and current systems* (eds. G. Wefer, S. Mulitza, and V. Ratmeyer). Springer, pp. 461-497.

Furukawa, Y. and Barnes, H.L. (1995) Reactions forming pyrite from precipitated amorphous ferrous sulfide. In *Geochemical transformation of sedimentary sulfur* (eds. M.A. Vairavamurthy and M.A.A. Schoonen). ACS Symposium Series **612**, 194-205.

Garming, J.F.L., Bleil, U., and Riedinger, N. (in press) Alteration of magnetic mineralogy at the sulfate methane transition: Analysis of sediments from the Argentine continental slope. *Phys. Earth Planet. Inter*.

Groot, J.J., Groot, C.R., Ewing, M., Burckle, L., and Conolly, J.R. (1967) Spores, pollen, diatoms and provenance of the Argentine Basin sediments. *Progr. Oceanogr*. **4**, 179-217.

Haese, R.R., Petermann, H., Dittert, L., and Schulz, H.D. (1998) The early diagenesis of iron in pelagic sediments: A multidisciplinary approach. *Earth Planet. Sci. Lett*. **157**, 233-248.

Haese, R.R., Schramm, J., Rutgers van der Loeff, M.M., and Schulz, H.D. (2000) A comparative study of iron and manganese diagenesis in continental slope and deep sea basin sediments off Uruguay (SW Atlantic). *Int. J. Earth Sci.* **88**, 619-629.

Harris, L.C. and Whiting, B.M. (2000) Sequence-stratigraphic significance of Miocene to Pliocene glauconite-rich layers, on- and offshore of the US Mid-Atlantic margin. *Sed. Geol*. **134**, 129-147.

Hensen, C., Zabel, M., and Schulz, H.D. (2000) A comparison of benthic nutrient fluxes from deep-sea sediments off Namibia and Argentina. *Deep-Sea Res. II* **47**, 2029-2050.

Hensen, C., Zabel, M., Pfeifer, K., Schwenk, T., Kasten, S., Riedinger, N., Schulz, H.D., and Boetius, A. (2003) Control of sulfate pore-water profiles by sedimentary events and the significance of anaerobic oxidation of methane for burial of sulfur in marine sediments. *Geochim. Cosmochim. Acta* **67**, 2631-2647.

Iriondo, M.H. (1984) The Quaternary of Northeastern Argentina. In *Quaternary of South America and Antarctic Peninsula* (ed. J. Rabassa). A.A. Balkema **2**, pp. 51-78.

Iversen, N. and Jørgensen, B.B. (1993) Diffusion coefficients of sulfate and methane in marine sediments: Influence of porosity. *Geochim. Cosmochim. Acta* **57**, 571-578.

Jiang, W.-T., Horng, C.-S., Roberts, A.P., and Peacor, D.R. 2001. Contradictory magnetic polarities in sediments and variable timing of neoformation of authigenic greigite. *Earth Planet. Sci. Lett*. **193**, 1-12.

Jørgensen, B.B. (1982) Mineralization of organic matter in the sea bed – the role of sulphate reduction. *Nature* **296**, 643-645.

Jørgensen, B.B., Böttcher, M.E., Lüschen, H., Neretin, L.N. and Volkov, I.I. (2004) Anaerobic methane oxidation and a deep H_2S sink generate isotopically heavy sulfides in Black Sea sediments. *Geochim. Cosmochim. Acta* **68**, 2095–2118.

Kao, S.-J., Horng, C.-S., Roberts, A.P., and Liu, K.-K. (2004) Carbon–sulfur–iron relationships in sedimentary rocks from southwestern Taiwan: Influence of geochemical environment on greigite and pyrrhotite formation. *Chem. Geol*. **203**, 153-168.

Karlin, R. and Levi, S. (1983) Diagenesis of magnetite minerals in recent hemipelagic sediments. *Nature* **303**, 327-330.

Karlin, R. and Levi, S. (1985) Geochemical and sedimentological control of the magnetic properties of hemipelagic sediments. *J. Geophys. Res*. **90**, 10373-10392.

Karlin, R. (1990) Magnetite diagenesis in marine sediments from the Oregon Continental Margin. *J. Geophys. Res*. **95**, 4405-4419.

Kasten, S., Freudenthal, T., Gingele, F.X., and Schulz, H.D. (1998) Simultaneous formation of iron-rich layers at different redox boundaries in sediments of the Amazon deep-sea fan. *Geochim. Cosmochim. Acta* **62**, 2253–2264.

Kasten, S., Zabel, M., Heuer, V., and Hensen, C. (2003) Processes and signals of nonsteady-state diagenesis in deep-sea sediments and their pore waters. In *The South Atlantic in the Late Quaternary: Reconstruction of material budget and current systems* (eds. G. Wefer, S. Mulitza, and V. Ratmeyer). Springer, pp. 431-459.

Klaus, A. and Ledbetter, M.T. (1988) Deep-sea sedimentary processes in the Argentine Basin revealed by high-resolution seismic records (3.5 kHz echograms). *Deep-Sea Res*. **35**, 899-917.

Ledbetter, M.T. and Klaus, A. (1987) Influence of bottom currents on sediment texture and sea-floor morphology in the Argentine Basin. In *Geology and geochemistry of abyssal plains* (eds. P.P.E. Weaver, and J. Thomson). Geological Society of London Special Publication **31**, pp. 23-31.

Lovley, D.R. (1991) Dissimilatory Fe(III) and Mn(IV) reduction. *Microbiol. Rev*. **55**, 259-287.

Morse, J.W. and Cornwell (1987) Analysis and distribution of iron sulfide minerals in recent anoxic marine sediments. *Mar. Chem*. **22**, 55-69.

Morse, J.W. (2002) Sedimentary geochemistry of the carbonate and sulphide systems and their potential influence on toxic metal bioavailability. In *Chemistry of marine water and sediments* (eds. A. Gianguzza, E. Pelizzetti and S. Sammartano). Springer, pp. 165-189.

Neretin, L.N., Böttcher, M.E., Jørgensen, B.B., Volkov, I.I., Lüschen, H., and Hilgenfeldt, K. (2004) Pyritization processes and greigite formation in the advancing sulfidization front in the Upper Pleistocene sediments of the Black Sea. *Geochim. Cosmochim. Acta* **68**, 2081-2093.

Niewöhner, C., Hensen, C., Kasten, S., Zabel, M., and Schulz, H.D. (1998) Deep sulfate reduction completely mediated by anaerobic methane oxidation in sediments of the upwelling area off Namibia. *Geochim. Cosmochim. Acta* **62**, 455-464.

Odin, G.S. and Matter, A. (1981) De glauconiarum origine. *Sedimentology* **28**, 611–641.

Passier, H.F., Dekkers, M.J., and de Lange, G.J. (1998) Sediment chemistry and magnetic properties in an anomalously reducing core from the eastern Mediterranean Sea. *Chem. Geol*. **152**, 287–306.

Peterson, R.G. and Stramma, L. (1991) Upper-level circulation in the South Atlantic Ocean. *Progr. Oceanogr*. **26**, 1-73.

Piccolo, M.C. and Perillo, G.M.E. (1999) The Argentina estuaries: A review. In *Estuaries of South America* (eds. G.M.E. Perillo, M.C. Piccolo, and M. Pino-Quivira). Springer, pp. 101-132.

Postma, D. and Appelo, C.A.J. (2000) Reduction of Mn-oxides by ferrous iron in a flow system: Column experiment and reactive transport modelling. *Geochim. Cosmochim. Acta* **64**, 1237–1247.

Pyzik, A.J. and Sommer, S.E. (1981) Sedimentary iron monosulfides: Kinetics and mechanism of formation. *Geochim. Cosmochim. Acta* **45**, 687-698.

Reitz, A., Hensen, C., Kasten, S., Funk, J.A., and de Lange, G.J. (2004) A combined geochemical and rock-magnetic investigation of a redox horizon at the last glacial/interglacial transition. *Phys. Chem. Earth*. **29**, 921-931.

Rickard, D., Schoonen, M.A.A., and Luther, G.W. (1995) Chemistry of iron sulfides in sedimentary environments. In *Geochemical transformation of sedimentary sulfur* (eds. M.A. Vairavamurthy and M.A.A. Schoonen). ACS Symposium Series **612**, pp. 168-193.

Rickard, D. (1997) Kinetics of pyrite formation by the H_2S oxidation of iron (II) monosulfides in aqueous solutions between 25 and 125°C: The rate equation. *Geochim. Cosmochim. Acta* **61**, 115-134.

Roberts, A.P. and Turner, G.M. (1993) Diagenetic formation of ferrimagnetic iron sulphide minerals in rapidly deposited marine sediments, South Island, New Zealand. *Earth Planet. Sci. Lett*. **115**, 257-273.

Romero, O. and Hensen, C. (2002) Oceanographic control of biogenic opal and diatoms in surface sediments of the South Western Atlantic. *Mar. Geol*. **186**, 263-280.

Sachs, S.D. and Ellwood, B.B. (1988) Controls on magnetic grain size variations and concentration in the Argentine Basin, South Atlantic Ocean. *Deep-Sea Res*. **35**, 929-942.

Schippers, A. and Jørgensen, B.B. (2001) Oxidation of pyrite and iron sulfide by manganese dioxide in marine sediments. *Geochim. Cosmochim. Acta* **65**, 915-922.

Schneider, R., Probst, U., and Donner, B. (1991) Stratigraphie. Bericht und Erste Ergebnisse der *Meteor*-Fahrt M 16/2, Recife – Belem, 28.04. - 21.05.1991. *Ber. Fachb. Geowiss. Univ. Bremen* **19**, 51-67.

Schoonen, M.A.A. and Barnes, H.L. (1991) Reactions forming pyrite and marcasite from solution: II. Via FeS precursors below 100°C. *Geochim. Cosmochim. Acta* **55**, 1505-1514.

Schulz, H.D., and cruise participants (2001) Report and preliminary results of *Meteor* cruise M 46/2 Recife - Montevideo, 02.12.–29.12.1999. *Ber. Fachb. Geowiss. Univ. Bremen* **174**.

Schulz, H.D. (2000) Quantification of early diagenesis: Dissolved constituents in marine pore water. In *Marine Geochemistry* (eds. H.D. Schulz and M. Zabel). Springer, pp. 85-128.

Tarduno, J.A. and Wilkison, S.L. (1996) Non-steady state magnetic mineral reduction, chemical lock-in, and delayed remanence acquisition in pelagic sediments. *Earth Planet. Sci. Lett*. **144**, 315–326.

Wilson, T.R.S., Thomson, J., Hydes, D.J., Colley, S., Culkin, F., and Sørensen, J. (1986) Oxidation fronts in pelagic sediments: Diagenetic formation of metal-rich layers. *Science* **232**, 972-975.

Vogt, C., Lauterjung, J., and Fischer, R.X. (2002) Investigation of the clay fraction (<2 μm) of the clay minerals society reference clays. *Clays Clay Minerals* **50**, 388–400.

Zabel, M., and Schulz, H.D. (2001) Importance of submarine landslides for non-steady state conditions in pore water systems. *Mar. Geol*. **176**, 87-99.

Alteration of magnetic mineralogy at the sulfate methane transition: Analysis of sediments from the Argentine continental slope

J.F.L. Garming, U. Bleil, and N. Riedinger

Fachbereich Geowissenschaften, Universität Bremen, Klagenfurter Str., 28359 Bremen, Germany

Abstract

On the Argentine continental slope off the Rio de la Plata estuary, the sulfate-methane transition (SMT) has been encountered at shallow depths of a few meters below the seafloor. At around this horizon, where sulfate diffusing downward from the bottom water is met and reduced by methane rising from deeper in the sediment column, intense alteration affects the detrital magnetic mineral assemblage. Less than 10% of the dominant primary low coercivity ferrimagnetic (titano-)magnetite remains after alteration. In the upper part of the suboxic environment, underlying the iron redox boundary, which is located at a depth of ~ 0.1 m, approximately 60% of the finer grained detrital fraction is already dissolved. While the high coercivity minerals are relatively unaffected in the suboxic environment, large portions (> 40%) are diagenetically dissolved in the sulfidic SMT zone. Nevertheless, the characteristics of the magnetic residue are entirely controlled by a high coercivity mineral assemblage. Unlike common observations, that diagenetic alteration produces coarser magnetic grain-sizes in suboxic milieus, a distinct overall fining is found in the sulfidic zone. Different factors should contribute to this effect. Scanning electron microscope analysis, combined with X-ray microanalysis, identified fine grained (titano-)magnetite preserved as inclusions in silicates and between high Ti titanohematite lamellae, and possibly of prime importance, a comprehensive fragmentation of larger grains in the course of maghemitization. The only secondary iron sulfide mineral detected is pyrite, which is present as clusters of euhedral crystals or directly replaces (titano-)magnetite. The thermomagnetic measurements did not provide evidence for the presence of ferrimagnetic sulfides such as greigite. Different from other studies reporting a marked magnetic enhancement at around the SMT due to the precipitation and preservation of such metastable ferrimagnetic sulfides, a complete pyritization process will cause a distinct magnetic depletion, like in the present case.

Alteration of manganese minerals and release of ferrous iron in deeper subsurface marine sediments from the western Argentine Basin

N. Riedinger[1] and S. Kasten[1,2]

[1] *Fachbereich Geowissenschaften, Universität Bremen, Klagenfurter Straße, 28359 Bremen, Germany*

[2] *current address: Alfred Wegener Institute for Polar and Marine Research, Am Handelshafen 12, 27570 Bremerhaven, Germany*

Abstract

To study diagenetic alteration of iron and manganese minerals, geochemical and mineralogical investigations of sediments from the western Argentine Basin were carried out. The dynamic depositional conditions prevailing in the study area were found to be mirrored in the solid phase and pore water concentration profiles of manganese. The data further show a relationship between manganese and hydrogen sulfide (H_2S) pore water profiles, suggesting the precipitation of manganese in the sulfidic zone. Above and below the sulfate/methane transition (SMT), release of divalent Mn occurs, which indicates the presence of reactive Mn-phases. The reduction of these phases are assumably due to biomediated processes. We discuss the occurrence of ferrous iron in pore water below the SMT as process of ferric iron reduction mediated by methanogens. This is the first study which gives geochemical evidence for this recently found biogeochemical process – which has been proposed on the base of laboratory studies – to occur in natural aquatic environments. We predict that the biogeochemical processes observed in the methanic zone could be relevant to advance the understanding of processes in the deep biosphere.

Keywords: Manganese; Hydrogen sulfide; Methanic zone; Ferrous iron; Microorganisms; Argentine Basin

1. INTRODUCTION

In marine surface sediments manganese is highly mobile due to early diagenetic processes (Goldberg and Arrhenius, 1958; Lynn and Bonatti, 1965; Calvert and Price, 1972; Froelich, 1979; Berner, 1981; Baturin, 1988; Lovley, 1991; Canfield et al., 1993; Thamdrup, 2000; a.o.). The reduction of Mn-oxides driven by the degradation of organic matter releases divalent Mn into the pore water (Froelich et al., 1979; Lovley and Phillips, 1988). A further reduction of Mn-oxides occurs due to ferrous iron oxidation (Postma, 1985; Canfield et al., 1993) as well as by anaerobic oxidation of iron sulfide, as demonstrated experimentally by Aller and Rude (1988) and Schippers and Jørgensen (2001). Migration of manganous ions from deeper suboxic/anoxic layers towards oxic levels near the sediment-water interface results in the precipitation of Mn-oxides (Lynn and Bonatti, 1965; Berner, 1981; Thamdrup et al., 1994). This diagenetic process leads to an enrichment of Mn-oxides at the Mn-redox boundary (e.g. Li et al., 1969; Canfield et al., 1993; Haese et al., 2000). The described redox cycling of manganese can be found in the upper layers of marine sediments, at the boundary between oxic and postoxic zone (Berner, 1981). In the postoxic zone released manganeous ions also diffuse downwards into the sulfidic zone, where they can either precipitate as Mn-carbonates (rhodochrosite) or Mn-sulfides (alabandite, e.g. Suess, 1979; Berner, 1981; Appelo and Postma, 1994; Lepland and Stevens, 1998), or they can co-precipitate with iron sulfides (Arakaki and Morse, 1993). The precipitation of Mn-sulfides requires high concentrations of divalent Mn in the pore water. The only known Mn-sulfides from recent marine sediments were found in the Baltic Sea (Suess, 1979; Böttcher and Huckriede, 1997; Lepland and Stevens, 1998). The cycling of manganese requires a significant amount of reactive Mn-phases in the sediment, resulting from hydrothermal sources or terrigenous input (Li et al., 1969), or an initial enrichment of Mn-oxides at the sediment/water inteface due to oxidation of formerly anoxic water column and precipitation of Mn-oxides (Sternbeck and Sohlenius, 1997; Neumann et al., 2002). In environments of rather slow sedimentation Mn-oxides alter quite fast and manganese cycling processes are restricted to the uppermost sediment layer (Suess, 1979). Only in areas with high accumulation rates Mn-oxides are buried rapidly and a considerable amount could be shielded from reduction (Canfield and Berner, 1987; Riedinger et al., in press). At greater sediment depth Mn-oxides could be relevant for biomediated processes along with iron conversion. These processes still require more investigations.

The sedimentary environment along the continental margin off Argentina and Uruguay is characterized by highly dynamic depositional conditions (Ewing et al., 1971; Biscay and Dasch, 1971; Ledbetter and Klaus, 1987; Hensen et al., 2000). Riedinger et al. (in press) could show that high sedimentation rates shield iron oxides from reduction, resulting in burial of these minerals in deeper sediment layers. Thus the western Argentine Basin provides a unique study area to investigate geochemical processes regarding the alteration of manganese in deeper subsurface sediments. In this study, we investigate the influence of depositional settings and anaerobic oxidation of methane (AOM) on the diagenetic overprint of Mn-oxides and the release of manganous ions into the pore water, presenting geochemical and

mineralogical data. Additionally, we discuss the processes causing the release of ferrous iron into the pore water below the sulfidic zone.

2. MATERIALS AND METHODS

2.1. Geological Settings

The sites of investigation are located in the western South Atlantic on the continental margin off Argentina and Uruguay (Fig. 1) between a water depth of 1100 and 4300 m.

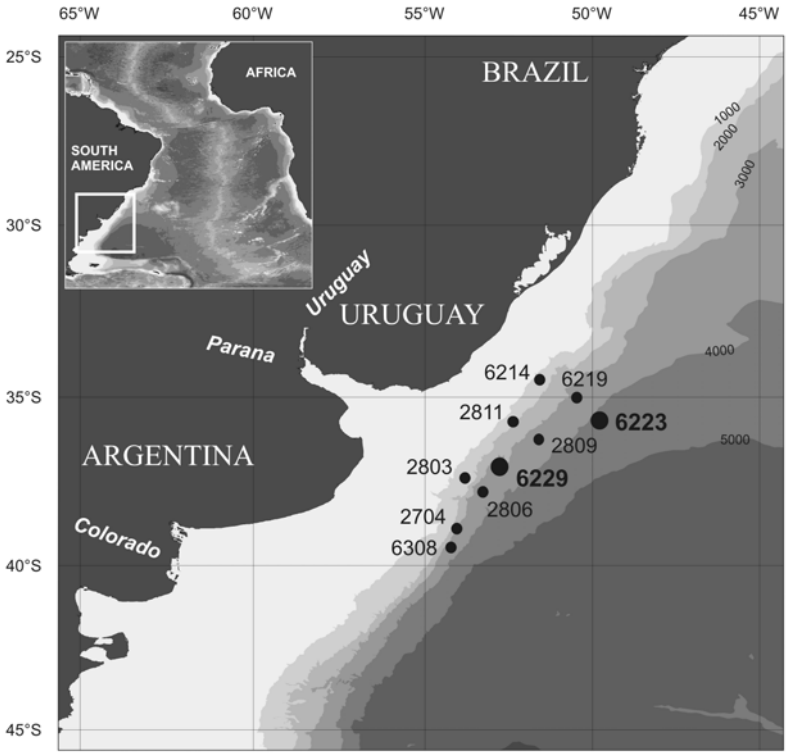

Fig. 1. Location map of the investigated gravity cores at GeoB stations in the western Argentine Basin. The sites discussed in more detail are indicated as bold symbols.

The depositional environment of this study area is characterized by strong current circulation and gravity-controlled sediment transport (Ewing and Leonardi, 1971; Klaus and Ledbetter, 1988). The extensive sediment transport along the western margin of the Argentine Basin from the shelf to the basin is controlled by gravity-driven mass transports, such as debris flows and turbidity currents (Ewing et al., 1971; Biscay and Dasch, 1971; Klaus and Ledbetter, 1988; Sachs and Ellwood, 1988; Hensen et al., 2003). Currents winnow and entrain sediments deposited by gravity-controlled mass flows, and the fine material is transported into the deep basin (Groot et al., 1967; Ewing et al., 1971; Ledbetter and Klaus, 1987; Sachs and Ellwood, 1988). The sediment at the study sites is characterized by low calcium carbonate contents, as well as relatively high amounts of organic carbon and iron (oxyhydr)oxides (Hensen et al., 2003; Riedinger et al., in press; Garming et al., in press).

2.2. Sampling an Sample Processing

The investigated gravity cores (Table 1) were retrieved east of the Rio de la Plata at the western boundary of the Argentine Basin, during expeditions M29/1-2 (1994) and M46/2-3 (1999-2000) of the RV *Meteor*.

Table 1. Studied gravity cores with geographical positions and water depths.

Station	Longitude [W]	Latitude [S]	Water Depth [m]	SMT[a] [mbsf]
GeoB 2704-2	53°55.30'	38°55.10'	3226	-
GeoB 2803-3	53°42.40'	37°24.40'	1163	-
GeoB 2806-5	53°08.60'	37°50.00'	3538	3.7
GeoB 2809-4	51°31.20'	36°20.30'	3561	9.3
GeoB 2811-2	52°16.30'	35°45.20'	1774	5.9
GeoB 6214-7	51°26.57'	34°31.52'	1566	4.9
GeoB 6219-2	50°33.88'	35°11.14'	3551	4.3
GeoB 6223-6	49°40.86'	35°44.42'	4280	5.1
GeoB 6229-6	52°39.00'	37°12.41'	3446	5.6
GeoB 6308-4	53°08.70'	39°10.00'	3620	5.0

[a] The sulfate/methane transition (SMT) was defined on the base of the sulfate penetration depth (see Hensen et al., 2003).

The sampling procedures and analytical techniques are only briefly described below and were described in more detail for the investigated sites by Hensen et al., 2003 and Riedinger et al., in press. For detailed information regarding analytical methods and devices, the reader is referred to Schulz (2000) and the homepage of the geochemistry group http://www.geochemie.uni-bremen.de at the University of Bremen.

To prevent a warming of the sediments after retrieval on board, all cores were immediately placed in a cooling laboratory and maintained at a temperature of about 4°C. Gravity cores were cut into 1 m segments on deck, and syringe samples were taken from every cut segment surface for methane analysis. For H_2S analysis of higher concentrations 1 mL sub-samples of the pore water were added to a ZnAc-solution in order to fix all sulfide present as ZnS. Within the first two days after recovery, gravity cores were cut lengthwise into two halves and processed within a glove box under argon atmosphere. E_H and pH were determined by punch-in electrodes and sediment samples were taken every 25 cm for pressure filtration of pore water. Solid phase samples for total digestions, sequential extractions and mineralogical analyses were taken at 10 cm intervals and kept in gas-tight glass bottles under argon atmosphere. The storage temperature for all sediments was -20°C to avoid dissimilatory oxidation of reduced species. For pressure filtration Teflon-squeezers were used, operated with argon (5 bar). The pore water was retrieved through 0.2 µm cellulose acetate membrane filters. The parameters hydrogen sulfide (H_2S), sulfate, alkalinity, and iron (Fe^{2+}) were determined by standard methods, within a few hours after retrieval of the pore water. All further analyses were carried out at the University of Bremen. Methane was measured with a gas chromatograph (Varian 3400) and the concentrations were subsequently corrected for

sediment porosity. Aliquots of the remaining pore water were diluted and acidified with HNO_3 for determination of cations using inductively coupled plasma atomic emission spectrometry (ICP-AES) techniques (Perkin Elmer Optima 3000 RL). Total digestions of the sediment were performed on anoxic subsamples, and analyzed by ICP-AES techniques. Total carbon (TC) and total organic carbon (TOC) contents were determined by measuring freeze-dried and homogenized samples using a LECO CS-300 carbon sulfur analyzer. The data that we report here can be accessed at the World Data Centers for Marine Environmental Sciences (http://www.pangaea.de/PangaVista).

2.3. Mineral Analysis

Mineral identification was carried out by X-ray diffraction (XRD). XRD was performed at a few selected depths of core GeoB 6229-6 by Philips X´Change (Cu-tube) with fixed divergence slit. The measurement was carried out with a first angle of 3° 2Θ and a last angle of 100° 2Θ. The step size was 0.02° 2Θ, and the time per step was 12 s/step. Samples of cores GeoB 6223-6 and GeoB 6308-4 were measured by X'Pert Pro MD, X'Celerator detector system, with a step size of 0.033° 2Θ, and the calculated time per step was 219.71 seconds. Mineral content quantification was carried out with QUAX (for further information see Vogt et al. 2002). Special mineral identification was performed on frozen and anoxic stored subsamples. Gravity separation was applied on the samples to enrich the heavy mineral phases. Glass capillars (0.5 mm) were filled with the sample material and sealed afterwards. The measurement was carried out with a STOE image plate diffractometer system (IPDS), with monochromatic Mo-ray. The image plate distance was 150 mm and the exposure time was 480 min, at 50 kV and 40 mA. The data qualification was carried out with X'Pert HighScore. Geophysical analysis using low-temperature mineral magnetic techniques were carried out at a few selected samples (for further details see Frederichs et al., 2003).

3. RESULTS AND DISCUSSION

3.1. Manganese Pore Water Profiles

The pore water profiles of manganese indicate the release of manganous ions in the postoxic zone, and an immobilization of divalent Mn in the sulfidic zone (Fig. 2). Furthermore at several sites an increase in Mn pore water concentrations within the methanic zone below the SMT is observed. In the sulfidic zone the pore water concentration profiles of H_2S and Mn show a relationship, where H_2S is consumed the immobilization of divalent Mn occurs. At the investigated sites the Mn-redox boundary, coinciding with the oxic/postoxic interface, is located at about 5 to 15 cm depth as shown by Haese et al. (2000).

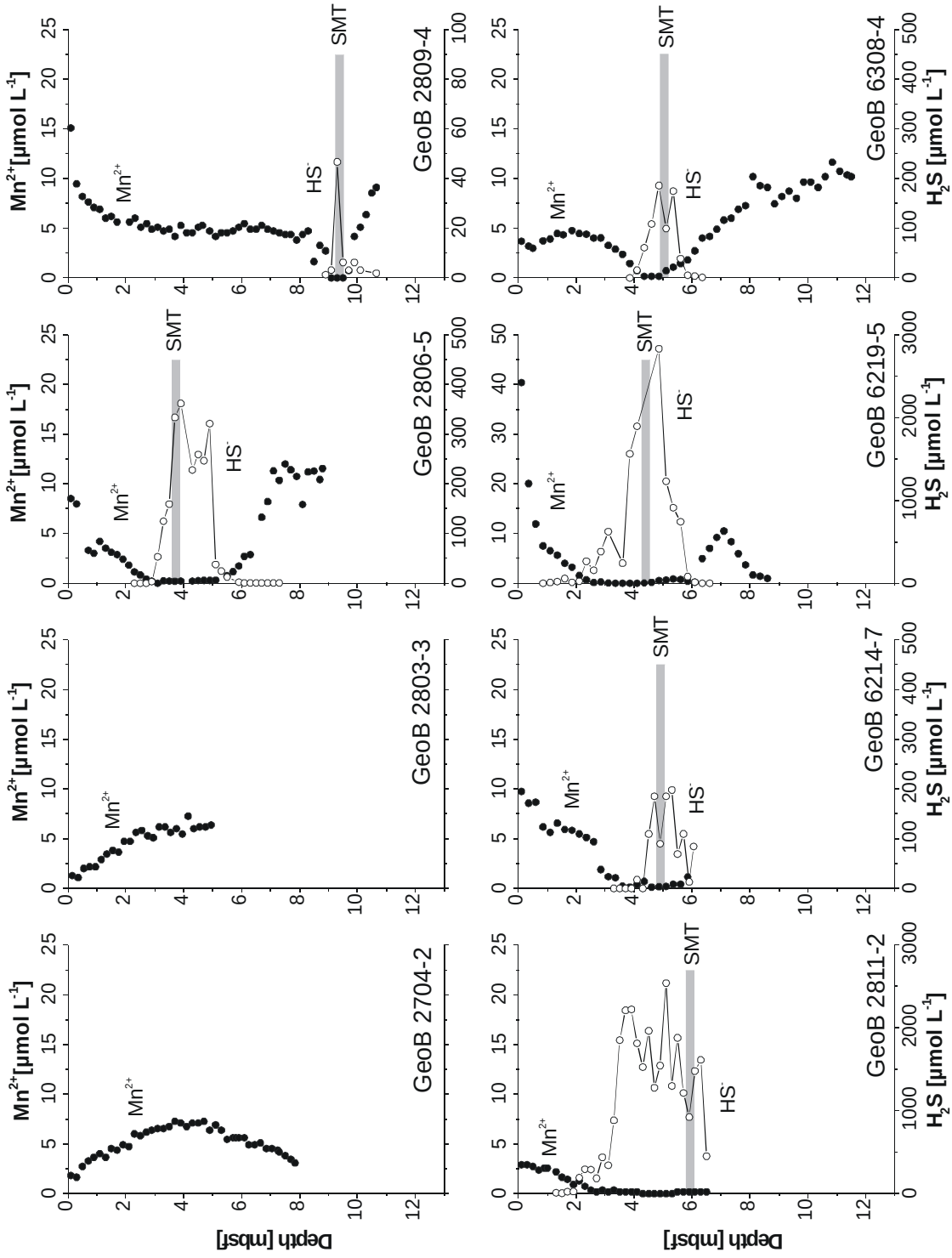

Fig. 2. Pore water concentration profiles of Mn (black dots) and H_2S (open circles) indicating a relationship between the decreasing manganous ions and depleted H_2S. The gray bars mark the location of the sulfate/methane transition (SMT). Pore water data of H_2S are taken from Hensen et al., 2003 and Riedinger et al., in press.

In contrast to divalent Mn, which was primarily released from Mn-oxides below the Mn-redox boundary, pore water sulfate has its dominant (unlimited) source in seawater. Hensen et al. (2003) discussed in detail sulfate concentration gradients of pore water profiles for the study area, which are characterized by non-steady state processes. They discussed the impact of young sedimentary events on the shape of sulfate pore water profiles. The impact of such depositional dynamics can also be found in the profiles of pore water manganese. For example at sites GeoB 2809 and GeoB 6214 the sulfate profiles show s-type and a kink-type shapes, respectively. These shapes can be explained by younger depositional events as sedimentary slides or slumps (Hensen et al., 2003).

Although the western Argentine Basin is characterized by highly dynamic sedimentary conditions (Ledbetter and Klaus, 1987; Hensen et al., 2000), Riedinger et al. (in press) could show that areas with constant and rather slow sedimentation rates since the Pleistocene/Holocene transition exist. Sediments at these sites are characterized by linear sulfate pore water profiles (Riedinger et al., in press), indicating that the pore water system is currently in steady state, such as at sites GeoB 6229 and GeoB 6223. The manganese profile at site GeoB 6229 shows a release of divalent Mn into the pore water at about 10 cm below the surface, at the oxic/postoxic boundary. The released divalent Mn is transported by diffusion upward to the Mn-redox boundary and downward into the sulfidic zone (Fig. 3).

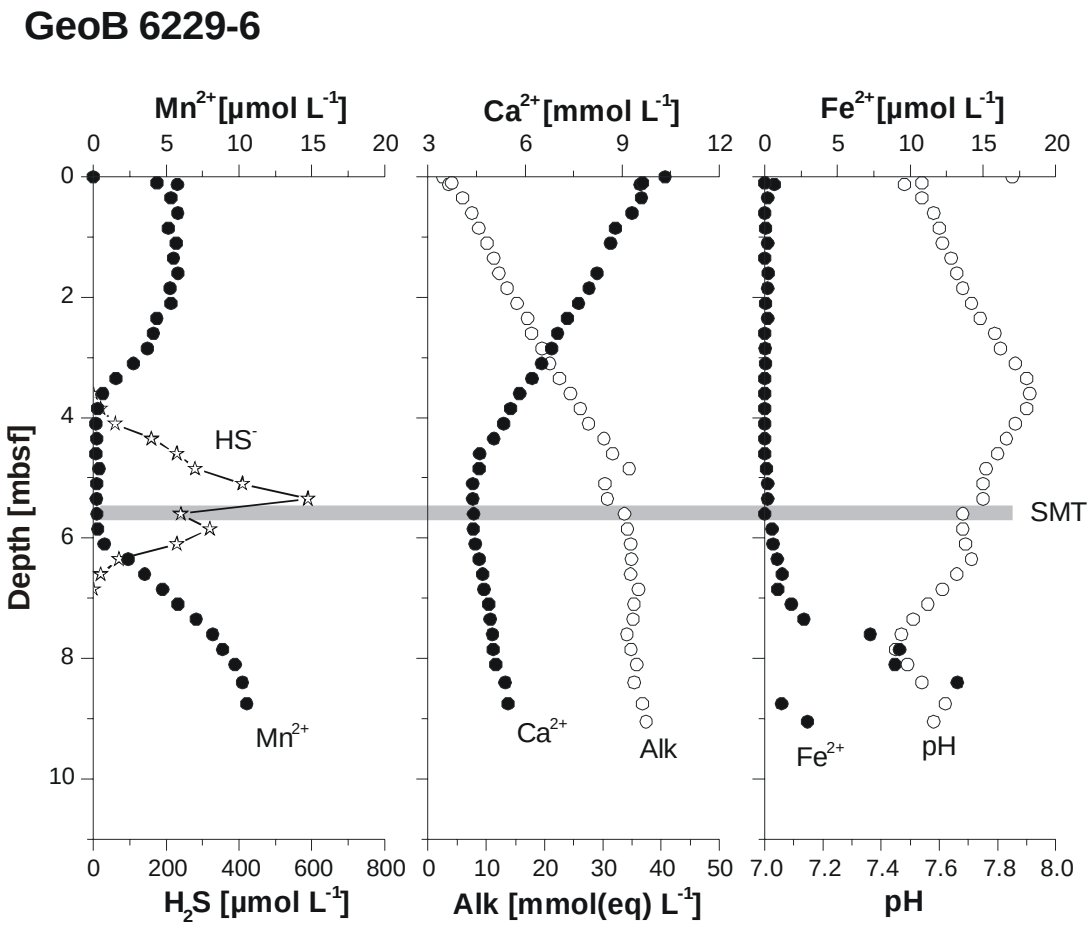

Fig. 3. Pore water data at site GeoB 6229 showing a double precipitation front of manganese in the sulfidic zone. The gray bar marks the location of the sulfate/methane transition (SMT).

Solid phase data of sediments from site GeoB 6223 display an enrichment of manganese in the upper 5 cm (Fig. 4). In contrast to site GeoB 6229 the Mn pore water profile at site GeoB 6223 does not show a release of divalent Mn slightly below the Mn-redox boundary which is located at about 15 cm below the sediment surface, but at a depth of about 2.5 mbsf. The absence of released manganous ions directly below the Mn-redox boundary could be explained by very low sediment deposition. As a result of sediments accumulating at small rates, the Mn-oxides have not been buried below the Mn-redox boundary and remain in the oxic zone. Thus no reduction of the Mn-oxides is taking place. Furthermore, a low input of organic matter, at site GeoB 6229 the current input of TOC is about twice as high as at site GeoB 6223 (Riedinger et al., in press), results in a deepening of the Mn-redox zone.

The increase of divalent Mn at about 2.5 mbsf indicates the presence of an additional manganese source. Mineralogical measurements show that at 2.55 mbsf enhanced amounts of glauconite are present and also Mn-oxides were detected. Because of the high amount of glauconite at this depth we assume that also higher amounts of Mn-oxides must have been initially present due to a sedimentary event, for example, a turbidity flow.

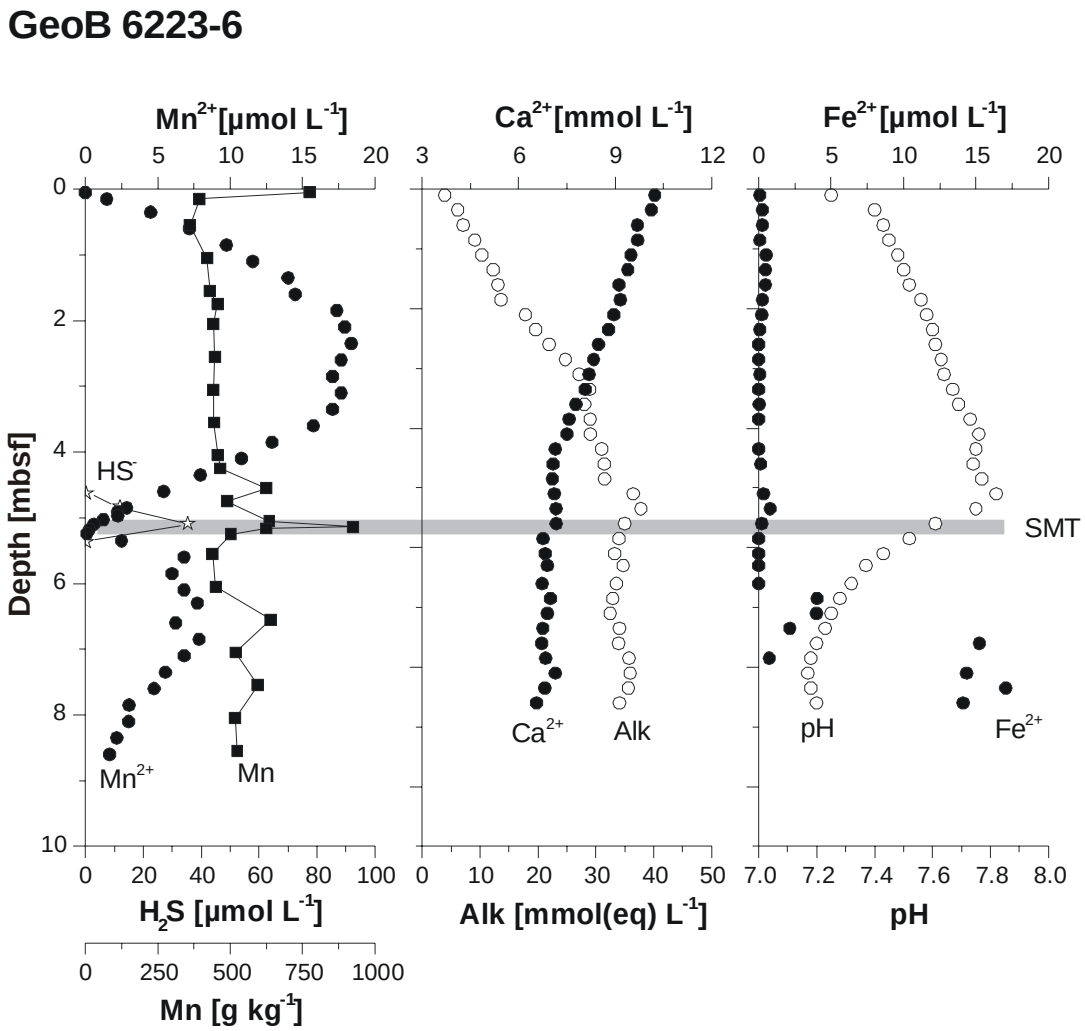

Fig. 4. Solid phase Mn at site GeoB 6223 showing an enrichment of manganese where manganese in pore water data is consumed – at the oxic/postoxic boundary and in the sulfidic zone. The gray bar represents the sulfate/methane transition (SMT).

In this way, downward transported surface sediments could have enriched oxidized minerals at this site, which were buried without or minor reduction because of high sedimentation rates. We suggest that the ongoing reduction of Mn-phases unstable in this postoxic environment has only left a minor fraction. The released manganous ions are transported upward by diffusion to the oxic/postoxic boundary and downwards to the sulfidic zone, resulting in the observed shape of the pore water profile (Fig. 4), and leading to enrichments in the solid phase at these sediment levels as shown in the model in Fig. 5, which is based on numerical modeling using the transport and reaction program CoTReM (Adler et al., 2000). A similar Mn profile of pore water and solid phase was observed by Thomson et al. (1986), in deep marine sediments from the north Atlantic. Enrichment of Mn-oxides at the sediment surface were rapidly buried due to turbidity emplacements. The downward and upward diffusion of divalent Mn in the pore water resulted from the reduction of this Mn-oxide front. The by Thomson et al. (1986) discussed Mn profiles, which were found in marine sediments, show a good correlation with the assumed initial situation in our theoretical approach, and thus emphases the plausibility of our model. However, the pore water data for both sites show that although the sulfate profiles already regained steady state conditions after sedimentary events or changes in depositional conditions, the impact of these sedimentary dynamics can still be found in pore water profiles of manganese.

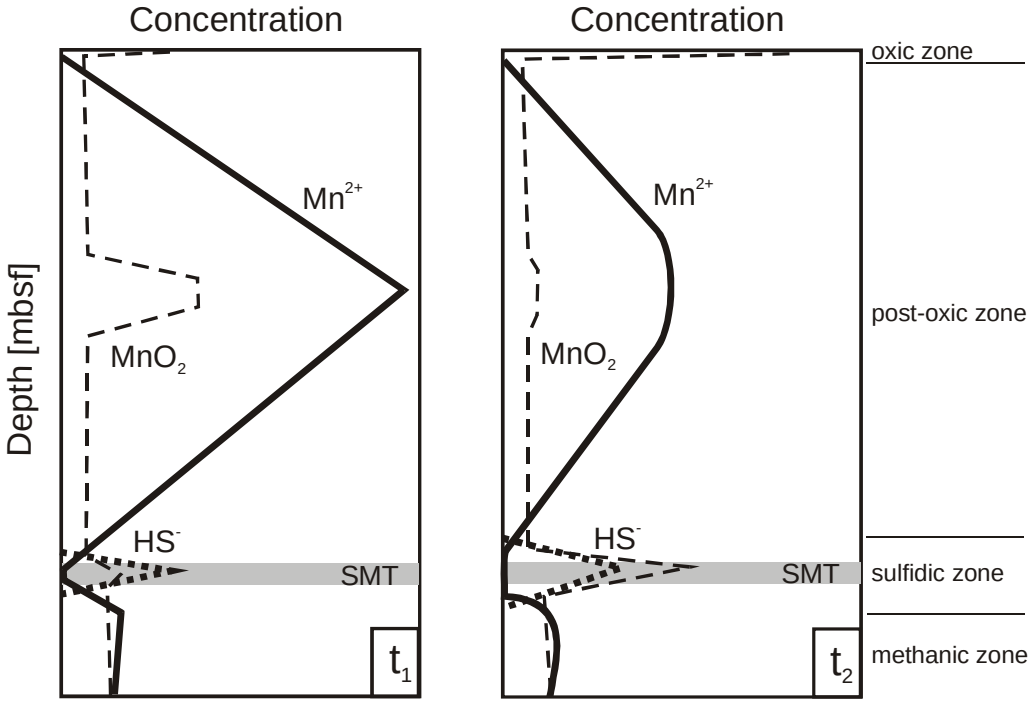

Fig. 5. Theoretical approach to explain the shape of the Mn pore water profile found at site GeoB 6223. Reduction of solid tetravalent Mn (the reactive Mn-phases are summarized as MnO_2, dashed line) releases divalent Mn into the pore water (Mn^{2+}, solid line). Manganous ions are transported upward and downward by diffusion and are consumed at the oxic/postoxic boundary and within the sulfidic zone (t_1). This process leads to an enrichment of solid phase manganese in the sulfidic zone and at the oxic/postoxic boundary. Due to a very low accumulation rate the Mn-oxides in the oxic zone still have not been buried below the Mn-redox boundary. The absence or very low amount of further reducible Mn-phases in the postoxic zone would smooth the shape of the pore water profile of Mn because of no or a very low release of divalent Mn into the pore water (t_2). The gray bars mark the sulfate/methane transition (SMT).

3.2. Precipitation of Mn(II) in the sulfidic zone

The diffusion of manganous ions into the sulfidic zone occurs from the postoxic zone as well as from the methanic zone. In the sulfidic zone the pore water profiles of manganese depicted in Fig. 2 show a complete consumption of divalent Mn. These minima correlate quite good with the H_2S peaks and thus indicates a precipitation of Mn-phases in the sulfidic zone. The pore water data would suggest a precipitation of Mn-sulfides like e.g. alabandite (MnS) (Berner, 1981):

$$HS^- + MnO_2 + 3H^+ \rightarrow Mn^{2+} + S^0 + 2H_2O \quad (1)$$

$$Mn^{2+} + HS^- \rightarrow MnS + H^+. \quad (2)$$

However, XRD measurements do not show any Mn-sulfides, what would also suggest that Mn-sulfide is present in amounts below the detection limit of XRD. The pore water composition of samples from the sulfidic zone modeled using the code PHREEQC 2.10 (Parkhurst and Appelo, 1999) show an undersaturation of MnS. A precipitation of MnS would require a more alkaline environment or much higher concentrations of divalent Mn in the pore water (e.g. Suess, 1979). Furthermore the modeling using PHREEQC 2.10 only indicates the precipitation of rhodochrosite ($MnCO_3$) or rather Ca-Mn-carbonates (Franklin and Morse, 1983; Dromgoole and Walter, 1990; Alvi and Winterhalter, 2001). Li et al. (1969) suggested the precipitation of $MnCO_3$ on the base of pore water profiles:

$$Mn^{2+} + HCO_3^- \rightarrow MnCO_{3(s)} + H^+. \quad (3)$$

However, neither XRD measurements nor geophysical analysis of samples from this depth did show any indication of rhodochrosite. If a precipitation of Mn incorporated in Ca-carbonate would take place, we would assume that the Mn pore water profile would show a similarity to the one of Ca. This is, however, in contradiction to the observed pore water profiles (Fig. 3 and 4). The calcium profile implies a consumption at one distinct layer, in the same way as the alkalinity profile. This indicates a $CaCO_3$ precipitation at a restricted horizon, which can be shown for site GeoB 6229 (Fig. 6). In contrast, the Mn pore water profile for site GeoB 6229 shows a consumption at two distinct horizons. Nevertheless, if there is a Mn precipitation associated with carbonate, we assume Ca-rich rhodochrosite is present (e.g. Neumann et at., 1997).

The consumption of divalent Mn in the sulfidic zone could be furthermore explained by coprecipitation with and/or adsorption of manganous ions on fine-grained iron monosulfides (mackinawite) as discussed by Arakaki and Morse (1993). But in that case, corresponding to ferrous iron, no manganese should be detected in the pore water where sulfide is present. However, at e.g. site GeoB 6223 (Fig. 4), there is still divalent Mn in the sulfidic zone, thus we assume that the reaction of Mn^{2+} and H_2S is thermodynamically rather slow compared to iron, and can only occur when the availability of H_2S exceeds Fe^{2+}, as was also discussed by

Lepland and Stevens (1998). A coprecipitation of divalent Mn and iron monosulfide could not be found in the investigated sediment on base of XRD and SEM analytical techniques. SEM analysis shows that the occurrence of manganese can only be associated with Fe-oxides but not with Fe-sulfides (Garming et al., in press). Regarding all the data from the sulfidic zone, our assumption is that either excessive H_2S is somehow affecting/facilitating the Mn-carbonate precipitation or Mn-sulfides.

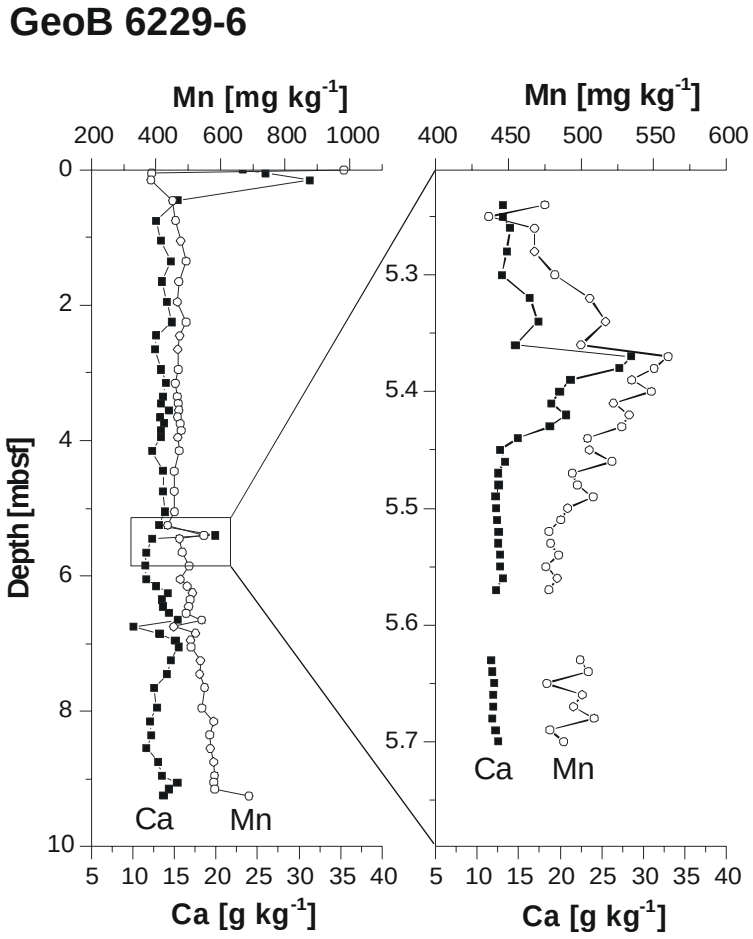

Fig. 6. Solid phase data at site GeoB 6229 showing in detail the enrichment of calcium at 5.37 mbsf (Ca data shown on the left side were taken from Riedinger et al., in press). An increase in the concentration of Mn at the same depth was found.

3.3. Dissolved Manganese in the Methanic Zone

To occurrence of manganous ions in pore water below the sulfidic zone can be related to the depositional conditions. An intense decrease in sedimentation rate would result in a stagnation of the formerly rapidly upward moving SMT as discussed by Riedinger et al. (in press) for the investigated area. The released H_2S could cause a drop in the previously linear Mn profile, where the new zone of SMT has established (Fig. 7). Thus, the concentration of Mn in pore water below the new SMT could be seen as a relict of the former profile. Furthermore, a high sedimentation rate leads to a preservation of iron oxides below the zone of AOM (Riedinger et al., in press). As summarized by Thamdrup (2000), abiotic reduction of highly reactive iron

hydroxides by HS^- occurs at higher rates than the reduction of Mn-oxides. This can explain the availability of Mn-oxides in the methanic zone, providing a source for divalent Mn. The released manganous ions move downward and upward by diffusion. In the sulfidic zone the divalent Mn is consumed, which leads to a drop in the pore water profile.

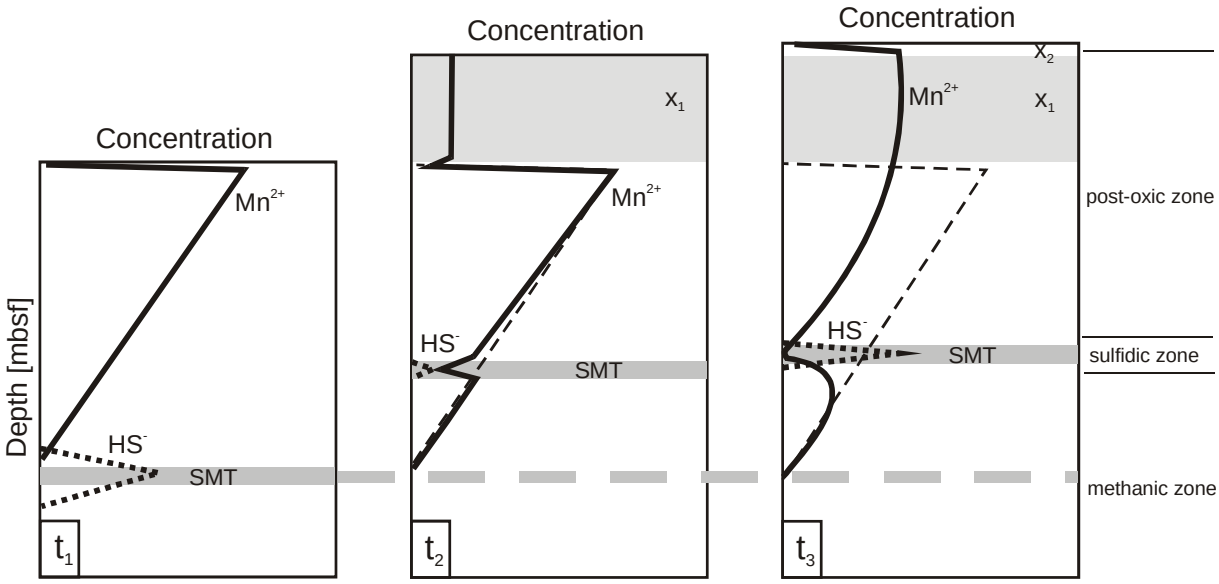

Fig. 7. Theoretical influence of a drastic change in sedimentation rate on the pore water profile of Mn. The initial situation shows a linear pore water profile of Mn with consumption in the sulfidic zone and release below the oxic/postoxic boundary (t_1). On the basis of high mean sedimentation rate (x_1) the SMT (gray bar) moves up rapidly resulting in a constant but rather low release of divalent Mn into pore water (t_2), on top of the linear concentration profile (t_1). A drastic decrease in the sedimentation rate (x_2) causes a fixation of the SMT (t_3). This leads to an increase of H_2S liberation resulting in a consumption of manganous ions at a distinct layer. In the postoxic zone the pore water profile is adjusting to the new depositional and geochemical conditions. The dashed line represents the initial Mn pore water profile.

Comparing the theoretical profile in Fig. 7 with its rather smoothed curvature and the Mn profiles in Fig. 2, we suggest that the observed kinks in the measured profiles can be explained by such shielded Mn-oxides, providing an additional source of divalent Mn within the methanic zone. Because the rapid upward movement of the SMT as well as the deeper buried sources of divalent Mn are related to sedimentary conditions, we think that the observed Mn profile reflect the depositional dynamics at the investigated sites.

Assuming that the divalent Mn sources in the methanic zone are mainly Mn-oxides, the liberation of manganous ions could be the result of nonenzymatic oxidation of ferrous iron by Mn-oxides (Lovley and Phillips, 1988; Aller and Rude, 1988; Canfield, 1993; Jørgensen, 2000; Schippers and Jørgensen, 2002):

$$2Fe^{2+} + MnO_2 + 4H_20 \rightarrow Mn^{2+} + 2Fe(OH)_3 + 2H^+. \qquad (5)$$

Modeling of pore water data at a depth of 8.10 mbsf by using PHREEQC 2.10 indicate that the reduction of Mn-oxides by ferrous iron and a subsequent precipitation of iron hydroxides would not occur under the prevailing reducing conditions. Furthermore this process implies a release of divalent Mn into pore water with a concurrent consumption of ferrous iron (Postma and Appelo, 2000). Such a decrease cannot be found in the pore water profiles of core GeoB 6229-6 (Fig. 3), suggesting that below the SMT different processes are relevant for the release of manganous ions into the pore water. We suggest that the processes of liberation of manganous ions and ferrous iron in the methanic zone at the investigated sites are not related to each other by abiogenic reaction but we assume that they are rather microbially driven. Most of the microorganisms that are capable of reducing tetravalent Mn can also reduce ferric iron (Lovley, 1993; Thamdrup, 2000). Most of these microbial processes are (mostly based on laboratory results) described for the postoxic zone only, with relation to the degradation of organic matter (e.g. Burdige and Nealson, 1985; Hastings and Emerson, 1986; Myers and Nealson, 1988; Lovley, 1991; Thamdrup 1994), and are not directly transferable to the methanic zone.

Similar Mn-profiles to those we found in sediments of the investigated cores, can also be discovered in deeply buried sediments as for example in ODP cores at Leg 172 (Çağatay et al., 2001) and Leg 201 (D'Hondt et al., 2004). In contrast to ODP sites, the processes of manganese reduction and precipitation at the studied sites proceed over a small range of depth. However, understanding the processes taking place in the methanic zone at the investigated sites could be relevant to advance the comprehension of processes in the deep biosphere, for example, which electron acceptors are available in such depths for microbial mediated processes.

3.4. Iron Reduction in the Methanic Zone

Below the zone of AOM ferrous iron is released into the pore water, correlating with a decrease in pH (Fig. 3 and Fig. 4). Iron oxides and glauconite which contains high amounts of ferric iron (Odin and Matter, 1981) could serve as substrates for iron reduction (Riedinger et al., in press). The presence of glauconite in sediments of the methanic zone, despite its high reactivity towards H_2S (Berner, 1981), was verified by XRD. However, as discussed above for the released manganese, we assume that the ferric iron is not reduced abiotically. As proposed by Canfield (1989), bacterial iron reduction seems to be the most likely source for dissolved iron in sediments where sulfate reduction is absent. Assuming that the release of ferrous iron into the pore water is associated with the reduction of ferric iron driven by degradation of organic matter, we would expect an increase in pH rather than a decrease as observed. Although the pH cannot be used as a proof because it can be influenced by many processes, we assume that the reduction of ferric iron is due to microbial mediated processes.

Furthermore Lovley and Phillips (1988) discussed the inhibition of ferric iron reduction in the presence of tetravalent manganese. As we find the release of manganous ions as well as ferrous iron at a similar depth within the methanic zone, we propose that the reduction is a

result of microbial processes, which are different than compared to the occurring processes in the postoxic zone. We suggest that the release of ferrous iron into pore water below the zone of AOM could be due to the reduction of ferric iron by methanogens – a new process which was reported recently by Bond and Lovley (2002) based on laboratory results. According to Bond and Lovley (2002) the reduction of Fe(III) by methanogens can only proceed in environments where methanogens and reducible iron oxides co-exist. Solid phase extractions e.g. of core GeoB 6223-6, in fact, show the presence of iron oxides below the sulfidic zone (Riedinger et al., in press). The reduction of ferric iron by microorganisms is coupled to the oxidation of H_2 (Lovley et al., 1989; Lovley, 1993):

$$2Fe^{3+} + H_2 \rightarrow 2Fe^{2+} + 2H^{+}. \qquad (6)$$

The excess hydrogen could be supplied by the oxidation of methane by methanogens (Lovley and Goodwin, 1988), but in the presence of ferric iron the production of methane is inhibited (Lovley and Philips, 1987; Lovley et al., 1995). However, the oxidation of iron monosulfides by H_2S also liberates hydrogen (Rickard, 1997) which could provide the energy source for the microbial metabolism (Drobner et al., 1990). Both the pH profiles at sites GeoB 6223 and GeoB 6229 show a drop where ferrous iron is liberated (Fig. 3 and Fig. 4). The decrease can be explained by the reduction of ferric iron by hydrogen-utilizing methanogens (Eq. 6). The reduction of ferric iron by methanogens could also be a promising candidate to explain processes concerning the release of ferrous iron in deeply buried sediments e.g. at ODP Leg 201 (D'Hondt et al., 2002).

4. CONCLUSIONS

Our study shows that sedimentary events or changes in depositional conditions can be identified by pore water profiles of manganese, when sulfate in pore water shows steady state profiles and cannot be used for such interpretation. Generally, pore water profiles of manganese should not be underestimated for interpretations of distinctive sedimentary settings. The shape of the pore water profile of manganese is not only influenced by depositional dynamics but also by the presence of ferrous iron and H_2S. Thus, manganese profiles can provide a good complementary tool for the reconstruction of sedimentary dynamics. However, we suggest that the term steady state/non-steady state has to be applied more careful discussing pore water or solid phase data. As we could show, single constituents in pore water can be already in steady state while others are still exposing non-steady state conditions and minerals although being unstable in particular geochemical environments can be present or preserved at considerable amounts in deeper subsurface sediments.

The pore water data suggest that the consumption of divalent manganese in the sulfidic zone is related to excess H_2S, although we cannot provide significant proof for direct precipitation of manganous ions by H_2S. The excessive H_2S is, however, likely to facilitate the precipitation of Mn-sulfides or Mn-carbonate. Because of the low amounts of the precipitated

Mn-phases it is difficult to detect these minerals by conventional techniques (e.g. XRD). However, we assume that the release of manganous ions into pore water within the methanic zone is microbially mediated corresponding to the processes of ferrous iron release. We suggest that ferrous iron released below the sulfidic zone is driven by the reduction of ferric iron by methanogens as described by Bond and Lovley (2002) on the base of laboratory results. The prerequisites stated by Bond and Lovley (2002) for this process to occur – namely the co-existence of methanogens and reactive iron (oxyhydr)oxides – are met in the study area. However, understanding the processes taking place in the methanic zone at the investigated sites, for example the release of ferrous iron and manganous ions in the methanic zone by e.g. methanogens, could be relevant to advance the understanding of processes in the deep biosphere, concerning the availability of electron acceptors for microbial mediated processes. Our findings emphasize the need for more intensive studies of the microbial mediated and geochemical processes in the methanic zone of deeply buried sediments and to identify the responsible microorganisms.

Acknowledgement. We thank the captains and crews of RV *Meteor* for their strong support during cruises M29/1-2 and M46/2-3. For technical assistance on board and in the home laboratory we are indebted to S. Hessler, S. Hinrichs, S. Siemer, and R. Krammer. We highly appreciate geophysical data provided by T. Frederichs and mineralogical measurements and discussions by M. Wendschuh and J. Birkenstock. Furthermore we would like to thank M. Böttcher, K. Pfeifer, and M. Zabel for detailed comments as well as M. Kölling and K. Seiter for reading an earlier draft of the manuscript. Our special appreciation goes to H.D. Schulz for helpful discussions. This research was funded by the Deutsche Forschungsgemeinschaft as part of the Research Center "Ocean Margins" (RCOM) of the University of Bremen contribution no. XXXX.

REFERENCES

Adler, M., Hensen, C., and Schulz, H.D. (2000) CoTReM – Column Transport and Reaction Model. http://www.geochemie.uni-bremen.de/downloads/cotrem/index.htm, User Guide, Version 2.3.

Aller, R.C. and Rude, P.D. (1988) Complete oxidation of solid phase sulfides by manganese and bacteria in anoxic marine sediments. *Geochim. Cosmochim. Acta* **52**, 751-765.

Alvi, K. and Winterhalter, B. (2001) Authigenic mineralisation in the temporally anoxic Gotland Deep, the Baltic Sea. *Baltica* **14**, 74-83.

Arakaki, T. and Morse, J.W. (1993) Coprecipitation and adsorption of Mn(II) with mackinawite (FeS) under conditions similar to those found in anoxic sediments. *Geochim. Cosmochim. Acta* **57**, 9-14.

Baturin, G.N. (1988) *The geochemistry of manganese and manganese nodules in the ocean*. Kluwer Academic Press.

Berner, R.A. (1981) A new geochemical classification of sedimentary environments. *J. Sed. Petrol.* **51**, 359-365.

Biscaye, P.E. and Dasch, E.J. (1971) The rubidium, strontium, strontium-isotope system in deep-sea sediments: Argentine Basin. *J. Geophys. Res.* **76**, 5087-5096.

Bond, D.R. and Lovley, D.R. (2002) Reduction of Fe(III) oxide by methanogens in the presence and absence of extracellular quinones. *Environ. Microbiol.* **4**(2), 115-124.

Böttcher, M.E. and Huckriede, H. (1997) First occurrence and stable isotope composition of authigenic γ-MnS in the central Gotland Deep (Baltic Sea). *Mar. Geol*. **137**, 201-205.

Burdige, D.J. and Nealson, K.H. (1985) Microbial manganese reduction by enrichment cultures from coastal marine sediments. *Appl. Environ. Microbiol*. **50**, 491-497.

Çağatay, M.N., Borowski, W.S., and Ternois, Y.G. (2001) Factors affecting the diagenesis of Quaternary sediments at ODP Leg 172 sites in western North Atlantic: evidence from pore water and sediment geochemistry. *Chem. Geol.* **175**, 467–484.

Calvert, S.E. and Price, N.B. (1972) Diffusion and reaction profiles of dissolved manganese in the pore water of marine sediments. *Earth Planet. Sci. Let.* **16**, 245-249.

Canfield, D.E. and Berner, R.A. (1987) Dissolution and pyritization of magnetite in anoxic marine sediments. *Geochim. Cosmochim. Acta*. **51**, 645-659.

Canfield, D.E. (1989) Reactive iron in marine sediments. *Geochim. Cosmochim. Acta* **53**, 619-632.

Canfield, D.E., Thamdrup, B., and Hansen, J.W. (1993) The anaerobic degradation of organic matter in Danish coastal sediments: Iron reduction, manganese reduction, and sulfate reduction. *Geochim. Cosmochim. Acta*. **57**, 3867-3883.

D'Hondt, S.L., Jørgensen, B.B., Miller, D.J. et al. (2002) Controls on microbial communities in deeply buried sediments, eastern equatorial Pacific and Peru Margin. *ODP Init. Reports* **201**.

D'Hondt, S., Jørgensen, B.B., Miller, D.J., et al., 2004. Distributions of microbial activities in deep subseafloor sediments. Science 306, 2216-2221.

Drobner, E., Huber, H., Wächtershäuser, D., Rose, D., and Stetter, K.O. (1990) Pyrite formation linked with hydrogen evolution under anaerobic conditions. *Nature*, **346**, 742-744.

Dromgoole, E.L. and Walter, L.M. (1990) Iron and manganese incorporation into calcite: Effects of growth kinetics, temperature and solution chemistry. *Chem. Geol.* **81**, 311-336.

Ewing, M. and Leonardi, A.G. (1971) Sediment transport and distribution in the Argentine Basin. 5. Sedimentary structure of the Argentine margin, basin, and related provinces. *Phys. Chem. Earth* **8**, 125-251.

Ewing, M., Eittreim, S.L., Ewing, J.I., and Le Pichon, X. (1971) Sediment transport and distribution in the Argentine Basin. 3. Nephloid layer and processes of sedimentation. *Phys. Chem. Earth* **8**, 51-77.

Franklin, M.L. and Morse, J.W. (1983) The interaction of manganese(II) with the surface of calcite in dilute solutions and seawater. *Mar. Chem.* **12**, 241-254.

Frederichs, T., von Dobeneck, T., Bleil, U., and Dekkers, M.J. (2003) Towards the identification of siderite, rhodochrosite, and vivianite in sediments by their low-temperature magnetic properties. *Phys. Chem. Earth* **28**, 669–679.

Froelich, P.N., Klinkhammer, G.P., Bender, M.L., Luedtke, N.A., Heath, G.R., Cullen, D., Dauphin, P., Hammond, D., Hartman, B., and Maynard, V. (1979) Early oxidation of organic matter in pelagic sediments of the eastern equatorial Atlantic: suboxic diagenesis. *Geochim. Cosmochim. Acta* **43**, 1075-1090.

Garming, J.F.L., Bleil, U., and Riedinger, N. (in press) Alteration of magnetic mineralogy at the sulfate methane transition: Analysis of sediments from the Argentine continental slope. *Phys. Earth Planet. Interiors*.

Goldberg, E.D. and Arrhenius, G.O.S. (1958) Chemistry of Pacific pelagic sediments. *Geochim. Cosmochim. Acta* **13**, 153-212.

Groot, J.J., Groot, C.R., Ewing, M., Burckle, L., and Conolly, J.R. (1967) Spores, pollen, diatoms and provenance of the Argentine Basin sediments. *Progr. Oceanogr*. **4**, 179-217.

Haese, R.R, Schramm, J., Rutgers van der Loeff, M.M., and Schulz, H.D. (2000) A comparative study of iron and manganese diagenesis in continental slope and deep sea basin sediments off Uruguay (SW Atlantic). *Int. J. Earth Sci.* **88**, 619-629.

Hastings, D. and Emerson, S. (1986) Oxidation of manganese by spores of a marine bacillus: Kinetic and thermodynamic considerations. *Geochim. Cosmochim. Acta* **50**, 1819-1824.

Hensen, C., Zabel, M., and Schulz, H.D. (2000) A comparison of benthic nutrient fluxes from deep-sea sediments of Namibia and Argentina. *Deep-Sea Res. II* **47** 2029-2050.

Hensen, C., Zabel, M., Peifer, K., Schwenk, T., Kasten, S., Riedinger, N., Schulz, H.D., and Boetius, A. (2003) Control of sulfate pore-water profiles by sedimentary events and the significance of anaerobic oxidation of methane for burial of sulfur in marine sediments. *Geochim. Cosmochim. Acta* **67**, 2631-2647.

Jørgensen, B.B. (2000) Bacteria and marine biogeochemistry. In *Marine Geochemistry* (eds. H.D. Schulz and M. Zabel). Springer, pp. 173-208.

Klaus, A. and Ledbetter, M.T. (1988) Deep-sea sedimentary processes in the Argentine Basin revealed by high-resolution seismic records (3.5 kHz echograms). *Deep-Sea Res*. **35**, 899-917.

Ledbetter, M.T. and Klaus, A. (1987) Influence of bottom currents on sediment texture and sea-floor morphology in the Argentine Basin. In *Geology and geochemistry of abyssal plains* (eds. P.P.E. Weaver, and J. Thomson). Geological Society Special Publication **31**, pp. 23-31.

Lepland, A. and Stevens, R.L. (1998) Manganese authigenesis in the Landsort Deep, Baltic Sea. *Mar. Geol*. **151**, 1-25.

Li, Y.-H., Bischoff, J., and Mathieu, G. (1969) The migration of manganese in the Arctic Basin sediment. *Earth Planet. Sci. Let.* **7**, 265-270.

Lovley, D.R. and Goodwin, S. (1988) Hydrogen concentrations as an indicator of the predominant terminal electron-accepting reactions in aquatic sediments. *Geochim. Cosmochim. Acta* **52**, 2993-3003.

Lovley, D.R. and Phillips, E.J.P. (1988) Manganese inhibition of microbial iron reduction in anaerobic sediments. *Geomicrobiol. J.* **6**, 145-155.

Lovley, D.R., Phillips, E.J.P., and Lonergan, D.J. (1989) Hydrogen and formate oxidation coupled to dissimilatory reduction of iron or manganese by *Alteromonas putrefaciens*. *Appl. Environ. Microbiol.* **55**, 700-706.

Lovley, D.R. (1991) Dissimilatory Fe(III) and Mn(IV) reduction. *Microbiol. Rev*. **55**, 259-287.

Lovley, D.R. (1993) Dissimilatory metal reduction. *Annu. Rev. Microbiol*. **47**, 263-290.

Lovley, D.R., Phillips, E.J.P., Lonergan, D.J., and Widman, P.K. (1995) Fe(III) and S^0 Reduction by *Pelobacter carbinolicus*. *Appl. Environ. Microbiol*. **61**, 2132–2138.

Lynn, D.C. and Bonatti, E. (1965) Mobility of manganese in diagenesis of deep-sea sediments. *Mar. Geol.* **3** 457-474.

Myers, C.R. and Nealson, K.H. (1988) Microbial reduction of manganese oxides: Interactions with iron and sulfur. *Geochim. Cosmochim. Acta* **52**, 2727-2732.

Neumann, T., Christiansen, C., Clasen, S., Emeis, K.-C., and Kunzendorf, H. (1997) Geochemical records of salt-water inflows into the deep basins of the Baltic Sea. *Cont. Shelf Res.* **17**, 95-115.

Neumann, T., Heiser, U., Leosson, M.A., and Kersten, M. (2002) Early diagenetic processes during Mn-carbonate formation: Evidence from the isotopic composition of authigenic Ca-rhodochrosites of the Baltic Sea. *Geochim. Cosmochim. Acta* **66**, 867–879.

Odin, G.S. and Matter, A. (1981) De glauconiarum origine. *Sedimentology* **28**, 611–641.

Parkhurst, D.L. and Appelo, C.A.J. (1999) User's guide to PHREEQC (Version 2.0). U.S. Geol. Surv. Water Resour. Inv. Rep., 99-4259.

Postma , D. (1985) Concentration of Mn and separation from Fe in sediments-I. Kinetics and stoichiometry of the reaction between birnessite and dissolved Fe(II) at 10°C. *Geochim. Cosmochim. Acta* **49**, 1023-1033.

Postma, D. and Appelo, C.A.J. (2000) Reduction of Mn-oxides by ferrous iron in a flow system: Column experiment and reactive transport modelling. *Geochim. Cosmochim. Acta* **64**, 1237–1247.

Rickard, D. (1997) Kinetics of pyrite formation by the H_2S oxidation of iron (II) monosulfides in aqueous solutions between 25 and 125°C: The rate equation. *Geochim. Cosmochim. Acta* **61**, 115-134.

Riedinger, N., Pfeifer, K., Kasten, S., Garming, J.F.L., Vogt, C., and Hensen, C. (in press) Diagenetic alteration of magnetic signals by anaerobic oxidation of methane related to a change in sedimentation rate. *Geochim. Cosmochim. Acta*

Schippers, A. and Jørgensen, B.B. (2001) Oxidation of pyrite and iron sulfide by manganese dioxide in marine sediments. *Geochim. Cosmochim. Acta* **65**, 915-922.

Schippers, A. and Jørgensen, B.B. (2002) Biogeochemistry of pyrite and iron sulfide oxidation in marine sediments. *Geochim. Cosmochim. Acta* **66**, 85-92.

Schulz, H.D. (2000) Quantification of early diagenesis: dissolved constituents in marine pore water. In *Marine Geochemistry* (eds. H.D. Schulz and M. Zabel). Springer, pp. 85-128.

Sternbeck, J. and Sohlenius, G. (1997) Authigenic sulfide and carbonate mineral formation in Holocene sediments of the Baltic Sea. *Chem. Geol.* **135**, 55-73.

Suess, E. (1979) Mineral phases formed in anoxic sediments by microbial decomposition of organic matter. *Geochim. Cosmochim. Acta* **43**, 339-352.

Thamdrup, B., Finster, K., Fossing, H., Hansen, W.J., and Jørgensen, B.B. (1994) Thiosulfate and sulfite distributions in porewater of marine sediments related to manganese, iron, and sulfur geochemistry. *Geochim. Cosmochim. Acta* **58**, 67-73.

Thamdrup, B. (2000) Bacterial manganese and iron reduction in aquatic sediments. In *Advances in Microbial Ecology* (ed. Schink, B.) **16**, 41-84.

Thomson, J., Higgs, N.C., Jarvis, I., Hydes, D.J., Colley, S., and Wilsom, T.R.S. (1986) The behaviour of manganese in Atlantic carbonate sediments. *Geochim. Cosmochim. Acta* **50**, 1807-1818.

Vogt, C., Lauterjung, J., and Fischer, R.X. (2002) Investigation of the clay fraction (<2 mm) of the clay minerals society reference clays. *Clays Clay Minerals* **50**, 388–400.

Active and buried authigenic barite fronts in sediments from the eastern Cape Basin

N. Riedinger[1], S. Kasten[1,2], J. Gröger[1], C. Franke[1,3], and K. Pfeifer[1]

[1] *Fachbereich Geowissenschaften, Universität Bremen, Klagenfurter Str., 28359 Bremen, Germany*

[2] *current adress: Alfred Wegener Institute for Polar and Marine Research, Am Handelshafen 12, 27570 Bremerhaven, Germany*

[3] *Paleomagnetic Laboratory ‚Fort Hoofddijk', Utrecht University, Budapestlaan 17, 3584 CD Utrecht, The Netherlands*

Abstract

Sediment cores retrieved in the Benguela coastal upwelling system off Namibia show very distinct enrichments of solid phase barium at the sulfate/methane transition (SMT). These barium peaks represent diagenetic barite ($BaSO_4$) fronts, which form by the reaction of upwardly diffusing barium with interstitial sulfate. Calculated enrichment times of these barium spikes indicate a formation time of at least 10,000 years. Barium enrichments a few meters below the SMT were observed at one of the investigated sites (GeoB 8455). Although this sulfate-depleted zone is undersaturated with respect to barite, the dominant mineral phase of these buried barium enrichments was identified as barite by scanning electron microscopy (SEM). This is the first study which reports the occurrence/preservation of pronounced barite enrichments in sulfate-depleted sediments buried a few meters below the SMT. Modeling the measured barium concentrations at site GeoB 8455, applying the numerical model CoTReM, reveals that the dissolution rate of barite directly below the SMT is about one order of magnitude higher than at the subjacent barium enrichments. This indicates that the dissolution of barite at these deeper buried fronts must be decelerated. A possible explanation for the preservation of the enrichments in solid phase barium in core GeoB 8455-2 could be a decreased dissolution of barite due to the high concentrations of dissolved barium in pore water. Furthermore, the alteration of barite into witherite ($BaCO_3$) via the transient phase barium sulfide could lead to the preservation of a former barite front. The calculations and modeling suggest that between the last glacial maxium (LGM) and the Pleistocene/Holocene transition occurred a relocation of the barite front to a shallower depth. Due to the prevailing, rather static depositional environment in this area we suggest that the upward shift of the SMT most likely is the result of an increase in the upward methane flux due to the burial of high amounts of organic matter below the SMT thus elevating the rates of methanogenesis.

1. INTRODUCTION

Sediments which underlay areas of high primary productivity are often enriched in barium bearing solid phases (e.g. Goldberg and Arrhenius, 1958; Church, 1979; Bishop, 1988; Dymond et al., 1992). The link between productivity and the amount of barium in the sediment is thought to be established by the formation of distinct barite ($BaSO_4$) particles in the water column associated with the decay of organic matter or rather the decay of phytoplankton (Chow and Goldberg, 1960; Dehairs et al., 1980; Bishop, 1988; Dehairs, 1991; Ganeshram et al., 2002). Thus, in marine deposits barite is often used as a tracer of paleoproductivity (e.g. Breymann et al., 1992; Gingele and Dahmke, 1994; Paytan et al., 1996; Gingele et al., 1999). Besides the utilization of barium, in particular barite, as a productivity-proxy several other indications can be drawn from barium compounds. Marine barite is often used to reconstruct past Sr isotope compositions of seawater, or for Sr isotope stratigraphy (e.g. Paytan et al., 1996; Mearon et al., 2002). Furthermore it can be applied to reconstruct the former sulfur isotope ratio of marine sulfate, or to draw conclusions about past changes in the upward flux of methane (Dickens, 2001). However, the use of barium as a proxy (e.g. for paleoproductivity) is clearly limited as shown in several studies (e.g. Breymann et al., 1992; McManus et al., 1998; Gingele et al., 1999). The alteration of the primary barium signal by diagenetic processes is one of the most important limitations for the application of barium and barium compounds as a proxy. Generally, barite is relatively resistant to alteration after burial (Paytan et al., 1993; 2002). However, in zones of sulfate depletion barite is dissolved and barium is released into the pore water. The upward transport of barium by diffusion into sulfate-bearing pore waters is leading to precipitation of authigenic barite in diagenetic fronts. Thus, barite fronts are mainly found directly above the sulfate penetration depth, at the sulfate/methane transition (SMT) (Cronan, 1974; Dean and Schreiber, 1978; von Breymann et al., 1992; Torres et al., 1996a; Dickens, 2001). The formation of authigenic barite fronts is affected by diagenetic alteration due to sulfate reduction and driven by anaerobic oxidation of methane (AOM) (e.g. Kasten and Jørgensen, 2000; Dickens, 2001). Non-steady state diagenesis greatly influences authigenic barite precipitation (Kasten et al., 2003). Drastic decreases in sedimentation rate can fix the barite front at a discrete interval, which can lead to the formation of large barite deposits (Torres et al., 1996a). Moreover, changes in methane flux can shift the SMT and thus the position of the barite front (Dickens, 2001). Thus, barite fronts above the SMT, which formed when the SMT was located at a shallower sediment depth in the past, can be used to reconstruct decreases in the upward flux of methane. However, generally only former barite fronts above the current depth of the SMT which formed in association with a downward migration of the SMT can be used. Burial of barite enrichments in sulfate-depleted sediments will result in their fast dissolution. Up to now, barium enrichments preserved below the SMT have only been described in deeply buried sediments, drilled by ODP (Ocean Drilling Program). These barium enrichments were mostly described as the result of hydrothermal intrusions or associated with fluid seeps (e.g. Varnavas, 1987; von Breymann et al., 1992; Torres et al, 1996b).

In this study we report on barite enrichments at the SMT and in addition we present data of solid phase Ba-enrichments in the sulfate-depleted zone. Scanning electron microscopy (SEM) and energy dispersive spectrometry (EDS) were carried out for identification and semi-quantification of the Ba phases in the sediment. Furthermore, we discuss the mechanisms and/or conditions which lead to the preservation of the barite enrichments below the SMT. To investigate the processes involved, we applied numerical modeling of the geochemical data and we calculated the time needed to produce the barium peaks observed.

2. MATERIALS AND METHODS

2.1. Sampling Sites

The two gravity cores investigated in this study were retrieved on a down slope transect (T2) on the continental margin off Namibia in the eastern South Atlantic (Fig. 1) during RV *Meteor* expedition M57/2 (Zabel et al., 2003). The cores GeoB 8426-3 (13°21.1'E, 25°28.9'S) and GeoB 8455-2 (13°11.0'E, 25°30.4'S) were recovered at water depths of 1045 and 1503 m, respectively.

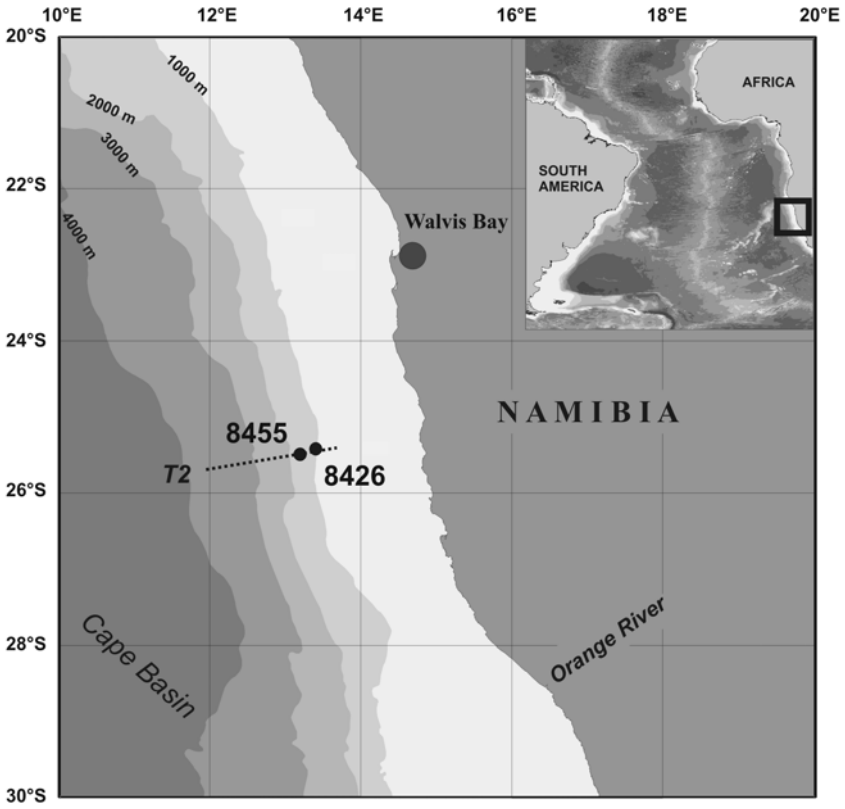

Fig. 1 Map displaying the location of the investigated gravity cores taken at GeoB stations on transect 2 (T2).

The sediments in the eastern Cape Basin are characterized by low input of terrigenous matter and high biogenic contents. The high amounts of organic matter (up to 12 wt% at site GeoB 8426, and 9 wt% at site GeoB 8455) in the sediment are due to the enhanced primary productivity in the surface water (Embley and Morley, 1980; Gingele and Dahmke, 1994). The Benguela upwelling system is controlled by the predominant southeasterly trade-winds, which drive the coastal upwelling of cold and nutrient-rich water (Shannon, 1985; Wefer and Fischer, 1993). Occasional berg winds, perpendicular to the coast, are the most important means of transport for terrestrial material (Wefer and Fischer, 1993; Shannon and Nelson, 1996). Minor amounts of terrigenous sediment are supplied by perennial rivers (Orange River) and rivers sporadically carrying water, like the Swakop River (Bremner and Willis, 1993). The deposition of river discharge is limited to the shelf, and the slope mainly consists of calcareous ooze (Rogers and Bremner, 1991; Bremner and Willis, 1993). Quaternary slumps and slides can only be found close to the Walvis Ridge (Summerhayes, 1979; Embley and Morley, 1980) and do not represent important sediment transport processes in the study area.

2.2. Sampling and Sample Processing

The sampling procedures and analytical techniques are only briefly described below. For detailed information regarding analytical methods and devices, the reader is referred to Schulz (2000) and to the homepage of the geochemistry group http://www.geochemie.uni-bremen.de at the University of Bremen. The set of pore water and solid phase data is available via the geological data network Pangaea (http://www.pangaea.de/PangaVista).

After retrieval on board, gravity cores were cut into 1-m segments on deck and syringe samples were taken from every cut segment bottom for methane analysis. Syringe samples of 5 ml of sediment were injected into 50 ml septum vials containing 20 ml of seawater, and were stored at -20°C. To prevent warming of the sediments, all cores were immediately placed in a cooling container and were maintained at a temperature of about 4°C. Within the first two days after recovery, gravity cores were cut lengthwise into two halves and were processed within a glove box under argon atmosphere. Sediment samples were taken every 25 cm for pressure filtration. Solid phase samples for total digestions, sequential extractions and mineralogical analyses were taken at 10 cm intervals and were kept in gas-tight glass bottles under argon atmosphere. The storage temperature for all sediments was -20°C to avoid dissimilatory oxidation of reduced species. Teflon-squeezers, provided with 0.2 µm cellulose acetate membrane filters, were used for pressure filtration (5 bar). For H_2S determination 1 mL sub samples of the pore water were added to a ZnAc-solution (400 µL) in order to fix all sulfide as ZnS. Sub samples for sulfate determination were diluted 1:20 and stored frozen for ion chromatography (HPLC). All further analyses were carried out at the University of Bremen. Methane was measured with a gas chromatograph (Varian 3400) equipped with a splitless injector, by injecting 20 µL of the headspace gas. The concentrations were subsequently corrected for sediment porosity. H_2S was determined using a titration method. Aliquots of the remaining pore water were diluted and acidified with HNO_3 for determination

of cations by atomic absorption spectrometry (AAS, Unicam Solaar 989 QZ) and inductively coupled plasma atomic emission spectrometry (ICP-AES, Perkin Elmer Optima 3000 RL).

All solid phase analyses were performed on anoxic subsamples. Sample solutions obtained by total acid digestion were analyzed by ICP-AES, with an analytical precision of less than 3%. Total carbon (TC) and total organic carbon (TOC) contents were determined by measuring freeze-dried and homogenized samples using a LECO CS-300 carbon sulfur analyzer. For organic carbon analysis, the samples were treated with 12.5% HCl, washed two times with Milli Q and dried at 60°C. The accuracy, checked by marble standards, was ± 3%. Sediment physical measurements of electrical resistivity, as a measure of porosity and density, were performed at a resolution of 1 cm on board using a GEOTEK Multi-Sensor Core Logger (MSCL). Selected dry bulk sediment samples were analyzed by scanning electron microscopy (SEM) using a Philips XL30 SFEG (operating between 10 kV to 12 kV) equipped with an EDAX energy dispersive spectrometer (EDS). Non-embedded powder samples were fixed on a carbon sticker, previously stuck onto the top of a standard SEM stub, and coated under argon atmosphere with a 5 nm Pt/Pd layer. For EDS analysis the analytical program AnalySIS Pro was applied.

3. RESULTS AND DISCUSSION

3.1. Authigenic Barite Fronts

In contrast to the non-reactive terrigenous Ba phase, biogenic barium is discussed as the labile Ba phase which is subject to (partial) remobilization in marine sediments due to sulfate depletion (e.g. McManus et al., 1994; Torres et al., 1996a). Because of the high productivity within the Benguela upwelling area the input of reactive (biogenic) barium into the sediment in this area is displayed by high concentrations, while the amount of terrigenous barium is low (Pfeifer et al., 2001). The pore water and solid phase barium profiles at site GeoB 8426 (Fig. 2) display the typical diagenetic cycling of barium as discussed by von Breymann et al. (1992).

The reactive solid phase barium is dissolved in the sulfate-depleted zone below the SMT and Ba^{2+} is released into the pore water. The upward migration of the dissolved barium into the sulfate-bearing zone is leading to the precipitation of authigenic barite at the SMT, which is currently located at about 3.20 mbsf at site GeoB 8426. Just below the SMT, the solid phase profile displays a pronounced Ba peak (Fig. 2). This Ba enrichment contains barite particles, which partially show dissolution structures (Fig. 3). This “double” barium peak indicates a recent upward shift in the SMT, with the small uppermost peak representing the site of the current/active barite front. Due to the diagenetic cycling of reactive barium, the authigenic barite peak is slowly but constantly growing. The active front slowly moves upward, keeping a constant offset to the sediment surface, corresponding to the SMT.

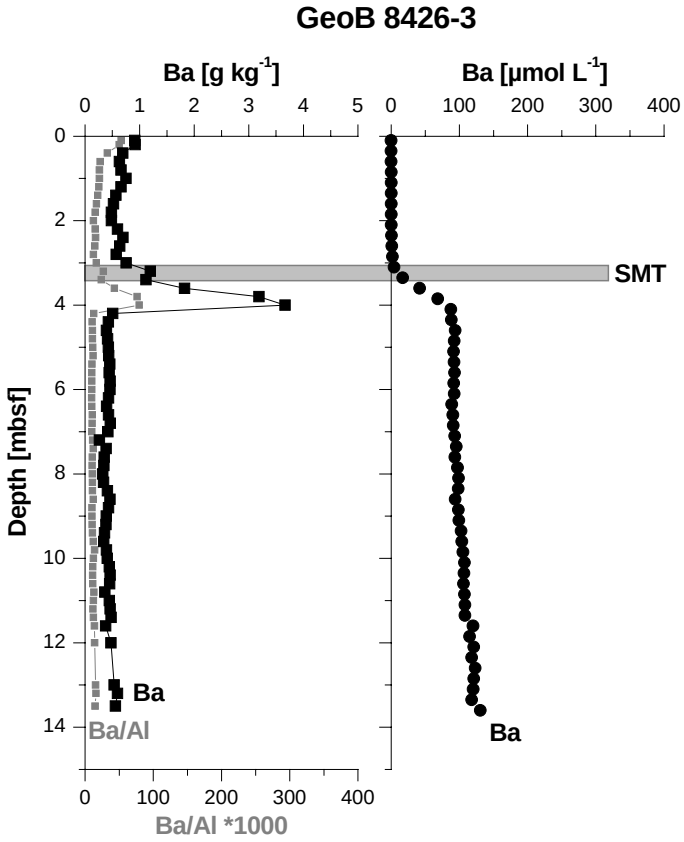

Fig. 2. Solid phase and pore water profiles of barium at site GeoB 8426. The current position of the barite front at the sulfate/methane transition (SMT) is indicated by the gray bar.

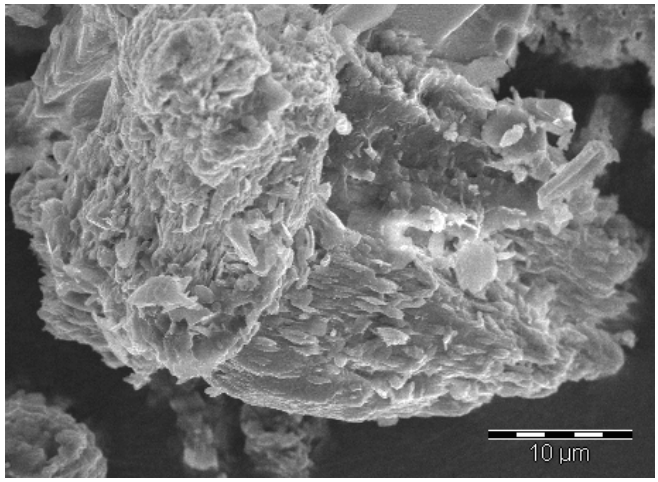

Fig. 3. Scanning electron micrograph of a larger barite particle at site GeoB 8426 slightly below the SMT (3.83 mbsf).

The penetration depth of sulfate in the study area is controlled by the anaerobic oxidation of methane (AOM) as shown by Niewöhner et al. (1998). At the SMT sulfate is consumed, and hydrogen sulfide is produced due to AOM (e.g. Barnes and Goldberg, 1976; Bernard, 1979).

The sulfate pore water profiles of the investigated cores GeoB 8426-3 and GeoB 8455-2 show a linear decrease with depth (Fig. 4). At site GeoB 8455 the SMT is located at about 3.80 mbsf, where solid phase barium is enriched similar to site GeoB 8426 with a second larger peak slightly below the SMT. In contrast to site GeoB 8426, the barium solid phase profile at site GeoB 8455 is characterized by the occurrence of two further distinct Ba peaks a few meters below the SMT (Fig. 5).

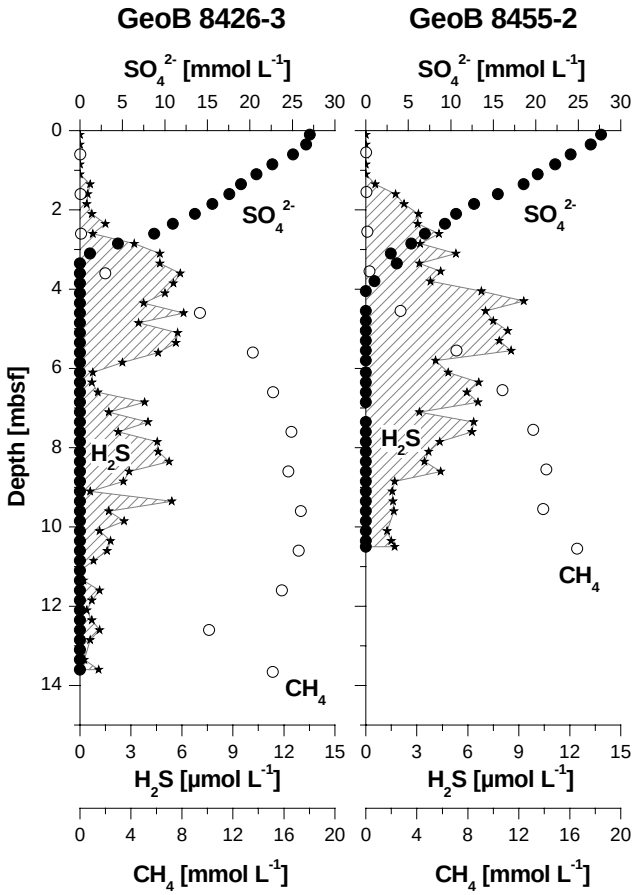

Fig. 4. Pore water profiles of sulfate, methane und hydrogen sulfide at the investigated sites.

The shape of the barium pore water profile reveals that the deeper buried barium enrichments provide an source for barium into the pore water. This indicates the presence of reactive Ba phases in the sediment. Selected, representative samples analyzed by SEM and EDS indicate, that the main Ba-mineral present in these enrichments is barite. Although the deeper buried barite fronts, at depths of about 7.69 and 9.18 mbsf, are dominated by rather small particles, the shape of the barite crystals is similar to those found within the barite peak at the SMT. Some barite crystals from the barite fronts in the sediments of core GeoB 8455-2 are displayed in Fig. 6 A-F. In contrast to the displayed barite particles at 4.22 mbsf, the barite grains at 7.69 and 9.18 mbsf show strong dissolution structures.

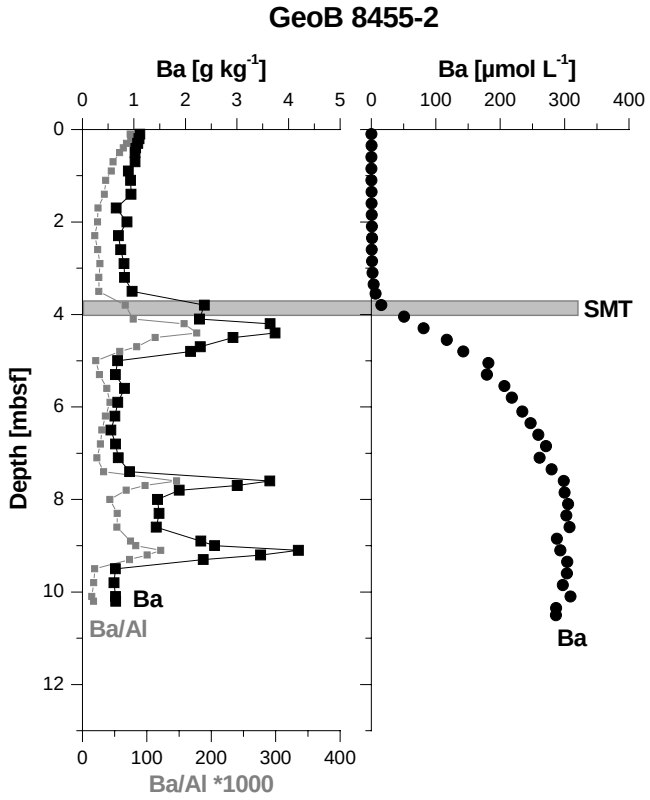

Fig. 5. Barium enrichments at site GeoB 8455. The gray bar marks the current barite front at the sulfate/methane transition (SMT). Two further barium enrichments are located a few meters below the SMT, indicating a release of barium into the pore water displayed by the dissolved barium profile.

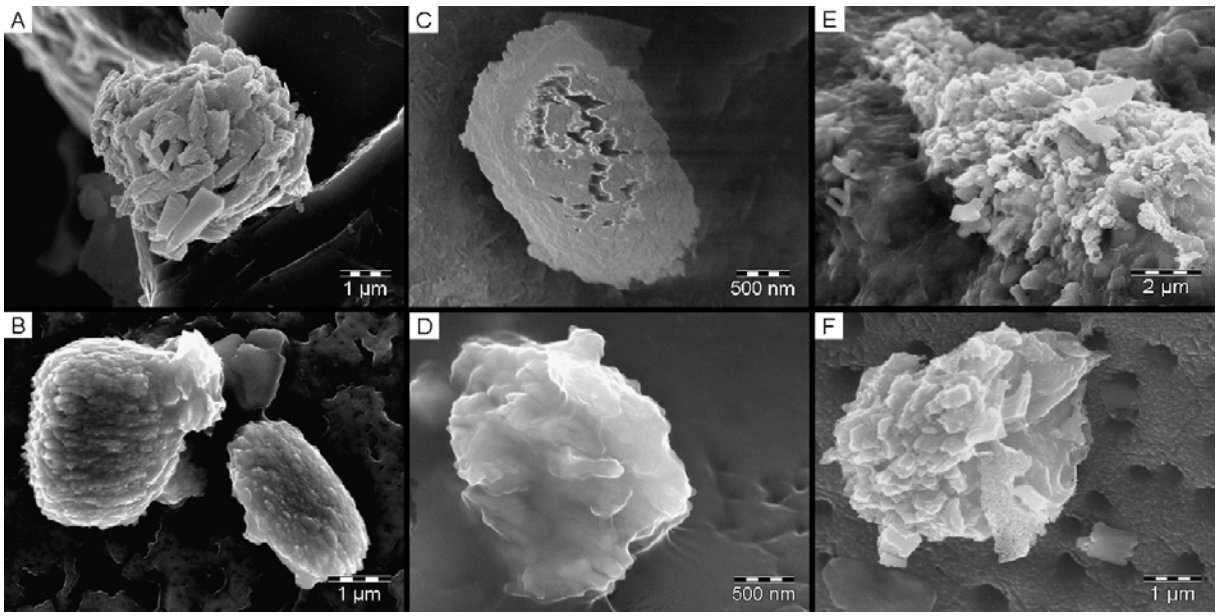

Fig. 6. Scanning electron microscope images of barite crystals at site GeoB 8455 at: A and B: 4.22 mbsf. C and D: 7.69 mbsf. E and F: 9.18 mbsf. The barite particles of the last four panels (C – F) show strong dissolution structures.

3.2. Enrichment Calculation

Under the premise of a constant diffusive upward flux of barium into the sulfate-bearing zone, we calculated the time needed to produce the measured barium enrichment in the solid phase at the SMT. The duration of barium precipitation can be simulated assuming linear diffusive concentration gradients over time (see also Dickens, 2001). Slight changes in the average porosity have substantial influence on the calculated enrichment periods. It has to be clearly pointed out that the calculated time needed for the formation of each barium enrichment is just an approximation due to these uncertainties. The calculation of the diffusive fluxes was performed according to Fick's first law with a diffusion coefficient in free solution (D_0) for barium of 147,6 cm^2 yr^{-1}, which was corrected for tortuosity (for details see Schulz, 2000). The relict concentration of solid phase barium at sites GeoB 8426 and GeoB 8455 amounts to 0.5 g kg^{-1} and 0.65 g kg^{-1}, respectively, and the dry density averages 2.7 g cm^{-3}. If we assume an average porosity of 75% for both cores, the time needed to produce the observed barium peaks at the SMT would be between 11,000 and 13,000 years. Assuming that the barium flux decreased with time, due to the decreased amount of reactive barite at the subjacent barium fronts or a decreased dissolution rate, the calculated times would be slightly overestimated. However, the results of the calculation emphasize that the barite enrichments in the deeper sediments at site GeoB 8455 were exposed to a sulfate-depleted environment for at least 10,000 years.

3.3. Numerical Modeling

To assess the influence of different mechanisms and/or conditions on the observed solid phase barium profiles observed in core GeoB 8455-2, such as dissolution rates, diffusive barium fluxes or variations in sedimentation rate or methane flux, we simulated different scenarios by numerical modeling. These computer simulations are based on the assumption that the amount of diagenetic barite, which precipitated at the SMT, was primarily supplied by upward diffusion of dissolved barium, resulting from the dissolution of barite at the subjacent peaks.

To simulate the process of barite dissolution and reprecipitation, the column transport and reaction model CoTReM was used. A detailed description of this computer software is given in the CoTReM User Guide (Adler et al., 2000; http://www.geochemie.uni-bremen.de/downloads/cotrem/index.htm) and by Adler et al. (2001). The model area, representing the core length of 12 m, was subdivided into cells of 5 cm thickness. The time step to fulfill numerical stability was set to 1 x 10^{-1} yr, and the porosity of the sediment was set to 75%. The sulfate bottom water concentration of 28 mmol/L was defined as the upper boundary condition. To define a diffusive flux of methane into the model area from below, we started with a fixed methane concentration of 36 mmol/L at the lower boundary. This methane value was defined to create the gradient necessary to simulate the measured influx of CH_4. The concentration of refractory solid phase barium below the SMT was set to 0.65 mg kg^{-1}

and the input concentration above the SMT was 1.0 mg kg^{-1}. For site GeoB 8455 we used a mean SR of 10 cm kyr^{-1}, adopted from adjacent sampling sites at similar water depths with sedimentation rates of 8-11 cm kyr^{-1} (Donner and Giese, 1992; Mollenhauer et al., 2002).

Modeling of the measured barium pore water profile of site GeoB 8455 reveals that the dissolution rate of barite directly below the SMT is much higher (about one order of magnitude) than at the deeper buried Ba enrichments. This indicates that the dissolution of barite at these deeper fronts must be decelerated compared to the dissolution rates directly below the SMT. Furthermore, the results of the simulations show that at steady state conditions the thickness of the barium peak at the SMT (mainly) depends on the sedimentation rate. At the investigated sites the barite peaks at the SMT are characterized by a large peak and a second, smaller one directly above, representing the current barite front. Thus, there must have been a slight recent upward shift of the SMT, resulting in the formation of the uppermost barite enrichment. To find out whether this process is limited to the investigated sites, we compared barium solid phase data of adjacent coring sites, e.g. site GeoB 3718 (Heuer et al., 2002, Kasten et al., 2003). The similarity in the shape of the barium profiles and the formation times reveals a more regional process.

Modeling the current positions of the barium peaks in core GeoB 8455-2 indicates an enrichment due to non-steady state conditions. Possible non-steady state processes causing the formation of the observed barite fronts could be related to the sediment composition, the depositional dynamics, such as drastic changes in the sedimentation rate, or variations in the upward methane flux. An increase in the upward flux of methane over a larger area can be caused by the degradation of organic matter in deeper sediments, or the decomposition of gas hydrate. Although the thermodynamic stability criteria for gas hydrate at the sampling sites are fulfilled, no indications of gas hydrates could be found in the sediments. High resolution echosounder profiles, as recorded by the PARASOUND shipboard system, indicate no depositional irregularities. An increase in methane concentrations could be explained by the burial of high amounts of non-refractive organic matter below the SMT and resulting elevated rates of methanogenesis due to the degradation of the organic matter. But this process would be assumed to be more regional. Regional processes can only account for the recent shift of the SMT leading to the formation of the small current barite peak, which was found at both studied sites. In contrast, the finding of additional barium enrichments below the SMT is limited to site GeoB 8455. However, because the sedimentary records do not indicate any sedimentary event, we assume that a change in the methane flux is the only process which also explains the prior pronounced shift in the SMT, and thus the preservation of additional barium fronts a few meters below the current SMT.

3.4. Barite Preservation

In sulfate-depleted marine sediments, barite is supposed to be highly instable. The results of a dissolution experiment performed by Schweizer et al. (subm.), using freshly precipitated barite in sulfate-free artificial seawater, demonstrate that barite dissolution is a fast process

which occurs on a time scale of minutes. This result is in good agreement with rates reported by Dove and Platt (1995). Adopting such high dissolution rates in the numerical model described above, the total amount of barite below the SMT would be dissolved within a very short time. In contradiction to these experimental dissolution rates, the modeled rates are about 6 orders of magnitudes lower. This emphasizes that the dissolution rates in natural marine environments are much lower than those obtained under laboratory conditions, which is documented by the occurrence of barite enrichments below the SMT at site GeoB 8455. Furthermore, it shows that additional processes or conditions decelerate the dissolution rate of barite in the sulfate-depleted sediments at site GeoB 8455.

One mechanism in this regard could be the strikingly high amount of total barium in the sediment system at site GeoB 8455 (Fig. 5). High concentrations of dissolved barium below the SMT could influence the dissolution rate of barite. Modeling such high barium concentrations in pore water by using PHREEQC 2.10 (Parkhurst and Appelo, 1999) indicates that very low concentrations of sulfate would be sufficient to obtain the barite saturation. Thus, at high barium pore water concentration the equilibrium with respect to barite is obtained with only low sulfate concentrations. Therefore, high concentration of barium in the pore water results in lower barite dissolution.

Further explanation concerning the enrichment of barium minerals in the sulfate-depleted zone could be the occurrence of other Ba phases, which show decreased amounts of oxygen compared to common barite element associations. Energy dispersive spectra of barium particles from the deeper buried barium enrichments at site GeoB 8455 reveal that some barium phases are decreased in oxygen concentrations while the amount of sulfur and barium is constant and only the carbon concentration increases (Fig. 7). This suggests that some barite particles were altered, or that primary sulfate-free Ba phases exist. González-Muñoz et al. (2003) reported microbially mediated precipitation of barite under laboratory conditions, and found that Ba phases were incorporated into spherical aggregates without sulfate. These spherical aggregates of 0.5 to 1 μm in diameter show a striking similarity to some of the barium particles which were found within the barium enrichments at site GeoB 8455 (Fig. 7C). The observed spherical aggregates described by González-Muñoz et al. (2003) mainly contained barium and phosphorus and were supposed to represent an early stage of crystal growth. This does not necessarily imply that the spherical aggregates found in core GeoB 8455-2 were formed by bacterially mediated processes, but that the crystals either are in an early stage of growth, or that the growth of the crystals was inhibited at an early stage.

Another process which could explain the occurrence of oxygen-depleted Ba phases compared to barite would be the dissimilatory reduction of sulfate from barite, as investigated by Baldi et al. (1996). On base of laboratory results, they discussed the microbial reduction of barite via the formation of other barium compounds, such as witherite ($BaCO_3$) and the transient species barium sulfide (BaS). These coexisting barium phases were also reported by Malysh

et al. (2002). They examined the influence of carbon-containing phases on the reduction of recycled barite in laboratory experiments.

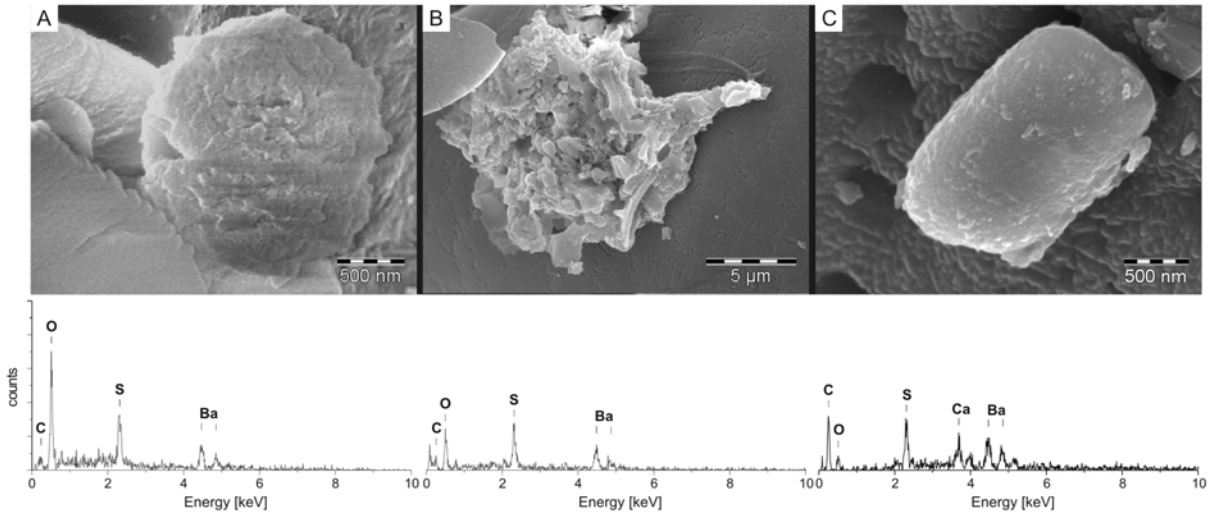

Fig. 7. Energy dispersive spectra (EDS) of barium particles (site GeoB 8455). A: Barite crystal at 7.69 mbsf with a characteristic barite ratio of barium, sulfur, and oxygen. B: Larger barite crystal with strong dissolution structures at 9.18 msbf. The EDS spectrum indicates a decreased oxygen concentration. C: Barium particle at 9.18 mbsf with calcium incorporations and carbon, but low oxygen concentrations.

The reduction of barite, or more precisely the reduction of barium-sulfate, with carbon leads to the formation of the mineral witherite via the transient phase barium sulfide:

$$BaSO_4 + 2C \rightarrow BaS + 2CO_2 \qquad (1)$$

$$BaS + CO_2 + H_2O \rightarrow BaCO_3 + H_2S. \qquad (2)$$

This process is accelerated due to the catalyzing effect of the formed barium sulfide particles (Malysh et al., 2002). Furthermore, the conversion of barite into barium sulfide could lead to a coating sulfide rim, which can be compared with coatings of ferric iron minerals by iron sulfides in sulfidic sediments (e.g. Garming et al., in press). This process could shield the barite particle, covered with barium sulfide, from further dissolution. It would also provide a small sink for hydrogen sulfide in deeper sediments. One indication for the process of barite reduction to occur in this environment is the increasing amount of carbon with decreasing oxygen concentrations found in some of the barium particles from the deeper buried barite fronts at site GeoB 8455 (Fig. 7). The sediments of the coring sites are characterized by high concentrations of hydrogen sulfide, high alkalinity (up to 80 mmol(eq) L^{-1}), and high amounts of TOC, and thus would provide a suitable environment for the alteration of barite into witherite (via barium sulfide). However, these processes in marine sediments require further investigations.

4. CONCLUSIONS

Sediments of two site from the eastern Cape Basin were examined for pore water and solid phase geochemistry. Small uppermost barium enrichments at both sites at the current SMT and large barium peaks slightly below imply a slightly upward shift of the SMT in the recent past, which is likely to be a widespread regional phenomenon in the study area. At one site, distinct solid phase barium enrichments occur a few meters below the SMT in sulfate-depleted sediments, which are dominated by small barite particles. These preserved buried barite fronts indicate former positions of the SMT. We assume that the abrupt relocation of the SMT, and thus the formation of new barite fronts, is most likely triggered by an increase in the upward flux of methane. Calculations of the formation time of these enrichments and numerical modeling suggest that this shift of the SMT occurred between the last glacial maximum (LGM) and the Pleistocene/Holocene transition. High amounts of non-refractive organic matter buried below the SMT, which lead to higher rates of methanogenesis, could explain such increases in methane concentrations and fluxes. Our results highlight the importance of quantity and quality of settling organic matter concerning biochemical processes in deeper sediments. Furthermore, the detection of barite below the SMT indicates that although being metastable/instable in the prevailing geochemical environments, such minerals can be preserved/shielded from dissolution by specific processes or mechanisms, and thus be buried into deeper sediments. At such depths barite, for example, could fuel/support AOM to proceed below the SMT. Thus, reactive minerals buried in deeper sediments can have great influence on biogeochemical processes in the deep biosphere by providing terminal electron acceptors.

Acknowledgements. We thank the crew and scientists aboard the RV *Meteor* for their strong support during cruise M57/2. For technical assistance on board and in the home laboratory we are indebted to S. Hessler and S. Siemer. SEM analyses were carried out at Utrecht University, EMSA. The people there are thanked for their hospitality and cooperation. Furthermore we would like to thank G. Bohrmann, G.R. Dickens, M. Kölling, and M. Zabel for detailed comments. Our special appreciation goes to H.D. Schulz for helpful discussions. This research was funded by the Deutsche Forschungsgemeinschaft as part of the Research Center "Ocean Margins" (RCOM) of the University of Bremen contribution no. XXXX.

REFERENCES

Adler, M., Hensen, C., and Schulz, H.D. (2000) CoTReM – Column Transport and Reaction Model. http://www.geochemie.uni-bremen.de/downloads/cotrem/index.htm, User Guide, Version 2.3.

Adler, M., Hensen, C., Wenzhöfer, F., Pfeifer, K., and Schulz, H.D. (2001) Modeling of subsurface calcite dissolution by oxic respiration in supralysoclinal deep-sea sediments. *Mar. Geol.* **177**, 167-189.

Baldi, F., Pepi, M., Burrini, D., Kniewald, G., Scali, D., and Lanciotti, E. (1996) Dissolution of barium from barite in sewage sludges and cultures of *Desulfovibrio desulfuricans. Appl. Environ. Microbiol.* **62**, 2398-2404.

Barnes, R.O. and Goldberg, E.D. (1976) Methane production and consumption in anoxic marine sediments. *Geology*, **4**, 297-300.

Bernard, B.B. (1979) Methane in marine sediments. *Deep-Sea Res*. **26A**, 429-443.

Bishop, J.K. (1988) The barite-opal-organic carbon association in oceanic particular matter. *Nature* **24**, 341-343.

Bremner, J.M. and Willis, J.P. (1993) Mineralogy and geochemistry of the clay fraction of sediments from the Namibian continental margin and the adjacent hinterland. *Mar. Geol.* **115**, 85-116.

Chow, T.J. and Goldberg, E.D. (1960) On the marine geochemistry of barium. *Geochim. Cosmochim. Acta* **20**, 192-198.

Church, T.M. (1979) Marine Barite. In *Marine Minerals* (ed. R.G. Burns). Rev. Mineral., Miner. Soc. Am. **6**, pp. 175-209.

Cronan, D.S. (1974) Authigenic minerals in deep-sea sediments. In *The sea,* **5** (ed. E.D. Goldberg). Wiley Interscience, pp. 491-525.

Dean, W.E. and Schreiber, B.C. (1978) Authigenic barite, Leg 41 Deep Sea Drilling Project. In *Proc. ODP, Init. Repts.* **41** (eds. Y. Lancelot, E. Seibold, et al.). U.S. Gov. Off., Washington, D.C., pp. 915-931.

Dehairs, F., Chesselet, R., and Jedwab, J. (1980) Discrete suspended particles of barite and the barium cycle in the open ocean. *Earth Planet. Sci. Lett.* **49**, 915-931.

Dehairs, F., Stroobants, N., and Goeyens, L. (1991) Suspended barite as a tracer of biological activity in the Southern Ocean. *Mar. Chem.* **35**, 399-410.

Dickens, G.R. (2001) Sulfate profiles and barium fronts in sediment on the Blake Ridge: Present and past methane fluxes through a large gas hydrate reservoir. *Geochim. Cosmochim. Acta* **65**, 529-543.

Donner, B. and Giese, M. (1992) Stratigraphie und Smear-Slide-Analysen. In *Berichte und erste Ergebnisse über die Meteor-Fahrt M20/2, Abidjan – Dakar, 27.12.1991 – 2.2.1992* (eds. H.D. Schulz and cruise participants). *Ber. Fachb. Geowiss. Univ. Bremen* **25**, pp. 51-80.

Dove, P.M. and Platt, F.M. (1995) Compatible real-time rates of mineral dissolution by Atomic Force Microscopy (AFM). *Chem. Geol.* **127**, 331-338.

Dymond, J., Suess, E., and Lyle, M. (1992) Barium in deep-sea sediment: A geochemical proxy for paleoproductivity. *Paleoceanography* **7**, 163-181.

Embley, R.W. and Morley, J.J. (1980) Quaternary sedimentation and paleoenvironmental studies off Namibia (South-West Africa). *Mar. Geol.* **36**, 183-204.

Ganeshram, R.S., Franc, R., Commeau, J., and Brown-Leger, S.L. (2003) An Experimental Investigation of Barite Formation in Seawater. *Geochim. Cosmochim. Acta* **67**, 2599-2605.

Garming, J.F.L., Bleil, U., and Riedinger, N. (in press) Alteration of magnetic mineralogy at the sulfate methane transition: Analysis of sediments from the Argentine continental slope. *Phys. Earth Planet. Inter.*

Gingele, F. and Dahmke, A. (1994) Discrete barite particles and barium as tracers of paleoproductivity in South Atlantic sediments. *Paleoceanography* **9**, 151-168.

Gingele, F.X., Zabel, M., Kasten, S., Bonn, W.J., and Nürnberg, C.C. (1999) Biogenic Barium as a Proxy for Paleoproductivity: Methods and Limitations of Application. In *Use of proxies in paleoceanography: Examples from the South Atlantic* (eds. G. Fischer and G. Wefer). Springer, pp. 345-364.

Goldberg, E.D. and Arrhenius, G.O.S. (1958) Chemistry of Pacific pelagic sediments. *Geochim. Cosmochim. Acta* **13**, 153-212.

Gonzáles-Muñoz, M.T., Fernández-Luque, B., Martínez-Ruiz, F., Cheroun, K.B., Arias, J.M., Rodríguez-Gallego, M., Martínez-Cañamero, M., de Linares, C., and Paytan, A. (2003) Precipitation of barite by *Myxococcus xanthus*: Possible implications for the biogeochemical cycle of barium. *Appl. Environ. Microbiol.* **69**, 5722–5725.

Heuer, V. (2002) Spurenelemente in Sedimenten des Südatlantik: Primärer Eintrag und frühdiagenetische Überprägung. Ph.D. Dissertation, *Ber. Fachb. Geowiss. Univ. Bremen* **209**.

Kasten, S. and Jørgensen, B.B. (2000) Sulfate reduction in marine sediments. In *Marine Geochemistry* (eds. H.D. Schulz and M. Zabel). Springer, pp. 263-281.

Kasten, S., Zabel, M., Heuer, V., and Hensen, C. (2003) Processes and Signals of Nonsteady-State Diagenesis in Deep-Sea Sediments and their Pore Waters. In *The South Atlantic in the Late Quaternary: Reconstruction of material budget and current systems* (eds. G. Wefer, S. Mulitza, and V. Ratmeyer). Springer, pp. 431-459.

Malysh, L.A., Gaisin, L.G., Volkova, M.F., Prokhorov, A.G., and Tkachev, K.V. (2002) Reduction of recycled barium sulfate. *Russ. J. Appl. Chem.* **75**, 14-17.

McManus, J., Berelson, W.M., Klinkhammer, G.P., Kilgore, T.E., and Hammond, D.E. (1994) Remobilization of barium in continental margin sediments. *Geochim. Cosmochim. Acta* **58**, 4899-4907.

McManus, J., Berelson, W.M., Klinkhammer, G.P., Johnson, K.S., Coale, K.H., Anderson, R.F., Kumar, N., Burdige, D.J., Hammond, D.E., Brumsack, H.J., Mccorkle, D.C., and Rushdi, A. (1998) Geochemistry of barium in marine sediments: Implications for its use as a paleoproxy. *Geochim. Cosmochim. Acta* 62, 3453–3473.

Mearon, S., Paytan, A., and Bralower, T.J. (2002) Cretaceous strontium isotope stratigraphy using marine barite. *Geology* **31**, 15–18.

Mollenhauer G., Schneider, R.R., Müller, P.J., Spieß, V., and Wefer, G. (2002) Glacial/interglacial variability in the Benguela upwelling system: Spatial distribution and budgets of organic carbon accumulation. *Global Biogeochem. Cycles* **16,** 1134.

Niewöhner, C., Hensen, C., Kasten, S., Zabel, M., and Schulz, H.D. (1998) Deep sulfate reduction completely mediated by anaerobic methane oxidation in sediments of the upwelling area off Namibia. *Geochim. Cosmochim. Acta* **62**, 455-464.

Parkhurst, D.L. and Appelo, C.A.J. (1999) *User's guide to PHREEQC (Version 2.0)*. U.S. Geol. Surv., Water Resour. Inv. Rep., pp. 99-4259.

Paytan, A., Kastner, M., Martin, E.E., Macdougall, J.D., and Herbert, T. (1993) Marine barites as a monitor of seawater strontium isotope compostion. *Nature* **366**, 445-449.

Paytan, A., Kastner, M., and Chavez, F.P. (1996) Glacial to interglacial fluctuations in productivity in the Equatorial Pacific as indicated by marine barite. *Science*, **274**, 1355-1357.

Paytan, A., Mearon, S., Cobb, K., and Kastner, M. (2002) Origin of marine barite deposits: Sr and S isotope characterization. *Geology* **30**, 747-750.

Pfeifer, K., Kasten, S., Hensen, C., and Schulz, H.D. (2001) Reconstruction of primary productivity from the barium contents in surface sediments of the Atlantic Ocean. *Mar. Geol.* **177**, 13-27.

Rogers, J. and Bremner, J.M. (1991) The Benguela ecosystem. Part VII. Marine-geological aspects. Oceanogr. *Mar. Biol. Annu. Rev.* **29**, 1-85.

Schulz, H.D. (2000) Quantification of early diagenesis: dissolved constituents in marine pore water. In *Marine Geochemistry* (eds. H.D. Schulz and M. Zabel). Springer, pp. 85-128.

Schweizer, M., Kasten, S., Pfeifer, K., and Schulz, H.D. (subm.) Gas hydrate decomposition recorded by authigenic barite precipitates: A process study from the northern Congo Fan. *Mar. Geol.*

Shannon, L.V. (1985) The Beguela ecosystem part 1: Evolution of the Benguela, physical features and processes. *Oceanogr. Mar. Biol. Annu. Rev.* **23**, 105-182.

Shannon, L.V. and Nelson., G. (1996) The Benguela: Large Scale Features and Processes and System Variability. In The South Atlantic: Present and Past Circulation (eds. G. Wefer, W. Berger, G. Siedler, and D. Webb). Springer, pp. 163-210.

Summerhayes, C.P., Bornhold, B.D., and Embley, R.W. (1979) Surficial slides and slumps on the continental slope and rise off South-West Africa. *Mar Geol.* **31**, 265-277.

Torres, M.E., Brumsack, H.J., Bohrmann, G., and Emeis, K.C. (1996a) Barite fronts in continental margin sediments: A new look at barium remobilization in the zone of sulfate reduction and formation of heavy barites in diagenetic fronts. *Chem. Geol.* **127**, 125-139.

Torres, M.E., Bohrmann, G., and Suess, E. (1996b). Authigenic barites and fluxes of barium associated with fluid seeps in the Peru subduction zone. *Earth Planet. Sci. Lett.* **144**, 469-481.

Varnavas, S.P. (1987) Marine barite in sediments from deep sea drilling project sites 424 and 424A (Galapagos hydrothermal mounds field). *Mar. Chem.* **20**, 245-253.

von Breymann, M.T., Brumsack, H., and Emeis, K.-C. (1992). Depositional and diagenetic behavior of barium in the Japan Sea. In *Proc. ODP, Sci. Resul.* **127/128** (eds. K.A. Pisciotto, J.C. Ingle, M.T. von Breymann, J. Barron, et al.). College Station, Texas, pp. 651-663.

Wefer, G. and Fischer, G. (1993) Seasonal patterns of vertical flux in equatorial and coastal upwelling areas of the eastern Atlantic. *Deep-Sea Res. I* **40**, 1613-1645.

Zabel, M. and cruise participants (2003) Report and preliminary results of *Meteor* cruise M 57/2, Walvis Bay – Walvis Bay, 11.02. - 12.03.2003, *Ber. Fachb. Geowiss. Univ. Bremen* **220**.

Microbial alteration of pyrite under anoxic conditions

N. Riedinger*[1], M. Krüger[2,3], K. Zengler,[2,4] and S. Kasten[1,5]

[1] *Fachbereich Geowissenschaften, Universität Bremen, Klagenfurter Straße, 28359 Bremen, Germany*
[2] *Max Planck Institute for Marine Microbiology, Celsiusstrasse 1, 28359 Bremen, Germany*
[3] *current address: Geomicrobiology, Federal Institute for Geosciences and Resources (BGR), Stilleweg 2, 30655 Hannover, Germany*
[4] *current address: Diversa Corporation, San Diego, CA 92121, USA*
[5] *current address: Alfred Wegener Institute for Polar and Marine Research, Am Handelshafen 12, 27570 Bremerhaven, Germany*

Abstract

Pyrite is the dominant iron sulfide in marine sediments, while in deeper sediments other iron sulfide minerals are often enriched compared to pyrite. We hypothesize that in anoxic sediments microorganisms can use hydrogen (H_2) as electron donor to reduce pyrite (FeS_2) to iron monosulfide (FeS). Therefore, the role of indigenous microbial communities in the process of pyrite reduction to FeS with H_2 as the required electron donor in anoxic marine sediments was investigated. To reveal the capability of microorganisms to perform the postulated process, different assays containing pyrite inoculated with marine inoculum as well as abiotic controls were continuously sampled for microbiological and geochemical investigations over a time period of about one year. We assigned the observed release of ferrous iron into the medium to the reduction of pyrite to FeS mediated by microorganisms. This assumed mechanism of microbial pyrite reduction is a promising approach to explain the alteration of minerals which are generally assumed to be stable in anoxic marine environments.

Key words: Anoxic marine sediments, Hydrogen, Iron monosulfide (FeS), Microbial reduction, Pyrite (FeS_2)

1. Introduction

In anoxic marine sediments, authigenic iron sulfides are formed as the result of bacterial sulfate reduction. The degradation of organic matter by sulfate reducing bacteria and sulfate reduction driven by anaerobic oxidation of methane (AOM), release substantial amounts of hydrogen sulfide (H_2S) into the pore water (Barnes and Goldberg, 1976; Jørgensen, 1982; Blair and Aller, 1995; Niewöhner et al., 1998). The liberated H_2S can react with dissolved iron or reactive iron phases to form iron sulfide minerals (e.g. Berner, 1984; Canfield and Berner, 1987; Canfield, 1989). The formation of pyrite (FeS_2) is presumably due to the oxidation of FeS by H_2S or with polysulfides (Berner, 1970; Morse et al., 1987; Luther, 1991; Schoonen and Barnes, 1991; Rickard and Luther, 1997; Morse, 2002). Donald and Southam (1999) suggested that sulfate reducing bacteria are able to stimulate the transformation of FeS into pyrite. The released H_2, as a result of this oxidation process, provides an (additional) energy source for microbial metabolism (Drobner et al., 1990; Rickard, 1997). However, the different proposed pathways of pyrite formation have only been demonstrated in laboratory experiments (Morse, 2002), thus it is still not clear which parameters drive the formation of pyrite in natural marine environments.

At the sediment surface, pyrite is chemically oxidized by O_2 (Ferdelman et al., 1997). Only in deeper subsurface sediments under anoxic conditions pyrite is supposed to be stable (Berner, 1971). In contrast, biologically mediated anaerobic FeS oxidation by MnO_2 in marine sediments was shown by Aller and Rude (1988). In addition, Schippers and Jørgensen (2002) demonstrated that in anoxic marine sediments also pyrite can be oxidized by MnO_2. Furthermore, they studied the potential of NO_3^{2-} and Fe(III)-oxides as electron acceptors. Although these oxidizing processes using the latter electron acceptors are possible according to thermodynamic considerations, they could not be detected by Schippers and Jørgensen (2002).

Although pyrite is the predominant iron sulfide mineral in marine sediments, iron sulfides like greigite and pyrrhotite, which are intermediates in pyrite formation, have been reported to accumulate in marine sediments as well (Roberts and Turner, 1993, Kao et al., 2004). In deeper sediments intermediate iron sulfides even dominate the sediment composition compared to pyrite (Kasten et al., 1998). So, the question arises, whether in deeper sediments these minerals are only initial/intermediate phases in the sequence of reactions leading to pyrite formation, as discussed for Black Sea sediments (Jørgensen et al., 2004, Neretin et al., 2004), or possibly result from the reverse reaction, the alteration of pyrite into FeS.

In this study we investigated the role of indigenous microbial communities in the process of pyrite reduction to FeS in anoxic marine sediments using H_2 as the electron donor – a process that is reverse to the formation of pyrite. To reveal the capability of microorganisms to perform/mediate the postulated process, different set-ups of pyrite inoculated with marine

inoculum from wadden sea as well as abiotic controls, were continuously sampled and measured over a time period of approximately one year.

2. Material and Methods

2.1. Extraction of Microorganisms from Sediments

The extraction of microorganisms from anoxic sediments was carried out by a method modified after Bakken and Lindahl (1995). Nycodenz®, a non-ionic tri-iodinated derivative of benzoic acid with three aliphatic hydrophilic side chains, was used to carry out the separation of intact living cells from the sediment by centrifugation. To prepare the Nycodenz® solution, 8 g of Nycodenz® were dissolved in 10 mL sulfate reduced medium. The anoxic, sulfate reduced artificial seawater medium was prepared as described by Widdel and Bak (1992).

Microorganisms were extracted from anoxic wadden sea sediment retrieved from the intertidal mud flats at the Padingbütteler Deich, close to Misselwarden, Germany. To homogenize the sediment, about 4 kg of fresh anoxic marine sediment with a temperature of about 4°C were mixed with cold oxygen-free seawater (1:1). The suspension was kept cool and stirred 2 times on a magnetic stirrer for 15 min, interrupted to be ultrasonicated twice for 1.5 min. Afterwards, the suspension was transferred into 500 mL centrifuge bottles and centrifuged at 800 x *g* for 15 min at 4°C to pellet the sediment. The supernatant was decanted into separate 500 mL centrifuge bottles and stored at 4°C. The sediment pellet was extracted again with cold, oxygen-free seawater. This step was repeated twice. The pooled supernatant containing microbes was centrifuged at 800 x *g* for 15 min at 4°C to remove residual sediment. Then, the supernatant was transferred into new 500 mL centrifuge bottles and centrifuged at 14,000 x *g* for 25 min at 4°C to pellet microbial cells. The supernatant was poured into a new bottle and the pellet was thoroughly resuspended to a final volume of 10 mL. This suspension was transferred into a 25 mL centrifuge tube and an equal volume of Nycodenz® solution was added below the sediment resuspension, creating a cushion. To produce a distinct layer the Nycodenz® - sediment resuspension was centrifuged in a swing-out rotor at 10,000 x *g* for 2 h at 4°C. The middle layer, containing the bacterial cells, was carefully transferred (under anoxic conditions) into a new tube. To remove the remaining Nycodenz®, the pellet was resuspended in medium and centrifuged again at 10,000 x *g* for 15 min. This step was repeated twice and afterwards the pellet was resuspended in medium to the final volume (1-2 mL) and stored anoxically. The presence of living microorganisms was verified by microscopic analysis.

2.2. Pyrite Preparation

The pyrite used in the experiment was collected from the lime pit Lägerdorf, Company Alsen AG. A few kg of the pyrite nodules were broken up into smaller pieces in a jaw crusher and

afterwards sieved to gain the <63 µm fraction. To remove oxidized iron and FeS from the surface, the fine grained pyrite was washed with boiling 6 molar HCl and subsequently rinsed with oxygen-free, deionized water (MilliQ). Afterwards, free sulfur was removed from the surface of the remaining pyrite by washing with boiling acetone and rinsing with oxygen-free MilliQ (modified after Schippers and Jørgensen, 2001). The washing steps were carried out under anoxic conditions (argon), using a vacuum filtration with a regenerated cellulose filter of 0.65 µm pore size. In the final step the pyrite was dried under permanent argon supply. In the treated sample, pyrite was the only mineral detected by X-ray diffraction (XRD). The surface area of the extracted pyrite fraction averages 0.4 m^2 g^{-1}, measured by using the BET-method (Brunauer et al., 1938).

2.3. Anoxic Pyrite Oxidation Experiments

For the experiment we chose closeable, flat flange glass vessels with a diameter of 120 mm (Fig. 1), where the upper part of the glass vessel is divided by a gas permeable disk. The vents in the flat flange lid used for sampling were sealed with butyl-rubber septa and the centered fermentation cap was filled with water. The HCl washed glass vessels were filled with medium under anoxic conditions, in a N_2 flushed glove box, adding pyrite and bacteria depending on the assay requirement (Table 1). Assay BP 1, containing pyrite inoculated with the extracted microorganisms and flushed with H_2/CO_2, where the postulated process is assumed to proceed, is termed the positive assay. BP 2 is flushed with N_2/CO_2 instead of H_2/CO_2, to investigate the role of H_2 as electron donor.

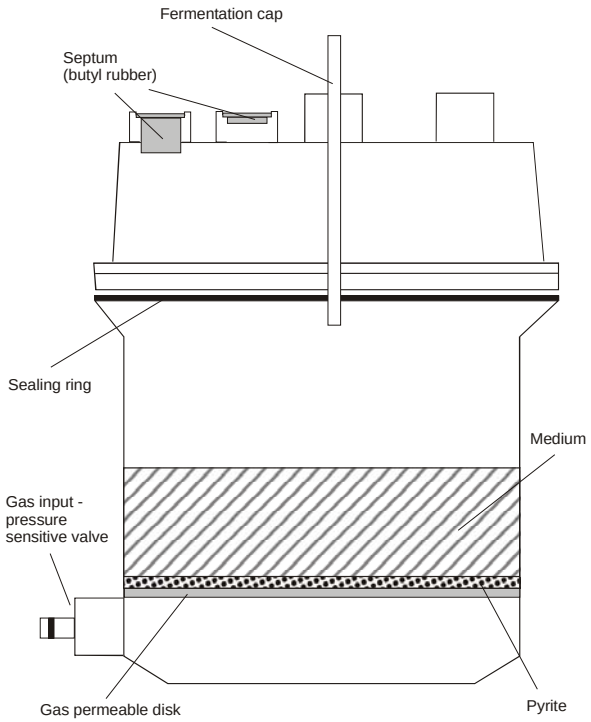

Fig. 1. Sketch of the flat fledge glass vessels used in the experiment. Due to the pressure of the gas mixture the medium is prevented from sinking below the gas permeable disk.

In the BP 3 assay no pyrite is added to define the background concentration for ferrous iron in the medium. BP 4 is the abiotic control and BP 7 is a identical replicate of BP 1. The assays BP 5, BP 6 and BP 8 are the replicates of assay BP 1, BP 3 and BP 4, respectively, without gas supply.

The glass vessels were kept light protected at room temperature and the temperature was recorded over the whole time of the experiment. The assays were daily flushed for a constant time interval with a mixture of H_2/CO_2 (80/20, v/v) and CO_2/N_2 (10/90, v/v), respectively.

Table 1. Complementary list of the experiment with the description of the set ups of each assays.

Glass vessel	FeS_2 [g]	Medium [mL]	Bacteria	H_2/CO_2	N_2/CO_2	Remarks
BP 1	30.5	300	+	+		positive
BP 2	30.5	300	+		+	
BP 3	0.0	300	+	+		
BP 4	30.6	300		+		abiotic control
BP 5	30.4	300				
BP 6	0.0	300	+			
BP 7	30.5	300	+	+		positive replicate
BP 8	30.5	300	+			

A routine oxygen measurement was applied during the experiments by using optical oxygen sensors to exclude the penetration of oxygen into the glass vessels (for detailed information see Hecht and Kölling, 2001).

2.4. Chemical Analysis

Samples were taken weekly for the measurement of pH, E_H and biological studies. All further analyses were carried out on filtered (0.2 µm) samples. Subsamples for sulfate determination were diluted 1:20 for ion chromatography (HPLC). For H_2S determination by titration, 1 mL of the pore water was added to a ZnAc-solution (400 µL) in order to fix all sulfide as ZnS. Aliquots of the remaining pore water were diluted and acidified with HCl for determination of iron and sulfur by ICP-AES techniques (Perkin Elmer Optima 3000 RL). The precision of ICP-AES analyses was better than 3%. Methane was determined using a GC 14B gas chromatograph (Shimadzu) as described in Nauhaus et al. (2002). Short chain fatty acids in pore water samples were determined via analysis with an HPLC equipped with UV and RI detectors (Rabus et al., 1996).

To determine the amount of FeS, solid phase samples were treated with 6 molar HCl and the released H_2S was precipitated in a trap containing a ZnAc solution (Zhabina and Volkov, 1978; Fossing and Jørgensen, 1989), which was adapted to the expected H_2S concentration. To determine the amount of H_2S, the residual Zn concentration of the ZnAc solutions was measured using ICP-AES techniques.

2.5. Microbial Analysis

Epifluorescence microscopy of bacteria
At several time points during the incubations samples were withdrawn for microscopical investigation of microbial growth. Samples (0.5 mL) were fixed with 4% paraformaldehyde solution as described by Eller et al. (2001) and stored in ethanol : phosphate buffered saline (PBS) (1:2) at –20°C until hybridization. Dilutions of these samples were filtered on polycarbonate filters (GTBP, 0.2 µm pore size; Millipore, Eschborn, Germany), stained with Acridine Orange (Meyer-Reil, 1983) and analyzed with an Axioplan microscope (Zeiss, Oberkochen, Germany).

Molecular community analysis
The DNA extraction was carried out using the Fast DNA Kit for Soil (BIO USA) according to the manufacturers instructions. To amplify the 16S ribosomal RNA (rRNA) gene of bacteria, the primer set GM3f/GM4r (Ravenschlag et al., 1999) was used. For sulfate-reducing bacteria a primer set targeting the gene for the adenosine-phosphosulfate-reductase (APS-reductase) was used (Friedrich, 2002). The 16S rDNA of Archaea was amplified with the primer set Arch20F/Arch958R (DeLong, 1992). Furthermore, a primer set targeting the mcrA gene of the methyl coenzyme-M reductase, a key enzyme for methanogenic Archaea was used: HAME1F/HAME2R (Hales et al., 1996).

3. Results and Discussion

Among other iron sulfide minerals pyrite is the dominant iron sulfide species in marine sediments (e.g Berner, 1970). In iron dominated anoxic sediments mostly iron monosulfides (FeS) occur, while in hydrogen sulfide (H_2S) dominated sediments pyrite is dominant. Once pyrite is formed and buried in anoxic sediments, it is supposed to be stable (Berner, 1967; 1971). However, Schippers and Jørgensen (2001, 2002) could show that in anoxic marine sediments MnO_2 chemically oxidizes pyrite to sulfate. This demonstrates, that alteration of pyrite in anoxic marine sediments is possible. Theoretically, in anoxic marine sediments microorganisms could reduce pyrite with a suitable electron donor like hydrogen (H_2) to FeS.

To study the role of indigenous microbial communities to perform the postulated process, 8 different setups were continuously sampled and measured. The positive assay contained pyrite inoculated with marine inoculum. The results of the geochemical solid phase measurements performed in this study showed that less than 0.01 wt% of FeS were present. This finding indicates that the reduction of pyrite to FeS indeed took place, although the concentration was too low for a verification by XRD. Overall, the results of the liquid phase measurements showed a slight decrease in the pH (Fig. 2) and an increase in ferrous iron (Fe^{2+}) and sulfur (S) concentration (Fig. 3), except for the N_2/CO_2 flushed assay BP 2.

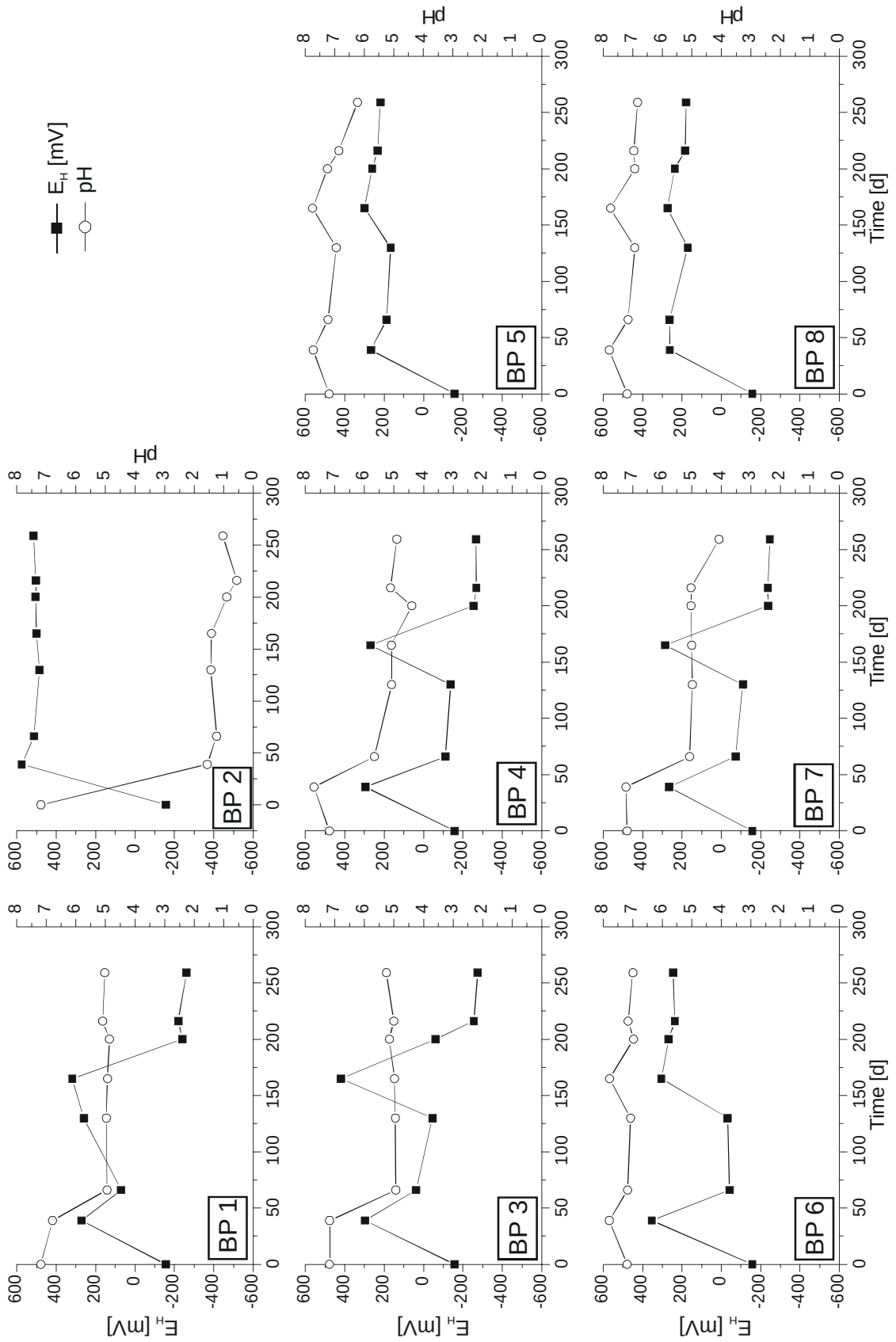

Fig. 2. E_H and pH values plotted over time for each assay.

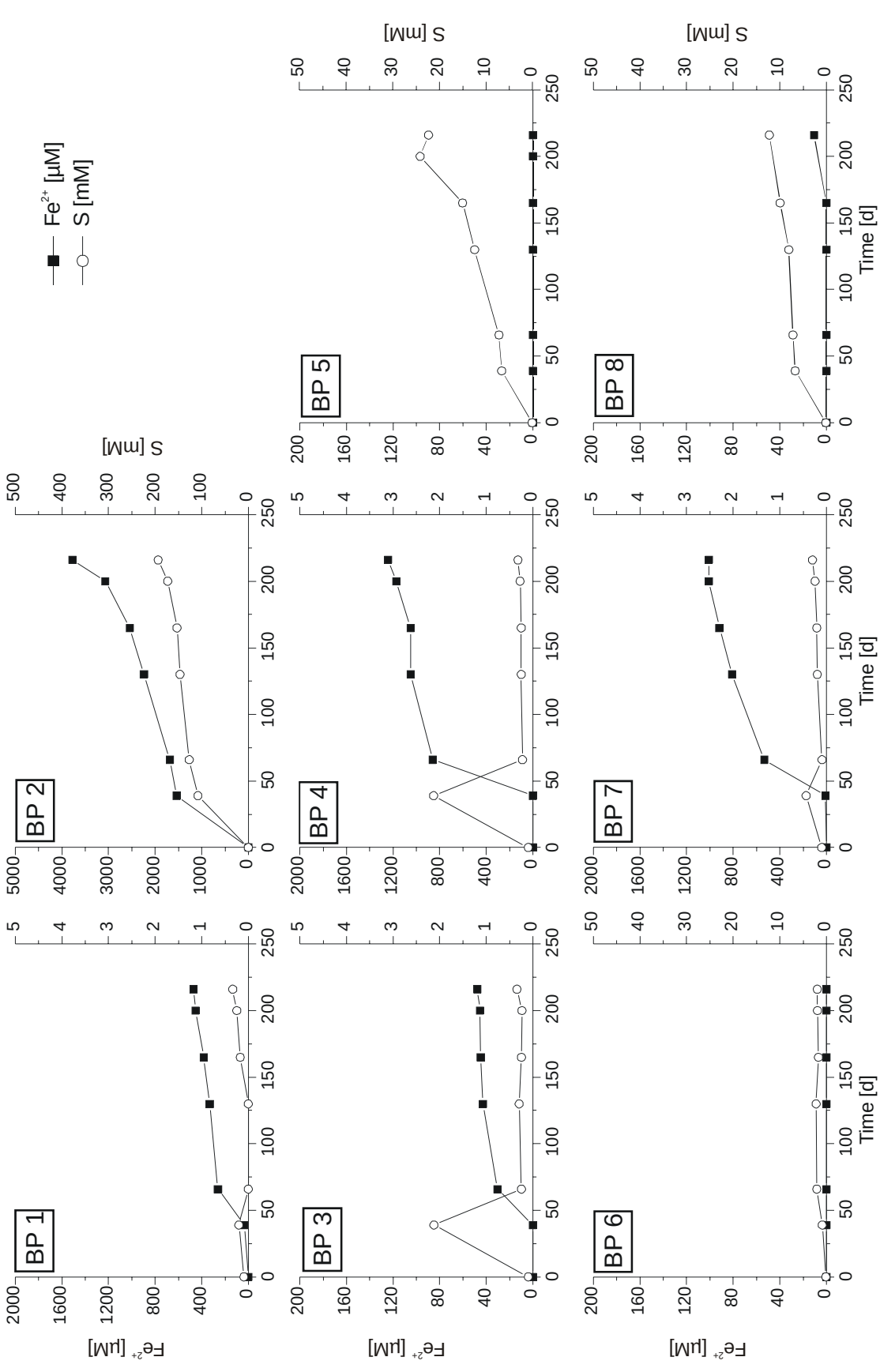

Fig. 3. Concentrations of total dissolved iron and sulfur (diagrams with different scales) plotted over time. Note that there is a resemblance between the assays BP 1, BP 4 and BP 7 of the experiment.

Due to a damage in the equipment of assay BP 2, the medium got oxidized and pyrite oxidation with the release of sulfate occurred. The assay was set up again with two other assays and marked as BP V2. The duration of the new experiment was decreased to 120 days but the sampling resolution was increased. In the retried experiment of assay 2 (BP V2) we replaced the pressure sensitive glass valves by injection needles with pressure sensitive valves. Due to the rather low pressure this equipment is more applicative for the experiment. The results expose almost no release of iron but little release of sulfur into the medium (Fig. 4) and thus are comparable with the results of assay BP 8 (Fig. 2 and 3). The assays BP 5 and BP 8, which were not supplied with gas, show very similar results in E_H and pH values as well as in the sulfur and iron concentrations. In some extent BP 6 is comparable to BP 5 and BP 8, only differing in the amount of released S.

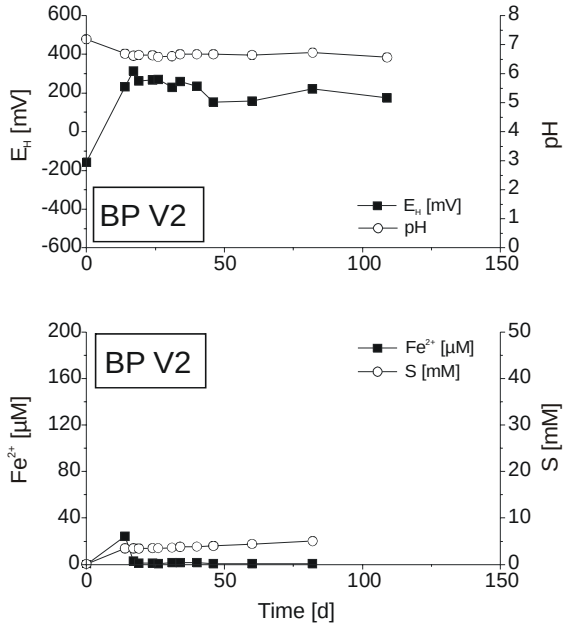

Fig. 4. Retried experiment of assay BP 2.

The concentration profiles of total dissolved iron and sulfur in Fig. 3 show, that there is a resemblance between assays BP 1, BP 4 and BP 7. Except for the low iron amount, BP 3 shows a similarity to assays BP 1, BP 4 and BP 7. Because the assays, which were not supplied with gas or gassed with nitrogen, show no or very low concentrations of iron in the medium, the release of ferrous iron into the medium in the positive assays BP 1, BP 4, and BP 7 indicates a dissolution of the iron phases related to hydrogen. After about 40 days the pressure sensitive glass valve got tilted in assay BP 4, and microscopic analysis showed that some bacteria were introduced. Thus, this abiotic control got altered into a positive replicate assay. Nevertheless, we suggest that the reaction of pyrite with H_2 is microbially mediated by bacteria using H_2 as the electron donor to reduce pyrite to FeS:

$$H_2 \leftrightarrow 2e^- + 2H^+ \qquad (1)$$

$$FeS_2 + H_2 \leftrightarrow HS^- + H^+ + FeS. \qquad (2)$$

But due to the alteration of the abiotic assay BP 4 into a positive assay we have no proof that a chemical reaction can be excluded. However, considering the standard free energy change for the reaction (Eq. 2) of 32.94 kJ (compare Rickard, 1997), we assume that the reaction is unlikely to proceed abiotically. Modeling the observed data using PHREEQC 2.10 (Parkhurst and Appelo, 1999), supports this view, as pyrite is saturated in the model result. In contrast, FeS is undersaturated, explaining the low amounts of FeS in the solid phase. Due to its acid solubility protons dissolve FeS according to the equation (Schippers and Jørgensen, 2002):

$$H^+ + FeS \leftrightarrow HS^- + Fe^{2+}. \qquad (3)$$

This abiotic reaction releases ferrous iron into the medium with a free energy change for this reaction of –12.04 kJ mol^{-1} (compare Canfield, 1989; Krom et al., 2002). The reaction (Eq. 3) would suggest that equal amounts of iron and sulfur are released into the medium. The detected lower concentrations of sulfur compared to iron indicate either a leakage of H_2S or that the bacteria have consumed the released sulfur.

Microscopic analysis revealed that the total amount of bacteria in assay BP 1 slightly decreased while the amount of bacteria increased in assay BP 3. Geochemical results also reveal, that there is a small release of ferrous iron into the medium in assay BP 3. Because this assay only contains bacteria in the medium, we suggest that there is a reduction of iron phases due to some contamination e.g. from the extraction of microorganisms from the marine sediment, where some cells are attached to particles as implied by analysis. We took this into account to define the background concentration for the released iron.

Table 2. Results of PCR amplification of DNA with selected primer sets during and at the end of the incubations.

Number	Sample	Sampling Date	Archaea	Methanogens	SRB	Bacteria
1	BP 1	07.01.2003			++	+
2	BP 2					
3	BP 3					+
4	BP 5					
5	BP 6					+
6	BP 7		+		+	+
7	BP 1	03.02.2003			+	+
8	BP 2				+	
9	BP 3				+	+
10	BP 5				+	
11	BP 6					+
12	BP 7					+
13	BP 1	03.07.2003	+	+	+	+
14	BP 2					
15	BP 3					+
16	BP 5					
17	BP 6					+
18	BP 7					

Furthermore, microscopic analysis showed high numbers of active/living bacteria of different shapes and forms, with no selective enrichment of one type, but rather specialized synthrophic communities/consortia in the positive assays. Furthermore, microbial analyses showed that bacteria dominate the microbial community (Table 2). In BP 1 the dominant organisms were probably homoacetogens, which produce acetate from H_2 and CO_2, especially when no methanogens or SRB are present. Comparison with HPLC results emphasize the presence of homoacetogens due to the high amounts of acetate (Table 3). Homoacetogens can live in symbioses with other microorganisms e.g. methanogens. They can use the H_2 produced , thus driving otherwise energetically rather unfavorable reactions. However, homoacetogens also could outcompete other organisms, and use the H_2 for pyrite reduction. It seems that methanogens were effectively inhibited, which was confirmed by gas chromatography.

Table 3. Results of short chain fatty acid analyses for selected sampling dates. Acetate is given in mM L^{-1}, presence of further fatty acids are indicated.

Sample	07.01.2003	03.02.2003	03.07.2003
BP 1	20.32 (P,F)	30.46 (P)	30.55 (B)
BP 2	-	-	-
BP 3	20.45 (P)	31.29 (P)	31.76 (P,B)
BP 5	-	-	-
BP 6	0.2	-	-
BP 7	18.00 (F)	34,48	30.96

P (propionate)
F (formiate)
B (butyrate)

A preliminary qualitative determination of microbial diversity revealed that Archaea were mostly absent and the number of active/living bacteria was highest in the assay BP 3 with the gas mixture H_2/CO_2 as substrate. The lower number of bacteria in the positive assays could indicate, that the reduction of pyrite with the accompanied release of trace elements (e.g. Cr, Ni) provides an unsuitable or almost toxic environment for some bacteria and only specialized synthrophic communities/consortia are present. However, microbial activity is dependent on the prevailing pH value (Brock et al., 1994). In marine sediments the pH values are more or less neutral due to carbonate buffering. In the experiment the pH dropped down to a value of 4 to 5 in the H_2/CO_2 gassed assays which can have an impact on the extent of microbially mediated reactions. The slight excess of H^+ coincides with the release of ferrous iron into the pore water.

4. Perspectives and Conclusions

Small amounts of FeS present in the solid phase of the positive assays were detected applying geochemical methods. However, the amounts were too low and thus the carried out measurements were not precise enough to quantify the exact amounts with high accuracy, or even be detected by X-ray diffraction (XRD). Thus, we recommend that measurements of using e.g. Mössbauer or scanning electron microscope (SEM) technique should be carried out.

Furthermore, we suggest that the fermentation cap should be filled with a ZnAc solution to trap released H_2S thus giving an indication for the presence of the postulated reaction. In addition, buffering of the medium by carbonate would reduce the influence of pH on bacterial activity and would better simulate conditions in natural marine environments.

Although the postulated reaction, the microbially mediated reduction of pyrite to FeS, could not be satisfactorily verified by our experiment, we assign the observed release of ferrous iron into the medium to the reduction of pyrite to FeS mediated by bacteria. We suggest that the reaction would be restricted to areas with high amounts of H_2, e.g. due to hydrothermal intrusions (Chapelle, et al., 2002), or with H_2 producing and H_2 consuming bacteria growing in close proximity (Conrad et al., 1986; Jørgensen, 2000). We think that this approach of microbial pyrite reduction is a promising candidate to explain alteration of some supposedly stable minerals in anoxic marine environments. However, the postulated process requires further investigation, especially concerning the microorganisms involved.

Acknowledgements. For technical assistance in the laboratory we are indebted to R. Appel, S. Hessler, and K. Nauhaus. Furthermore we would like to thank S. Bühring and M. Kölling for helpful discussions as well as F. Aspetsberger and K. Seiter for reading an earlier version of the manuscript. Our special appreciation goes to H.D. Schulz and F. Widdel for detailed comments. This research was funded by the Deutsche Forschungsgemeinschaft as part of the Research Center "Ocean Margins" (RCOM) of the University of Bremen contribution no. XXXX.

REFERENCES

Aakra, Å., Hesselsøe, M., and Bakken, L.R. (2000) Surface attachment of ammonia-oxidizing bacteria in soil. *Microbial Ecol.* **39**, 222-235.

Aller, R.C. and Rude, P.D. (1988) Complete oxidation of solid phase sulfides by manganese and bacteria in anoxic marine sediments. *Geochim. Cosmochim. Acta* **52**, 751-765.

Bakken, L.R. and Lindahl, V. (1995) Recovery of bacterial cells from soil. In *Nucleic acids in the environment: Methods and applications* (eds. J.T. Trevors and J.D. van Elsas). Springer, pp. 9-27.

Barnes, R.O. and Goldberg, E.D. (1976) Methane production and consumption in anoxic marine sediments. *Geology* **4**, 297-300.

Berner, R.A. (1967) Thermodynamic stability of sedimentary iron sulfides. *Am. J. Sci.* **265**, 773-785.

Berner, R.A. (1970) Sedimentary pyrite formation. *Am. J. Sci.* **268**, 1-23.

Berner, A.R. (1971) *Principles of Chemical Sedimentology*. McGraw-Hill, New York.

Berner, R.A. (1984) Sedimentary pyrite formation: An update. *Geochim. Cosmochim. Acta* **48**, 605-615.

Blair, N.E. and Aller, R.C. (1995) Anaerobic methane oxidation on the Amazon shelf. *Geochim. Cosmochim. Acta* **59**, 3707-3715.

Brock, T.D., Madigan, M.T., Martinko, J.M., and Parker, J. (1994) *Biology of microorganisms*. Prentice-Hall.

Brunauer, S., Emmet, P.H., and Teller, E. (1938) The adsorption of gases in multimolecular layers. *J. Am. Chem. Soc.* **60**, 309-319.

Canfield, D.E. and Berner, R.A. (1987) Dissolution and pyritization of magnetite in anoxic marine sediments. *Geochim. Cosmochim. Acta* **51**, 645-659.

Canfield, D.E. (1989) Reactive iron in marine sediments. *Geochim. Cosmochim. Acta* **53**, 619-632.

Chapelle, F.H., O'Neill, K., Bradley, P.M., Methé, B.A., Ciufo, S.A., Knobel, L.L., and Lovley D.R. (2002) A hydrogen-based subsurface microbial community dominated by methanogens. *Nature* **415**, 312-315.

Conrad, R., Schink, B., and Phelps, T.J. (1986) Thermodynamics of H2-consuming and H2-producing metabolic reactions in diverse methanogenic environments under in siu´tu conditions. *FEMS Microbiol. Ecol.* **38**, 353-360.

DeLong, E. F. (1992) Archaea in coastal marine environments. *Proc. Natl. Acad. Sci. USA* **89**, 5685–5689.

Donald, R. and Southam, G. (1999) Low temperature anaerobic bacterial diagenesis of ferrous monosulfide to pyrite. *Geochim. Cosmochim. Acta* **63**, 2019-2023.

Drobner, E., Huber, H., Wächtershäuser, D., Rose, D., and Stetter, K.O. (1990) Pyrite formation linked with hydrogen evolution under anaeobic conditions. *Nature* **346**, 742-744.

Eller, G., Stubner, S., and Frenzel, P. (2001) Group specific 16S rRNA targeted probes for the detection of type I and type II methanotrophs by fluorescence in situ hybridisation. *FEMS Microb. Lett.* **198**, 91-97.

Ferdelman, T.G., Lee, C., Pantoja, S., Harder, J., Bebout, B.M., and Fossing, H. (1997) Sulfate reduction and methanogenesis in a Thioploca-dominated sediment off the coast of Chile. *Geochim. Cosmochim. Acta* **61**, 3065-3079.

Fossing, H. and Jørgensen, B.B. (1989) Measurement of bacterial sulfate reduction in sediments: Evaluation of a single-step chromium reduction method. *Biogeochemistry* **8**, 205-222.

Friedrich, M.W. (2002) Phylogenetic analysis reveals multiple lateral transfers of adenosine-5'-phosphosulfate reductase genes among sulfate-reducing microorganisms. *J. Bacteriol.* **184**, 278-289.

Hales, B.A., Edwards, C., Ritchie, D.A., Hall, G., Pickup, R.W., and Saunders, J.R. (1996) Isolation and identification of methanogen-specific DNA from blanked bog peat by PCR amplification and sequence analysis. *Appl. Environ. Microbiol*. **62**, 668-675.

Hecht, H. and Kölling, M. (2001) A low-cost optode-array measuring system based on 1 mm plastic optical fibres – new technique for in-situ detection and quantification of pyrite weathering processes. *Sens. Actuat. B* **81**, 76-82.

Jørgensen, B.B. (1982) Mineralization of organic matter in the sea bed – the role of sulphate reduction. *Nature* **296**, 643-645.

Jørgensen, B.B. (2000) Bacteria and marine biogeochemistry. In *Marine geochemistry* (eds. H.D. Schulz and M. Zabel). Springer, pp. 173-207.

Jørgensen, B.B., Böttcher, M.E., Lüschen, H., Neretin, L.N., and Volkov, I.I. (2004) Anaerobic methane oxidation and a deep H2S sink generate isotopically heavy sulfides in Black Sea sediments. *Geochim. Cosmochim. Acta* **68**, 2095–2118.

Kao, S.-J., Horng, C.-S., Roberts, A.P., and Liu, K.-K. (2004) Carbon-sulfur-iron relationships in sedimentary rocks from southwestern Taiwan: influence of geochemical environments on greigite and pyrrhotite formation. *Chem. Geol.* **203**, 153-168.

Kasten, S., Freudenthal, T., Gingele, F.X., and Schulz, H.D. (1998) Simultaneous formation of iron-rich layers at different redox boundaries in sediments of the Amazon deep-sea fan. *Geochim. Cosmochim. Acta* **62**, 2253–2264.

Krom, M.D., Mortimer, R.J.G., Poulton, S.W., Hayes, P., Davies, I.M., Davison, W., and Zhang, H. (2002) In-situ determination of dissolved iron production in recent marine sediments. *Aqua. Sci.* **64**, 282–291.

Luther, G.W. (1991) Pyrite synthesis via polysulfide compounds. *Geochim. Cosmochim. Acta* **55**, 2839-2849.

Meyer-Reil, L.A. (1983) Benthic response to sedimentation events during autumn to spring at a shallow water station in the western Kiel Bight. *Mar. Biol.* **77**, 247–256.

Morse, J.W., Millero, F.J., Cornwell, J.C., and Rickard, D. (1987) The chemistry of the hydrogen sulfide and iron sulfide systems in natural waters. *Earth-Sci. Rev.* **24**, 1-42.

Morse, J.W. (2002) Sedimentary geochemistry of the carbonate and sulphide systems and their potential influence on toxic metal bioavailability. In *Chemistry of marine water and sediments* (eds. A. Gianguzza, E. Pelizzetti and S. Sammartano). Springer, pp. 165-189.

Nauhaus, K., Boetius, A., Krüger, M., and Widdel, F. (2002) In vitro demonstration of anaerobic oxidation of methane coupled to sulphate reduction in sediments from a marine gas hydrate area. *Environ. Microbiol.* **4**, 296–305.

Neretin, L., Böttcher, M.E., Jørgensen, B.B., Volkov, I.I., Lüschen, H., and Hilgenfeldt, K. (2004) Pyritization processes and greigite formation in the advancing sulfidization front in the Upper Pleistocene sediments of the Black Sea. *Geochim. Cosmochim. Acta* **68**, 2081-2093.

Niewöhner, C., Hensen, C., Kasten, S., Zabel, M., and Schulz, H.D. (1998) Deep sulfate reduction completely mediated by anaerobic methane oxidation in sediments of the upwelling area off Namibia. *Geochim. Cosmochim. Acta* **62**, 455-464.

Parkhurst, D.L. and Appelo, C.A.J. (1999) *User's guide to PHREEQC (Version 2.0)*. U.S. Geol. Surv., Water Resour. Inv. Rep., pp. 99-4259.

Rabus, R., Fukui, M., Wilkes, H., and Widdel, F. (1996) Degradative capacities and 16S rRNA-targeted whole-cell hybridization of sulfate-reducing bacteria in an anaerobic enrichment culture utilizing alkylbenzenes from crude oil. *Appl. Environ. Microbiol*. **62**, 3605–3613.

Ravenschlag, K., Sahm, K., Pernthaler, J., and Amann, R. (1999) High bacterial diversity in permanently cold marine sediments. *Appl. Environ. Microbiol.* **65**, 3982–3989.

Rickard, D. (1997) Kinetics of pyrite formation by the H_2S oxidation of iron (II) monosulfides in aqueous solutions between 25 and 125°C: The rate equation. *Geochim. Cosmochim. Acta* **61**, 115-134.

Rickard, D. and Luther, G.W. (1997) Kinetics of pyrite formation by the H_2S oxidation of iron (II) monosulfides in aqueous solutions between 25 and 125°C: The mechanismn. *Geochim. Cosmochim. Acta* **61**, 135-147.

Roberts, A.P. and Turner, G.M. (1993) Diagenetic formation of ferrimagnetic iron sulphide minerals in rapidly deposited marine sediments, South Island, New Zealand. *Earth Planet. Sci. Lett.* **115**, 257-273.

Schippers, A. and Jørgensen, B.B. (2001) Oxidation of pyrite and iron sulfide by manganese dioxide in marine sediments. *Geochim. Cosmochim. Acta* **65**, 915-922.

Schippers, A. and Jørgensen, B.B. (2002) Biogeochemistry of pyrite and iron sulfide oxidation in marine sediments. *Geochim. Cosmochim. Acta* **66**, 85-92.

Schoonen, M.A.A. and Barnes, H.L. (1991) Reactions forming pyrite and marcasite from solution: II. Via FeS precursors below 100°C. *Geochim. Cosmochim. Acta* **55**, 1505-1514.

Widdel, F. and Bak, F. (1992) Gram-negative mesophilic sulfate-reducing bacteria. In *The procaryotes* (eds. A. Balows, M.P. Starr, H. Stolp, H.G. Trüper and H.G. Schlegel). Springer, pp. 3352-3378.

Zhabina, N.N. and Volkov, I.I. (1978) A method of determination of various sulfur compounds in sea sediments and rocks. In *Environmental biogeochemistry and geomicrobiology. Vol. 3: Methods, metals and assessment* (ed. W.E. Krumbein). Ann Arbor Science Publishers, pp. 735-745.

Conclusions and perspectives

The manuscripts presented in this thesis are based on geochemical, geophysical and microbiological results. The interdisciplinary approach of combining different methods revealed a good tool to investigate processes which proceed in deeper subsurface sediments.

In our studies we could show that sedimentary events or changes in depositional conditions can be identified and in some cases even be reconstructed by the application of numerical modeling on pore water profiles and solid phase records. Sulfate pore water profiles are directly influenced by depositional dynamics such as gravity flows. Time estimates for younger sedimentary events (between tens to hundreds of years) can be gained by modeling the shape of sulfate pore water profiles. For the identification of older depositional events manganese profiles could provide a good complementary tool. In addition to pore water interpretations, solid phase records can provide valuable information on changes in depositional conditions and fluxes of oxidants and reductants over time.

Drastic decreases in sedimentation rate can result in a fixed or slow moving sulfate/methane transition (SMT). The sulfide released by anaerobic oxidation of methane (AOM) leads to enhanced dissolution of ferrimagnetic iron minerals and to the formation of paramagnetic pyrite. This diagenetic transformation causes a loss of the primary magnetic signal, which has a strong effect on the interpretation of paleomagnetic data. Our model results indicate, that gaps in magnetic susceptibility found within the sulfidic zone around the current depth of the SMT in sediments of the western Argentine Basin result from a strong decrease in sedimentation rate at the Pleistocene/Holocene transition. It could further be shown, that high mean sedimentation rates can lead to a burial of reactive minerals in considerable amounts in deeper sediments. The observed release of ferrous and manganous ions into pore water within the methanic zone indicates the alteration of reactive minerals at this depth, probably related to biomediated processes. Moreover we could show, that metastable minerals can be preserved or shielded from dissolution by specific processes or mechanisms, such as coating by non-reactive phases or high sedimentation rates, and thus be buried in deeper sediments. In sediments from the eastern Cape Basin we found authigenic barite enrichments below the SMT, in sulfate-depleted sediments. In these deeper sediments, barite could provide terminal electron acceptors for sulfate reducing bacteria and support the anaerobic oxidation of methane well below the SMT. Thus, deeper buried reactive minerals can fuel biogeochemical processes in deeper sediments.

Contrary to these processes would be the microbially mediated alteration of minerals, which are generally supposed to be stable under anoxic conditions. Based on our experimental results of microbial pyrite reduction, we assume that in deeper anoxic marine sediments biomediated processes can affect stable minerals such as pyrite. Our findings emphasize the need for more intensive studies of the microbially mediated and geochemical processes in the methanic zone of deeper buried sediments especially concerning the microorganisms involved.

In marine depositional environments such as the highly dynamic western Argentine Basin, compressed sequences of redox zones can be found, which show great similarities to geochemical zonations identified in sedimentary sequences of several hundreds of meters drilled by the ODP. We suggest, that understanding the processes taking place in the methanic zone at the investigated sites – like in the Argentine Basin – could be relevant to advance the comprehension of processes within the deep biosphere. It could help to understand for example, which electron acceptors are available at such depths for microbially mediated processes.

Overall, we could demonstrate that geophysical and geochemical properties, used for the interpretation of paleomagnetic data or as proxy for paleoproductivity, are strongly influenced by non-steady state diagenesis. Moreover we could show, that non-steady state diagenesis can have an impact on mineral assemblages in deeper marine sediments. Reactive minerals buried into deeper sediments can fuel microbiological processes. Thus, we suggest that processes observed in the studied sediments could help to understand biogeochemical processes occurring in the deep biosphere, and should be subject to further detailed investigation.

Danksagung

Für die Vergabe dieser Arbeit, seine Hilfsbereitschaft bei allen Fragen und seine Unterstützung möchte ich mich bei Herrn Prof. Dr. Horst D. Schulz bedanken. Herrn Prof. Dr. Ulrich Bleil danke ich für die Übernahme des Zweitgutachtens, sowie für die konstruktiven Kommentare.

Mein größter Dank gilt PD Dr. Sabine Kasten für die Betreuung dieser Arbeit, die in dem von ihr mitbeantragten Projekt eingegliedert war. Besonders möchte ich mich für ihr stetes Interesse an der Entwicklung der Arbeit, ihre Ideen und ihre uneingeschränkte Unterstützung auch in schwierigen Situationen bedanken. Neben den zahlreichen fachlichen Diskussionen und konstruktiven Anregungen kamen auch gute Stimmung und viel Spaß bei der Arbeit nicht zu kurz.

Allen Mitgliedern der Arbeitsgruppe Geochemie und Hydrogeologie der Universität Bremen danke ich für die angenehme Arbeitsatmosphäre und ständige Hilfsbereitschaft. Für die Unterstützung im Labor und bei technischen Fragen danke ich Silvana Hessler, Susanne Siemer und Karsten Enneking. Mein Dank gilt auch Simone Pannike, Esther Arning, Luzie Schnieders, Kathrin Küster, Markus Schmidt und Jens Gröger für die tatkräftige Hilfe bei den Arbeiten im Labor. Für die hilfreiche Unterstützung bei unzähligen Fragen danke ich meinen Kollegen, Veith Becker, Dr. Henrik Hecht, Maik Inthorn, Dr. Volker Karius, Dr. Tanja Lager, Cristian März, Kerstin Plewa, Michael Schweizer, Katharina Wien. Ganz besonders danke ich Fanni Aspetsberger für ihre sehr große Hilfe und ihre Geduld in der Endphase. Ein spezieller Dank geht auch an Dr. Kerstin Pfeifer und Dr. Katherina Seiter für die konstruktive und nette Zeit im TAB-Büro. Ein ganz besonderer Dank geht an Dr. Martin Kölling für seine technischen Optimierungen sowie seine Unterstützung und Geduld bei zahlreichen Fragen.

Für die anregenden Diskussionen und Kommentare möchte ich mich bei Dr. Christian Hensen, PD Dr. Matthias Zabel, Dr. Oscar Romero und Prof. Dr. Gerhard Bohrmann bedanken. Bei Dr. Christoph Vogt, Dr. Johannes Birkenstock und Dr. Michael Wendschuh bedanke ich mich für die tatkräftige analytische Unterstützung. Des weiteren danke ich Dr. Anja Reitz, Dr. Solveig Bühring und Dr. Verena Heuer für ihre Hilfe und Motivation.

Für die tatkräftige Hilfe bei den Messungen und Laborarbeiten am Max Planck Institut für Marine Mikrobiologie in Bremen (MPI) möchte ich mich bei Dr. Katja Nauhaus und Ramona Appel bedanken. Für die Unterstützung, Diskussionen und konstruktiven Kommentare danke ich Prof. Dr. Friedrich Widdel und besonders Dr. Martin Krüger.

Bei den Mitarbeitern der Arbeitsgruppe Geophysik bedanke ich mich für eine erfolgreiche und produktive Zusammenarbeit insbesondere bei Linda Garming, Christine Franke, Dr. Thomas Frederichs und Dr. David Heslop.

Für die diskussionsreichen und ausgelassenen Donnerstagabende möchte ich mich bei Fanni, Henner, Henrik, Ina, Katherina, Kerstin, Maik, Tanja, Urte und Volker bedanken.

Mein persönlicher Dank gilt meinen Freunden für die Motivation und die abwechslungsreichen und schönen Abende.

Zu guter Letzt möchte ich mich ganz herzlich bei meiner Familie für die uneingeschränkte Unterstützung bedanken, und dass sie immer für mich da war.

Publications of this series:

No. 1 **Wefer, G., E. Suess and cruise participants**
Bericht über die POLARSTERN-Fahrt ANT IV/2, Rio de Janeiro - Punta Arenas, 6.11. - 1.12.1985.
60 pages, Bremen, 1986.

No. 2 **Hoffmann, G.**
Holozänstratigraphie und Küstenlinienverlagerung an der andalusischen Mittelmeerküste.
173 pages, Bremen, 1988. (out of print)

No. 3 **Wefer, G. and cruise participants**
Bericht über die METEOR-Fahrt M 6/6, Libreville - Las Palmas, 18.2. - 23.3.1988.
97 pages, Bremen, 1988.

No. 4 **Wefer, G., G.F. Lutze, T.J. Müller, O. Pfannkuche, W. Schenke, G. Siedler, W. Zenk**
Kurzbericht über die METEOR-Expedition No. 6, Hamburg - Hamburg, 28.10.1987 - 19.5.1988.
29 pages, Bremen, 1988. (out of print)

No. 5 **Fischer, G.**
Stabile Kohlenstoff-Isotope in partikulärer organischer Substanz aus dem Südpolarmeer (Atlantischer Sektor). 161 pages, Bremen, 1989.

No. 6 **Berger, W.H. and G. Wefer**
Partikelfluß und Kohlenstoffkreislauf im Ozean.
Bericht und Kurzfassungen über den Workshop vom 3.-4. Juli 1989 in Bremen.
57 pages, Bremen, 1989.

No. 7 **Wefer, G. and cruise participants**
Bericht über die METEOR - Fahrt M 9/4, Dakar - Santa Cruz, 19.2. - 16.3.1989.
103 pages, Bremen, 1989.

No. 8 **Kölling, M.**
Modellierung geochemischer Prozesse im Sickerwasser und Grundwasser.
135 pages, Bremen, 1990.

No. 9 **Heinze, P.-M.**
Das Auftriebsgeschehen vor Peru im Spätquartär. 204 pages, Bremen, 1990. (out of print)

No. 10 **Willems, H., G. Wefer, M. Rinski, B. Donner, H.-J. Bellmann, L. Eißmann, A. Müller, B.W. Flemming, H.-C. Höfle, J. Merkt, H. Streif, G. Hertweck, H. Kuntze, J. Schwaar, W. Schäfer, M.-G. Schulz, F. Grube, B. Menke**
Beiträge zur Geologie und Paläontologie Norddeutschlands: Exkursionsführer.
202 pages, Bremen, 1990.

No. 11 **Wefer, G. and cruise participants**
Bericht über die METEOR-Fahrt M 12/1, Kapstadt - Funchal, 13.3.1990 - 14.4.1990.
66 pages, Bremen, 1990.

No. 12 **Dahmke, A., H.D. Schulz, A. Kölling, F. Kracht, A. Lücke**
Schwermetallspuren und geochemische Gleichgewichte zwischen Porenlösung und Sediment im Wesermündungsgebiet. BMFT-Projekt MFU 0562, Abschlußbericht. 121 pages, Bremen, 1991.

No. 13 **Rostek, F.**
Physikalische Strukturen von Tiefseesedimenten des Südatlantiks und ihre Erfassung in Echolotregistrierungen. 209 pages, Bremen, 1991.

No. 14 **Baumann, M.**
Die Ablagerung von Tschernobyl-Radiocäsium in der Norwegischen See und in der Nordsee.
133 pages, Bremen, 1991. (out of print)

No. 15 **Kölling, A.**
Frühdiagenetische Prozesse und Stoff-Flüsse in marinen und ästuarinen Sedimenten.
140 pages, Bremen, 1991.

No. 16 **SFB 261 (ed.)**
1. Kolloquium des Sonderforschungsbereichs 261 der Universität Bremen (14.Juni 1991):
Der Südatlantik im Spätquartär: Rekonstruktion von Stoffhaushalt und Stromsystemen.
Kurzfassungen der Vorträge und Poster. 66 pages, Bremen, 1991.

No. 17 **Pätzold, J. and cruise participants**
Bericht und erste Ergebnisse über die METEOR-Fahrt M 15/2, Rio de Janeiro - Vitoria,
18.1. - 7.2.1991. 46 pages, Bremen, 1993.

No. 18 **Wefer, G. and cruise participants**
Bericht und erste Ergebnisse über die METEOR-Fahrt M 16/1, Pointe Noire - Recife,
27.3. - 25.4.1991. 120 pages, Bremen, 1991.

No. 19 **Schulz, H.D. and cruise participants**
Bericht und erste Ergebnisse über die METEOR-Fahrt M 16/2, Recife - Belem, 28.4. - 20.5.1991.
149 pages, Bremen, 1991.

No. 20 **Berner, H.**
Mechanismen der Sedimentbildung in der Fram-Straße, im Arktischen Ozean und in der Norwegischen See. 167 pages, Bremen, 1991.

No. 21 **Schneider, R.**
Spätquartäre Produktivitätsänderungen im östlichen Angola-Becken: Reaktion auf Variationen im Passat-Monsun-Windsystem und in der Advektion des Benguela-Küstenstroms.
198 pages, Bremen, 1991. (out of print)

No. 22 **Hebbeln, D.**
Spätquartäre Stratigraphie und Paläozeanographie in der Fram-Straße. 174 pages, Bremen, 1991.

No. 23 **Lücke, A.**
Umsetzungsprozesse organischer Substanz während der Frühdiagenese in ästuarinen Sedimenten.
137 pages, Bremen, 1991.

No. 24 **Wefer, G. and cruise participants**
Bericht und erste Ergebnisse der METEOR-Fahrt M 20/1, Bremen - Abidjan, 18.11.- 22.12.1991.
74 pages, Bremen, 1992.

No. 25 **Schulz, H.D. and cruise participants**
Bericht und erste Ergebnisse der METEOR-Fahrt M 20/2, Abidjan - Dakar, 27.12.1991 - 3.2.1992.
173 pages, Bremen, 1992.

No. 26 **Gingele, F.**
Zur klimaabhängigen Bildung biogener und terrigener Sedimente und ihrer Veränderung durch die Frühdiagenese im zentralen und östlichen Südatlantik. 202 pages, Bremen, 1992.

No. 27 **Bickert, T.**
Rekonstruktion der spätquartären Bodenwasserzirkulation im östlichen Südatlantik über stabile Isotope benthischer Foraminiferen. 205 pages, Bremen, 1992. (out of print)

No. 28 **Schmidt, H.**
Der Benguela-Strom im Bereich des Walfisch-Rückens im Spätquartär. 172 pages, Bremen, 1992.

No. 29 **Meinecke, G.**
Spätquartäre Oberflächenwassertemperaturen im östlichen äquatorialen Atlantik.
181 pages, Bremen, 1992.

No. 30 **Bathmann, U., U. Bleil, A. Dahmke, P. Müller, A. Nehrkorn, E.-M. Nöthig, M. Olesch, J. Pätzold, H.D. Schulz, V. Smetacek, V. Spieß, G. Wefer, H. Willems**
Bericht des Graduierten Kollegs. Stoff-Flüsse in marinen Geosystemen.
Berichtszeitraum Oktober 1990 - Dezember 1992. 396 pages, Bremen, 1992.

No. 31 **Damm, E.**
Frühdiagenetische Verteilung von Schwermetallen in Schlicksedimenten der westlichen Ostsee.
115 pages, Bremen, 1992.

No. 32 **Antia, E.E.**
Sedimentology, Morphodynamics and Facies Association of a mesotidal Barrier Island Shoreface (Spiekeroog, Southern North Sea). 370 pages, Bremen, 1993.

No. 33 **Duinker, J. and G. Wefer (ed.)**
Bericht über den 1. JGOFS-Workshop. 1./2. Dezember 1992 in Bremen. 83 pages, Bremen, 1993.

No. 34 **Kasten, S.**
Die Verteilung von Schwermetallen in den Sedimenten eines stadtbremischen Hafenbeckens.
103 pages, Bremen, 1993.

No. 35 **Spieß, V.**
Digitale Sedimentographie. Neue Wege zu einer hochauflösenden Akustostratigraphie.
199 pages, Bremen, 1993.

No. 36 **Schinzel, U.**
Laborversuche zu frühdiagenetischen Reaktionen von Eisen (III) - Oxidhydraten in marinen Sedimenten.189 pages, Bremen, 1993.

No. 37 **Sieger, R.**
CoTAM - ein Modell zur Modellierung des Schwermetalltransports in Grundwasserleitern.
56 pages, Bremen, 1993. (out of print)

No. 38 **Willems, H. (ed.)**
Geoscientific Investigations in the Tethyan Himalayas. 183 pages, Bremen, 1993.

No. 39 **Hamer, K.**
Entwicklung von Laborversuchen als Grundlage für die Modellierung des Transportverhaltens von Arsenat, Blei, Cadmium und Kupfer in wassergesättigten Säulen. 147 pages, Bremen, 1993.

No. 40 **Sieger, R.**
Modellierung des Stofftransports in porösen Medien unter Ankopplung kinetisch gesteuerter Sorptions- und Redoxprozesse sowie thermischer Gleichgewichte. 158 pages, Bremen, 1993.

No. 41 **Thießen, W.**
Magnetische Eigenschaften von Sedimenten des östlichen Südatlantiks und ihre paläozeanographische Relevanz. 170 pages, Bremen, 1993.

No. 42 **Spieß, V. and cruise participants**
Report and preliminary results of METEOR-Cruise M 23/1, Kapstadt - Rio de Janeiro, 4.-25.2.1993. 139 pages, Bremen, 1994.

No. 43 **Bleil, U. and cruise participants**
Report and preliminary results of METEOR-Cruise M 23/2, Rio de Janeiro - Recife, 27.2.-19.3.1993 133 pages, Bremen, 1994.

No. 44 **Wefer, G. and cruise participants**
Report and preliminary results of METEOR-Cruise M 23/3, Recife - Las Palmas, 21.3. - 12.4.1993 71 pages, Bremen, 1994.

No. 45 **Giese, M. and G. Wefer (ed.)**
Bericht über den 2. JGOFS-Workshop. 18../19. November 1993 in Bremen. 93 pages, Bremen, 1994.

No. 46 **Balzer, W. and cruise participants**
Report and preliminary results of METEOR-Cruise M 22/1, Hamburg - Recife, 22.9. - 21.10.1992. 24 pages, Bremen, 1994.

No. 47 **Stax, R.**
Zyklische Sedimentation von organischem Kohlenstoff in der Japan See: Anzeiger für Änderungen von Paläoozeanographie und Paläoklima im Spätkänozoikum. 150 pages, Bremen, 1994.

No. 48 **Skowronek, F.**
Frühdiagenetische Stoff-Flüsse gelöster Schwermetalle an der Oberfläche von Sedimenten des Weser Ästuares. 107 pages, Bremen, 1994.

No. 49 **Dersch-Hansmann, M.**
Zur Klimaentwicklung in Ostasien während der letzten 5 Millionen Jahre: Terrigener Sedimenteintrag in die Japan See (ODP Ausfahrt 128). 149 pages, Bremen, 1994.

No. 50 **Zabel, M.**
Frühdiagenetische Stoff-Flüsse in Oberflächen-Sedimenten des äquatorialen und östlichen Südatlantik. 129 pages, Bremen, 1994.

No. 51 **Bleil, U. and cruise participants**
Report and preliminary results of SONNE-Cruise SO 86, Buenos Aires - Capetown, 22.4. - 31.5.93 116 pages, Bremen, 1994.

No. 52 **Symposium: The South Atlantic: Present and Past Circulation.**
Bremen, Germany, 15 - 19 August 1994. Abstracts. 167 pages, Bremen, 1994.

No. 53 **Kretzmann, U.B.**
^{57}Fe-Mössbauer-Spektroskopie an Sedimenten - Möglichkeiten und Grenzen. 183 pages, Bremen, 1994.

No. 54 **Bachmann, M.**
Die Karbonatrampe von Organyà im oberen Oberapt und unteren Unteralb (NE-Spanien, Prov. Lerida): Fazies, Zyklo- und Sequenzstratigraphie. 147 pages, Bremen, 1994. (out of print)

No. 55 **Kemle-von Mücke, S.**
Oberflächenwasserstruktur und -zirkulation des Südostatlantiks im Spätquartär. 151 pages, Bremen, 1994.

No. 56 **Petermann, H.**
Magnetotaktische Bakterien und ihre Magnetosome in Oberflächensedimenten des Südatlantiks. 134 pages, Bremen, 1994.

No. 57 **Mulitza, S.**
Spätquartäre Variationen der oberflächennahen Hydrographie im westlichen äquatorialen Atlantik. 97 pages, Bremen, 1994.

No. 58 **Segl, M. and cruise participants**
Report and preliminary results of METEOR-Cruise M 29/1, Buenos-Aires - Montevideo, 17.6. - 13.7.1994
94 pages, Bremen, 1994.

No. 59 **Bleil, U. and cruise participants**
Report and preliminary results of METEOR-Cruise M 29/2, Montevideo - Rio de Janiero 15.7. - 8.8.1994. 153 pages, Bremen, 1994.

No. 60 **Henrich, R. and cruise participants**
Report and preliminary results of METEOR-Cruise M 29/3, Rio de Janeiro - Las Palmas 11.8. - 5.9.1994. Bremen, 1994. (out of print)

No. 61 **Sagemann, J.**
Saisonale Variationen von Porenwasserprofilen, Nährstoff-Flüssen und Reaktionen in intertidalen Sedimenten des Weser-Ästuars. 110 pages, Bremen, 1994. (out of print)

No. 62 **Giese, M. and G. Wefer**
Bericht über den 3. JGOFS-Workshop. 5./6. Dezember 1994 in Bremen.
84 pages, Bremen, 1995.

No. 63 **Mann, U.**
Genese kretazischer Schwarzschiefer in Kolumbien: Globale vs. regionale/lokale Prozesse.
153 pages, Bremen, 1995. (out of print)

No. 64 **Willems, H., Wan X., Yin J., Dongdui L., Liu G., S. Dürr, K.-U. Gräfe**
The Mesozoic development of the N-Indian passive margin and of the Xigaze Forearc Basin in southern Tibet, China. – Excursion Guide to IGCP 362 Working-Group Meeting "Integrated Stratigraphy". 113 pages, Bremen, 1995. (out of print)

No. 65 **Hünken, U.**
Liefergebiets - Charakterisierung proterozoischer Goldseifen in Ghana anhand von Fluideinschluß - Untersuchungen. 270 pages, Bremen, 1995.

No. 66 **Nyandwi, N.**
The Nature of the Sediment Distribution Patterns in ther Spiekeroog Backbarrier Area, the East Frisian Islands. 162 pages, Bremen, 1995.

No. 67 **Isenbeck-Schröter, M.**
Transportverhalten von Schwermetallkationen und Oxoanionen in wassergesättigten Sanden. - Laborversuche in Säulen und ihre Modellierung -. 182 pages, Bremen, 1995.

No. 68 **Hebbeln, D. and cruise participants**
Report and preliminary results of SONNE-Cruise SO 102, Valparaiso - Valparaiso, 95.
134 pages, Bremen, 1995.

No. 69 **Willems, H. (Sprecher), U.Bathmann, U. Bleil, T. v. Dobeneck, K. Herterich, B.B. Jorgensen, E.-M. Nöthig, M. Olesch, J. Pätzold, H.D. Schulz, V. Smetacek, V. Speiß. G. Wefer**
Bericht des Graduierten-Kollegs Stoff-Flüsse in marine Geosystemen.
Berichtszeitraum Januar 1993 - Dezember 1995.
45 & 468 pages, Bremen, 1995.

No. 70 **Giese, M. and G. Wefer**
Bericht über den 4. JGOFS-Workshop. 20./21. November 1995 in Bremen. 60 pages, Bremen, 1996. (out of print)

No. 71 **Meggers, H.**
Pliozän-quartäre Karbonatsedimentation und Paläozeanographie des Nordatlantiks und des Europäischen Nordmeeres - Hinweise aus planktischen Foraminiferengemeinschaften.
143 pages, Bremen, 1996. (out of print)

No. 72 **Teske, A.**
Phylogenetische und ökologische Untersuchungen an Bakterien des oxidativen und reduktiven marinen Schwefelkreislaufs mittels ribosomaler RNA. 220 pages, Bremen, 1996. (out of print)

No. 73 **Andersen, N.**
Biogeochemische Charakterisierung von Sinkstoffen und Sedimenten aus ostatlantischen Produktions-Systemen mit Hilfe von Biomarkern. 215 pages, Bremen, 1996.

No. 74 **Treppke, U.**
Saisonalität im Diatomeen- und Silikoflagellatenfluß im östlichen tropischen und subtropischen Atlantik. 200 pages, Bremen, 1996.

No. 75 **Schüring, J.**
Die Verwendung von Steinkohlebergematerialien im Deponiebau im Hinblick auf die Pyritverwitterung und die Eignung als geochemische Barriere. 110 pages, Bremen, 1996.

No. 76 **Pätzold, J. and cruise participants**
Report and preliminary results of VICTOR HENSEN cruise JOPS II, Leg 6,
Fortaleza - Recife, 10.3. - 26.3. 1995 and Leg 8, Vítoria - Vítoria, 10.4. - 23.4.1995.
87 pages, Bremen, 1996.

No. 77 **Bleil, U. and cruise participants**
Report and preliminary results of METEOR-Cruise M 34/1, Cape Town - Walvis Bay, 3.-26.1.1996.
129 pages, Bremen, 1996.

No. 78 **Schulz, H.D. and cruise participants**
Report and preliminary results of METEOR-Cruise M 34/2, Walvis Bay - Walvis Bay, 29.1.-18.2.96
133 pages, Bremen, 1996.

No. 79 **Wefer, G. and cruise participants**
Report and preliminary results of METEOR-Cruise M 34/3, Walvis Bay - Recife, 21.2.-17.3.1996.
168 pages, Bremen, 1996.

No. 80 **Fischer, G. and cruise participants**
Report and preliminary results of METEOR-Cruise M 34/4, Recife - Bridgetown, 19.3.-15.4.1996. 105 pages, Bremen, 1996.

No. 81 **Kulbrok, F.**
Biostratigraphie, Fazies und Sequenzstratigraphie einer Karbonatrampe in den Schichten der Oberkreide und des Alttertiärs Nordost-Ägyptens (Eastern Desert, N'Golf von Suez, Sinai). 153 pages, Bremen, 1996.

No. 82 **Kasten, S.**
Early Diagenetic Metal Enrichments in Marine Sediments as Documents of Nonsteady-State Depositional Conditions. Bremen, 1996.

No. 83 **Holmes, M.E.**
Reconstruction of Surface Ocean Nitrate Utilization in the Southeast Atlantic Ocean Based on Stable Nitrogen Isotopes. 113 pages, Bremen, 1996.

No. 84 **Rühlemann, C.**
Akkumulation von Carbonat und organischem Kohlenstoff im tropischen Atlantik: Spätquartäre Produktivitäts-Variationen und ihre Steuerungsmechanismen. 139 pages, Bremen, 1996.

No. 85 **Ratmeyer, V.**
Untersuchungen zum Eintrag und Transport lithogener und organischer partikulärer Substanz im östlichen subtropischen Nordatlantik. 154 pages, Bremen, 1996.

No. 86 **Cepek, M.**
Zeitliche und räumliche Variationen von Coccolithophoriden-Gemeinschaften im subtropischen Ost-Atlantik: Untersuchungen an Plankton, Sinkstoffen und Sedimenten. 156 pages, Bremen, 1996.

No. 87 **Otto, S.**
Die Bedeutung von gelöstem organischen Kohlenstoff (DOC) für den Kohlenstoffffluß im Ozean. 150 pages, Bremen, 1996.

No. 88 **Hensen, C.**
Frühdiagenetische Prozesse und Quantifizierung benthischer Stoff-Flüsse in Oberflächensedimenten des Südatlantiks. 132 pages, Bremen, 1996.

No. 89 **Giese, M. and G. Wefer**
Bericht über den 5. JGOFS-Workshop. 27./28. November 1996 in Bremen. 73 pages, Bremen, 1997.

No. 90 **Wefer, G. and cruise participants**
Report and preliminary results of METEOR-Cruise M 37/1, Lisbon - Las Palmas, 4.-23.12.1996. 79 pages, Bremen, 1997.

No. 91 **Isenbeck-Schröter, M., E. Bedbur, M. Kofod, B. König, T. Schramm & G. Mattheß**
Occurrence of Pesticide Residues in Water - Assessment of the Current Situation in Selected EU Countries. 65 pages, Bremen 1997.

No. 92 **Kühn, M.**
Geochemische Folgereaktionen bei der hydrogeothermalen Energiegewinnung. 129 pages, Bremen 1997.

No. 93 **Determann, S. & K. Herterich**
JGOFS-A6 "Daten und Modelle": Sammlung JGOFS-relevanter Modelle in Deutschland. 26 pages, Bremen, 1997.

No. 94 **Fischer, G. and cruise participants**
Report and preliminary results of METEOR-Cruise M 38/1, Las Palmas - Recife, 25.1.-1.3.1997, with Appendix: Core Descriptions from METEOR Cruise M 37/1. Bremen, 1997.

No. 95 **Bleil, U. and cruise participants**
Report and preliminary results of METEOR-Cruise M 38/2, Recife - Las Palmas, 4.3.-14.4.1997. 126 pages, Bremen, 1997.

No. 96 **Neuer, S. and cruise participants**
Report and preliminary results of VICTOR HENSEN-Cruise 96/1. Bremen, 1997.

No. 97 **Villinger, H. and cruise participants**
Fahrtbericht SO 111, 20.8. - 16.9.1996. 115 pages, Bremen, 1997.

No. 98 **Lüning, S.**
Late Cretaceous - Early Tertiary sequence stratigraphy, paleoecology and geodynamics of Eastern Sinai, Egypt. 218 pages, Bremen, 1997.

No. 99 **Haese, R.R.**
Beschreibung und Quantifizierung frühdiagenetischer Reaktionen des Eisens in Sedimenten des Südatlantiks. 118 pages, Bremen, 1997.

No. 100 **Lührte, R. von**
Verwertung von Bremer Baggergut als Material zur Oberflächenabdichtung von Deponien - Geochemisches Langzeitverhalten und Schwermetall-Mobilität (Cd, Cu, Ni, Pb, Zn). Bremen, 1997.

No. 101 **Ebert, M.**
Der Einfluß des Redoxmilieus auf die Mobilität von Chrom im durchströmten Aquifer. 135 pages, Bremen, 1997.

No. 102 **Krögel, F.**
Einfluß von Viskosität und Dichte des Seewassers auf Transport und Ablagerung von Wattsedimenten (Langeooger Rückseitenwatt, südliche Nordsee). 168 pages, Bremen, 1997.

No. 103 **Kerntopf, B.**
Dinoflagellate Distribution Patterns and Preservation in the Equatorial Atlantic and Offshore North-West Africa. 137 pages, Bremen, 1997.

No. 104 **Breitzke, M.**
Elastische Wellenausbreitung in marinen Sedimenten - Neue Entwicklungen der Ultraschall Sedimentphysik und Sedimentechographie. 298 pages, Bremen, 1997.

No. 105 **Marchant, M.**
Rezente und spätquartäre Sedimentation planktischer Foraminiferen im Peru-Chile Strom. 115 pages, Bremen, 1997.

No. 106 **Habicht, K.S.**
Sulfur isotope fractionation in marine sediments and bacterial cultures. 125 pages, Bremen, 1997.

No. 107 **Hamer, K., R.v. Lührte, G. Becker, T. Felis, S. Keffel, B. Strotmann, C. Waschkowitz, M. Kölling, M. Isenbeck-Schröter, H.D. Schulz**
Endbericht zum Forschungsvorhaben 060 des Landes Bremen: Baggergut der Hafengruppe Bremen-Stadt: Modelluntersuchungen zur Schwermetallmobilität und Möglichkeiten der Verwertung von Hafenschlick aus Bremischen Häfen. 98 pages, Bremen, 1997.

No. 108 **Greeff, O.W.**
Entwicklung und Erprobung eines benthischen Landersystemes zur *in situ*-Bestimmung von Sulfatreduktionsraten mariner Sedimente. 121 pages, Bremen, 1997.

No. 109 **Pätzold, M. und G. Wefer**
Bericht über den 6. JGOFS-Workshop am 4./5.12.1997 in Bremen. Im Anhang: Publikationen zum deutschen Beitrag zur Joint Global Ocean Flux Study (JGOFS), Stand 1/1998. 122 pages, Bremen, 1998.

No. 110 **Landenberger, H.**
CoTReM, ein Multi-Komponenten Transport- und Reaktions-Modell. 142 pages, Bremen, 1998.

No. 111 **Villinger, H. und Fahrtteilnehmer**
Fahrtbericht SO 124, 4.10. - 16.10.199. 90 pages, Bremen, 1997.

No. 112 **Gietl, R.**
Biostratigraphie und Sedimentationsmuster einer nordostägyptischen Karbonatrampe unter Berücksichtigung der Alveolinen-Faunen. 142 pages, Bremen, 1998.

No. 113 **Ziebis, W.**
The Impact of the Thalassinidean Shrimp *Callianassa truncata* on the Geochemistry of permeable, coastal Sediments. 158 pages, Bremen 1998.

No. 114 **Schulz, H.D. and cruise participants**
Report and preliminary results of METEOR-Cruise M 41/1, Málaga - Libreville, 13.2.-15.3.1998. Bremen, 1998.

No. 115 **Völker, D.J.**
Untersuchungen an strömungsbeeinflußten Sedimentationsmustern im Südozean. Interpretation sedimentechographischer Daten und numerische Modellierung. 152 pages, Bremen, 1998.

No. 116 **Schlünz, B.**
Riverine Organic Carbon Input into the Ocean in Relation to Late Quaternary Climate Change. 136 pages, Bremen, 1998.

No. 117 **Kuhnert, H.**
Aufzeichnug des Klimas vor Westaustralien in stabilen Isotopen in Korallenskeletten. 109 pages, Bremen, 1998.

No. 118 **Kirst, G.**
Rekonstruktion von Oberflächenwassertemperaturen im östlichen Südatlantik anhand von Alkenonen. 130 pages, Bremen, 1998.

No. 119 **Dürkoop, A.**
Der Brasil-Strom im Spätquartär: Rekonstruktion der oberflächennahen Hydrographie während der letzten 400 000 Jahre. 121 pages, Bremen, 1998.

No. 120 **Lamy, F.**
Spätquartäre Variationen des terrigenen Sedimenteintrags entlang des chilenischen Kontinentalhangs als Abbild von Klimavariabilität im Milankovi- und Sub-Milankovi-Zeitbereich. 141 pages, Bremen, 1998.

No. 121 **Neuer, S. and cruise participants**
Report and preliminary results of POSEIDON-Cruise Pos 237/2, Vigo – Las Palmas, 18.3.-31.3.1998. 39 pages, Bremen, 1998

No. 122 **Romero, O.E.**
Marine planktonic diatoms from the tropical and equatorial Atlantic: temporal flux patterns and the sediment record. 205 pages, Bremen, 1998.

No. 123 **Spiess, V. und Fahrtteilnehmer**
Report and preliminary results of RV SONNE Cruise 125, Cochin – Chittagong, 17.10.-17.11.1997. 128 pages, Bremen, 1998.

No. 124 **Arz, H.W.**
Dokumentation von kurzfristigen Klimaschwankungen des Spätquartärs in Sedimenten des westlichen äquatorialen Atlantiks. 96 pages, Bremen, 1998.

No. 125 **Wolff, T.**
Mixed layer characteristics in the equatorial Atlantic during the late Quaternary as deduced from planktonic foraminifera. 132 pages, Bremen, 1998.

No. 126 **Dittert, N.**
Late Quaternary Planktic Foraminifera Assemblages in the South Atlantic Ocean: Quantitative Determination and Preservational Aspects. 165 pages, Bremen, 1998.

No. 127 **Höll, C.**
Kalkige und organisch-wandige Dinoflagellaten-Zysten in Spätquartären Sedimenten des tropischen Atlantiks und ihre palökologische Auswertbarkeit. 121 pages, Bremen, 1998.

No. 128 **Hencke, J.**
Redoxreaktionen im Grundwasser: Etablierung und Verlagerung von Reaktionsfronten und ihre Bedeutung für die Spurenelement-Mobilität. 122 pages, Bremen 1998.

No. 129 **Pätzold, J. and cruise participants**
Report and preliminary results of METEOR-Cruise M 41/3, Vítoria, Brasil – Salvador de Bahia, Brasil, 18.4. - 15.5.1998. Bremen, 1999.

No. 130 **Fischer, G. and cruise participants**
Report and preliminary results of METEOR-Cruise M 41/4, Salvador de Bahia, Brasil – Las Palmas, Spain, 18.5. – 13.6.1998. Bremen, 1999.

No. 131 **Schlünz, B. und G. Wefer**
Bericht über den 7. JGOFS-Workshop am 3. und 4.12.1998 in Bremen. Im Anhang: Publikationen zum deutschen Beitrag zur Joint Global Ocean Flux Study (JGOFS), Stand 1/ 1999. 100 pages, Bremen, 1999.

No. 132 **Wefer, G. and cruise participants**
Report and preliminary results of METEOR-Cruise M 42/4, Las Palmas - Las Palmas - Viena do Castelo; 26.09.1998 - 26.10.1998. 104 pages, Bremen, 1999.

No. 133 **Felis, T.**
Climate and ocean variability reconstructed from stable isotope records of modern subtropical corals (Northern Red Sea). 111 pages, Bremen, 1999.

No. 134 **Draschba , S.**
North Atlantic climate variability recorded in reef corals from Bermuda. 108 pages, Bremen, 1999.

No. 135 **Schmieder, F.**
Magnetic Cyclostratigraphy of South Atlantic Sediments. 82 pages, Bremen, 1999.

No. 136 **Rieß, W.**
In situ measurements of respiration and mineralisation processes – Interaction between fauna and geochemical fluxes at active interfaces. 68 pages, Bremen, 1999.

No. 137 **Devey, C.W. and cruise participants**
Report and shipboard results from METEOR-cruise M 41/2, Libreville – Vitoria, 18.3. – 15.4.98. 59 pages, Bremen, 1999.

No. 138 **Wenzhöfer, F.**
Biogeochemical processes at the sediment water interface and quantification of metabolically driven calcite dissolution in deep sea sediments. 103 pages, Bremen, 1999.

No. 139 **Klump, J.**
Biogenic barite as a proxy of paleoproductivity variations in the Southern Peru-Chile Current. 107 pages, Bremen, 1999.

No. 140 **Huber, R.**
Carbonate sedimentation in the northern Northatlantic since the late pliocene. 103 pages, Bremen, 1999.

No. 141 **Schulz, H.**
Nitrate-storing sulfur bacteria in sediments of coastal upwelling. 94 pages, Bremen, 1999.

No. 142 **Mai, S.**
Die Sedimentverteilung im Wattenmeer: ein Simulationsmodell. 114 pages, Bremen, 1999.

No. 143 **Neuer, S. and cruise participants**
Report and preliminary results of Poseidon Cruise 248, Las Palmas - Las Palmas, 15.2.-26.2.1999.
45 pages, Bremen, 1999.

No. 144 **Weber, A.**
Schwefelkreislauf in marinen Sedimenten und Messung von *in situ* Sulfatreduktionsraten.
122 pages, Bremen, 1999.

No. 145 **Hadeler, A.**
Sorptionsreaktionen im Grundwasser: Unterschiedliche Aspekte bei der Modellierung des Transportverhaltens von Zink. 122 pages, 1999.

No. 146 **Dierßen, H.**
Zum Kreislauf ausgewählter Spurenmetalle im Südatlantik: Vertikaltransport und Wechselwirkung zwischen Partikeln und Lösung. 167 pages, Bremen, 1999.

No. 147 **Zühlsdorff, L.**
High resolution multi-frequency seismic surveys at the Eastern Juan de Fuca Ridge Flank and the Cascadia Margin – Evidence for thermally and tectonically driven fluid upflow in marine sediments. 118 pages, Bremen 1999.

No. 148 **Kinkel, H.**
Living and late Quaternary Coccolithophores in the equatorial Atlantic Ocean: response of distribution and productivity patterns to changing surface water circulation. 183 pages, Bremen, 2000.

No. 149 **Pätzold, J. and cruise participants**
Report and preliminary results of METEOR Cruise M 44/3, Aqaba (Jordan) - Safaga (Egypt) – Dubá (Saudi Arabia) – Suez (Egypt) - Haifa (Israel), 12.3.-26.3.-2.4.-4.4.1999. 135 pages, Bremen, 2000.

No. 150 **Schlünz, B. and G. Wefer**
Bericht über den 8. JGOFS-Workshop am 2. und 3.12.1999 in Bremen. Im Anhang:
Publikationen zum deutschen Beitrag zur Joint Global Ocean Flux Study (JGOFS), Stand 1/ 2000.
95 pages, Bremen, 2000.

No. 151 **Schnack, K.**
Biostratigraphie und fazielle Entwicklung in der Oberkreide und im Alttertiär im Bereich der Kharga Schwelle, Westliche Wüste, SW-Ägypten. 142 pages, Bremen, 2000.

No. 152 **Karwath, B.**
Ecological studies on living and fossil calcareous dinoflagellates of the equatorial and tropical Atlantic Ocean. 175 pages, Bremen, 2000.

No. 153 **Moustafa, Y.**
Paleoclimatic reconstructions of the Northern Red Sea during the Holocene inferred from stable isotope records of modern and fossil corals and molluscs. 102 pages, Bremen, 2000.

No. 154 **Villinger, H. and cruise participants**
Report and preliminary results of SONNE-cruise 145-1 Balboa – Talcahuana, 21.12.1999 – 28.01.2000.
147 pages, Bremen, 2000.

No. 155 **Rusch, A.**
Dynamik der Feinfraktion im Oberflächenhorizont permeabler Schelfsedimente. 102 pages, Bremen, 2000.

No. 156 **Moos, C.**
Reconstruction of upwelling intensity and paleo-nutrient gradients in the northwest Arabian Sea derived from stable carbon and oxygen isotopes of planktic foraminifera. 103 pages, Bremen, 2000.

No. 157 **Xu, W.**
Mass physical sediment properties and trends in a Wadden Sea tidal basin. 127 pages, Bremen, 2000.

No. 158 **Meinecke, G. and cruise participants**
Report and preliminary results of METEOR Cruise M 45/1, Malaga (Spain) - Lissabon (Portugal),
19.05. - 08.06.1999. 39 pages, Bremen, 2000.

No. 159 **Vink, A.**
Reconstruction of recent and late Quaternary surface water masses of the western subtropical Atlantic Ocean based on calcareous and organic-walled dinoflagellate cysts. 160 pages, Bremen, 2000.

No. 160 **Willems, H. (Sprecher), U. Bleil, R. Henrich, K. Herterich, B.B. Jørgensen, H.-J. Kuß, M. Olesch, H.D. Schulz,V. Spieß, G. Wefer**
Abschlußbericht des Graduierten-Kollegs Stoff-Flüsse in marine Geosystemen.
Zusammenfassung und Berichtszeitraum Januar 1996 - Dezember 2000. 340 pages, Bremen, 2000.

No. 161 **Sprengel, C.**
Untersuchungen zur Sedimentation und Ökologie von Coccolithophoriden im Bereich der Kanarischen Inseln: Saisonale Flussmuster und Karbonatexport. 165 pages, Bremen, 2000.

No. 162 **Donner, B. and G. Wefer**
Bericht über den JGOFS-Workshop am 18.-21.9.2000 in Bremen:
Biogeochemical Cycles: German Contributions to the International Joint Global Ocean Flux Study.
87 pages, Bremen, 2000.

No. 163 **Neuer, S. and cruise participants**
Report and preliminary results of Meteor Cruise M 45/5, Bremen – Las Palmas, October 1 – November 3, 1999. 93 pages, Bremen, 2000.

No. 164 **Devey, C. and cruise participants**
Report and preliminary results of Sonne Cruise SO 145/2, Talcahuano (Chile) - Arica (Chile), February 4 – February 29, 2000. 63 pages, Bremen, 2000.

No. 165 **Freudenthal, T.**
Reconstruction of productivity gradients in the Canary Islands region off Morocco by means of sinking particles and sediments. 147 pages, Bremen, 2000.

No. 166 **Adler, M.**
Modeling of one-dimensional transport in porous media with respect to simultaneous geochemical reactions in CoTReM. 147 pages, Bremen, 2000.

No. 167 **Santamarina Cuneo, P.**
Fluxes of suspended particulate matter through a tidal inlet of the East Frisian Wadden Sea (southern North Sea). 91 pages, Bremen, 2000.

No. 168 **Benthien, A.**
Effects of CO_2 and nutrient concentration on the stable carbon isotope composition of C37:2 alkenones in sediments of the South Atlantic Ocean. 104 pages, Bremen, 2001.

No. 169 **Lavik, G.**
Nitrogen isotopes of sinking matter and sediments in the South Atlantic. 140 pages, Bremen, 2001.

No. 170 **Budziak, D.**
Late Quaternary monsoonal climate and related variations in paleoproductivity and alkenone-derived sea-surface temperatures in the western Arabian Sea. 114 pages, Bremen, 2001.

No. 171 **Gerhardt, S.**
Late Quaternary water mass variability derived from the pteropod preservation state in sediments of the western South Atlantic Ocean and the Caribbean Sea. 109 pages, Bremen, 2001.

No. 172 **Bleil, U. and cruise participants**
Report and preliminary results of Meteor Cruise M 46/3, Montevideo (Uruguay) – Mar del Plata (Argentina), January 4 – February 7, 2000. Bremen, 2001.

No. 173 **Wefer, G. and cruise participants**
Report and preliminary results of Meteor Cruise M 46/4, Mar del Plata (Argentina) – Salvador da Bahia (Brazil), February 10 – March 13, 2000. With partial results of METEOR cruise M 46/2. 136 pages, Bremen, 2001.

No. 174 **Schulz, H.D. and cruise participants**
Report and preliminary results of Meteor Cruise M 46/2, Recife (Brazil) – Montevideo (Uruguay), December 2 – December 29, 1999. 107 pages, Bremen, 2001.

No. 175 **Schmidt, A.**
Magnetic mineral fluxes in the Quaternary South Atlantic: Implications for the paleoenvironment.
97 pages, Bremen, 2001.

No. 176 **Bruhns, P.**
Crystal chemical characterization of heavy metal incorporation in brick burning processes.
93 pages, Bremen, 2001.

No. 177 **Karius, V.**
Baggergut der Hafengruppe Bremen-Stadt in der Ziegelherstellung. 131 pages, Bremen, 2001.

No. 178 **Adegbie, A. T.**
Reconstruction of paleoenvironmental conditions in Equatorial Atlantic and the Gulf of Guinea Basins for the last 245,000 years. 113 pages, Bremen, 2001.

No. 179 **Spieß, V. and cruise participants**
Report and preliminary results of R/V Sonne Cruise SO 149, Victoria - Victoria, 16.8. - 16.9.2000.
100 pages, Bremen, 2001.

No. 180 **Kim, J.-H.**
Reconstruction of past sea-surface temperatures in the eastern South Atlantic and the eastern South Pacific across Termination I based on the Alkenone Method. 114 pages, Bremen, 2001.

No. 181 **von Lom-Keil, H.**
Sedimentary waves on the Namibian continental margin and in the Argentine Basin – Bottom flow reconstructions based on high resolution echosounder data. 126 pages, Bremen, 2001.

No. 182 **Hebbeln, D. and cruise participants**
PUCK: Report and preliminary results of R/V Sonne Cruise SO 156, Valparaiso (Chile) - Talcahuano (Chile), March 29 - May 14, 2001. 195 pages, Bremen, 2001.

No. 183 **Wendler, J.**
Reconstruction of astronomically-forced cyclic and abrupt paleoecological changes in the Upper Cretaceous Boreal Realm based on calcareous dinoflagellate cysts. 149 pages, Bremen, 2001.

No. 184 **Volbers, A.**
Planktic foraminifera as paleoceanographic indicators: production, preservation, and reconstruction of upwelling intensity. Implications from late Quaternary South Atlantic sediments. 122 pages, Bremen, 2001.

No. 185 **Bleil, U. and cruise participants**
Report and preliminary results of R/V METEOR Cruise M 49/3, Montevideo (Uruguay) - Salvador (Brasil), March 9 - April 1, 2001. 99 pages, Bremen, 2001.

No. 186 **Scheibner, C.**
Architecture of a carbonate platform-to-basin transition on a structural high (Campanian-early Eocene, Eastern Desert, Egypt) – classical and modelling approaches combined. 173 pages, Bremen, 2001.

No. 187 **Schneider, S.**
Quartäre Schwankungen in Strömungsintensität und Produktivität als Abbild der Wassermassen-Variabilität im äquatorialen Atlantik (ODP Sites 959 und 663): Ergebnisse aus Siltkorn-Analysen. 134 pages, Bremen, 2001.

No. 188 **Uliana, E.**
Late Quaternary biogenic opal sedimentation in diatom assemblages in Kongo Fan sediments. 96 pages, Bremen, 2002.

No. 189 **Esper, O.**
Reconstruction of Recent and Late Quaternary oceanographic conditions in the eastern South Atlantic Ocean based on calcareous- and organic-walled dinoflagellate cysts. 130 pages, Bremen, 2001.

No. 190 **Wendler, I.**
Production and preservation of calcareous dinoflagellate cysts in the modern Arabian Sea. 117 pages, Bremen, 2002.

No. 191 **Bauer, J.**
Late Cenomanian – Santonian carbonate platform evolution of Sinai (Egypt): stratigraphy, facies, and sequence architecture. 178 pages, Bremen, 2002.

No. 192 **Hildebrand-Habel, T.**
Die Entwicklung kalkiger Dinoflagellaten im Südatlantik seit der höheren Oberkreide. 152 pages, Bremen, 2002.

No. 193 **Hecht, H.**
Sauerstoff-Optopoden zur Quantifizierung von Pyritverwitterungsprozessen im Labor- und Langzeit-in-situ-Einsatz. Entwicklung - Anwendung – Modellierung. 130 pages, Bremen, 2002.

No. 194 **Fischer, G. and cruise participants**
Report and Preliminary Results of RV METEOR-Cruise M49/4, Salvador da Bahia – Halifax, 4.4.-5.5.2001. 84 pages, Bremen, 2002.

No. 195 **Gröger, M.**
Deep-water circulation in the western equatorial Atlantic: inferences from carbonate preservation studies and silt grain-size analysis. 95 pages, Bremen, 2002.

No. 196 **Meinecke,G. and cruise participants**
Report of RV POSEIDON Cruise POS 271, Las Palmas - Las Palmas, 19.3.-29.3.2001. 19 pages, Bremen, 2002.

No. 197 **Meggers, H. and cruise participants**
Report of RV POSEIDON Cruise POS 272, Las Palmas - Las Palmas, 1.4.-14.4.2001. 19 pages, Bremen, 2002.

No. 198 **Gräfe, K.-U.**
Stratigraphische Korrelation und Steuerungsfaktoren Sedimentärer Zyklen in ausgewählten Borealen und Tethyalen Becken des Cenoman/Turon (Oberkreide) Europas und Nordwestafrikas. 197 pages, Bremen, 2002.

No. 199 **Jahn, B.**
Mid to Late Pleistocene Variations of Marine Productivity in and Terrigenous Input to the Southeast Atlantic. 97 pages, Bremen, 2002.

No. 200 **Al-Rousan, S.**
Ocean and climate history recorded in stable isotopes of coral and foraminifers from the northern Gulf of Aqaba. 116 pages, Bremen, 2002.

No. 201 **Azouzi, B.**
Regionalisierung hydraulischer und hydrogeochemischer Daten mit geostatistischen Methoden.
108 pages, Bremen, 2002.

No. 202 **Spieß, V. and cruise participants**
Report and preliminary results of METEOR Cruise M 47/3, Libreville (Gabun) - Walvis Bay (Namibia), 01.06 - 03.07.2000. 70 pages, Bremen 2002.

No. 203 **Spieß, V. and cruise participants**
Report and preliminary results of METEOR Cruise M 49/2, Montevideo (Uruguay) - Montevideo, 13.02 - 07.03.2001. 84 pages, Bremen 2002.

No. 204 **Mollenhauer, G.**
Organic carbon accumulation in the South Atlantic Ocean: Sedimentary processes and glacial/interglacial Budgets. 139 pages, Bremen 2002.

No. 205 **Spieß, V. and cruise participants**
Report and preliminary results of METEOR Cruise M49/1, Cape Town (South Africa) - Montevideo (Uruguay), 04.01.2000 - 10.02.2000. 57 pages, Bremen, 2003.

No. 206 **Meier, K.J.S.**
Calcareous dinoflagellates from the Mediterranean Sea: taxonomy, ecology and palaeoenvironmental application. 126 pages, Bremen, 2003.

No. 207 **Rakic, S.**
Untersuchungen zur Polymorphie und Kristallchemie von Silikaten der Zusammensetzung $Me_2Si_2O_5$ (Me:Na, K). 139 pages, Bremen, 2003.

No. 208 **Pfeifer, K.**
Auswirkungen frühdiagenetischer Prozesse auf Calcit- und Barytgehalte in marinen Oberflächen-sedimenten. 110 pages, Bremen, 2003.

No. 209 **Heuer, V.**
Spurenelemente in Sedimenten des Südatlantik. Primärer Eintrag und frühdiagenetische Überprägung. 136 pages, Bremen, 2003.

No. 210 **Streng, M.**
Phylogenetic Aspects and Taxonomy of Calcareous Dinoflagellates. 157 pages, Bremen 2003.

No. 211 **Boeckel, B.**
Present and past coccolith assemblages in the South Atlantic: implications for species ecology, carbonate contribution and palaeoceanographic applicability. 157 pages, Bremen, 2003.

No. 212 **Precht, E.**
Advective interfacial exchange in permeable sediments driven by surface gravity waves and its ecological consequences. 131 pages, Bremen, 2003.

No. 213 **Frenz, M.**
Grain-size composition of Quaternary South Atlantic sediments and its paleoceanographic significance. 123 pages, Bremen, 2003.

No. 214 **Meggers, H. and cruise participants**
Report and preliminary results of METEOR Cruise M 53/1, Limassol - Las Palmas – Mindelo, 30.03.2002 - 03.05.2002. 81 pages, Bremen, 2003.

No. 215 **Schulz, H.D. and cruise participants**
Report and preliminary results of METEOR Cruise M 58/1, Dakar – Las Palmas, 15.04..2003 - 12.05.2003. Bremen, 2003.

No. 216 **Schneider, R. and cruise participants**
Report and preliminary results of METEOR Cruise M 57/1, Cape Town – Walvis Bay, 20.01. – 08.02.2003. 123 pages, Bremen, 2003.

No. 217 **Kallmeyer, J.**
Sulfate reduction in the deep Biosphere. 157 pages, Bremen, 2003.

No. 218 **Røy, H.**
Dynamic Structure and Function of the Diffusive Boundary Layer at the Seafloor. 149 pages, Bremen, 2003.

No. 219 **Pätzold, J., C. Hübscher and cruise participants**
Report and preliminary results of METEOR Cruise M 52/2&3, Istanbul – Limassol – Limassol, 04.02. – 27.03.2002. Bremen, 2003.

No. 220 **Zabel, M. and cruise participants**
Report and preliminary results of METEOR Cruise M 57/2, Walvis Bay – Walvis Bay, 11.02. – 12.03.2003. 136 pages, Bremen 2003.

No. 221 **Salem, M.**
Geophysical investigations of submarine prolongations of alluvial fans on the western side of the Gulf of Aqaba-Red Sea. 100 pages, Bremen, 2003.

No. 222 **Tilch, E.**
Oszillation von Wattflächen und deren fossiles Erhaltungspotential (Spiekerooger Rückseitenwatt, südliche Nordsee). 137 pages, Bremen, 2003.

No. 223 **Frisch, U. and F. Kockel**
Der Bremen-Knoten im Strukturnetz Nordwest-Deutschlands. Stratigraphie, Paläogeographie, Strukturgeologie. 379 pages, Bremen, 2004.

No. 224 **Kolonic, S.**
Mechanisms and biogeochemical implications of Cenomanian/Turonian black shale formation in North Africa: An integrated geochemical, millennial-scale study from the Tarfaya-LaAyoune Basin in SW Morocco. 174 pages, Bremen, 2004. Report online available only.

No. 225 **Panteleit, B.**
Geochemische Prozesse in der Salz- Süßwasser Übergangszone. 106 pages, Bremen, 2004.

No. 226 **Seiter, K.**
Regionalisierung und Quantifizierung benthischer Mineralisationsprozesse. 135 pages, Bremen, 2004.

No. 227 **Bleil, U. and cruise participants**
Report and preliminary results of METEOR Cruise M 58/2, Las Palmas – Las Palmas (Canary Islands, Spain), 15.05. – 08.06.2003. 123 pages, Bremen, 2004.

No. 228 **Kopf, A. and cruise participants**
Report and preliminary results of SONNE Cruise SO175, Miami - Bremerhaven, 12.11 - 30.12.2003. 218 pages, Bremen, 2004.

No. 229 **Fabian, M.**
Near Surface Tilt and Pore Pressure Changes Induced by Pumping in Multi-Layered Poroelastic Half-Spaces.
121 pages, Bremen, 2004.

No. 230 **Segl, M. , and cruise participants**
Report and preliminary results of POSEIDON cruise 304 Galway – Lisbon, 5. – 22. Oct. 2004, 27 pages, Bremen 2004

No. 231 **Meinecke, G. and cruise participants**
Report and preliminary results of POSEIDON Cruise 296, 42 pages, Bremen 2005.

No. 232 **Meinecke, G. and cruise participants**
Report and preliminary results of POSEIDON Cruise 310, 49 pages, Bremen 2005.

No. 233 **Meinecke, G. and cruise participants**
Report and preliminary results of METEOR Cruise 58/3, Bremen 2005.

No. 234 **Feseker, T.**
Numerical Studies on Groundwater Flow in Coastal Aquifers. 219 pages. Bremen 2004.

No. 235 **Sahling, H. and cruise participants**
Report and preliminary results of R/V POSEIDON Cruise P317/4, Istanbul-Istanbul , 16 October - 4 November 2004. 92 pages, Bremen 2004.

No. 236 **Meinecke, G. and cruise participants**
Report and preliminary results of POSEIDON Cruise 305, Bremen 2005.

No. 237 **Ruhland, G. and cruise participants**
Report and preliminary results of POSEIDON Cruise 319, Bremen 2005.

No. 238 **Chang, T.S.**
Dynamics of fine-grained sediments and stratigraphic evolution of a back-barrier tidal basin of the German Wadden Sea (southern North Sea). 102 pages, Bremen 2005.

No. 239 **Lager, T.**
Predicting the source strength of recycling materials within the scope of a seepage water prognosis by means of standardized laboratory methods. 141 pages, Bremen 2005.

No. 240 **Meinecke, G.**
DOLAN - Operationelle Datenübertragung im Ozean und Laterales Akustisches Netzwerk in der Tiefsee. Abschlußbericht. 42 pages, Bremen 2005.

No. 241 **Guasti, E.**
Early Paleogene environmental turnover in the southern Tethys as recorded by foraminiferal and organic-walled dinoflagellate cysts assemblages. 203 pages, Bremen 2005.

No. 242 **Riedinger, N.**
Preservation and diagenetic overprint of geochemical and geophysical signals in ocean margin sediments related to depositional dynamics. 91 pages, Bremen 2005.